

# Technical Report

## TR-13-28

### **Precipitation of barite in the biosphere and its consequences for the mobility of Ra in Forsmark and Simpevarp**

Maria Jaremalm, Hifab AB

Stephan Köhler, Swedish University of Agricultural Sciences

Fredrik Lidman, Jarec AB

December 2013

**Svensk Kärnbränslehantering AB**

Swedish Nuclear Fuel  
and Waste Management Co

Box 250, SE-101 24 Stockholm  
Phone +46 8 459 84 00



ISSN 1404-0344

SKB TR-13-28

ID 1419023

# **Precipitation of barite in the biosphere and its consequences for the mobility of Ra in Forsmark and Simpevarp**

Maria Jaremalm, Hifab AB

Stephan Köhler, Swedish University of Agricultural Sciences

Fredrik Lidman, Jarec AB

December 2013

This report concerns a study which was conducted for SKB. The conclusions and viewpoints presented in the report are those of the authors. SKB may draw modified conclusions, based on additional literature sources and/or expert opinions.

A pdf version of this document can be downloaded from [www.skb.se](http://www.skb.se).

## Abstract

In the safety analysis of a repository of spent nuclear fuel  $^{226}\text{Ra}$  dominates the long term risk. It is therefore vital that its behaviour in the environment is well-understood and that the radionuclide transport models can be adequately and reliably parameterised. Due to the low concentrations of radium in the environment it is, however, rarely included in standard multielement analyses. Biogeochemically radium is often assumed to behave similarly to other alkaline earth metals such as barium, strontium and calcium, which therefore often are used as natural analogues for radium. However, previous measurements of site specific  $K_d$  values for various elements in the Forsmark and Simpevarp areas have in many cases revealed considerable differences between Ca and Sr on one hand and Ba on the other.

In order to explain these differences this report investigates the possible occurrence of barite ( $\text{BaSO}_4$ ) in the Forsmark and Simpevarp areas and its importance for the mobility of primarily Ba and Ra. Thermodynamic modelling in Visual MINTEQ 3.0 was used to study the solubility of alkaline earth metals (Ca, Sr, Ba and Ra) in all available water samples from the site investigations with sufficient background data ( $n=424$ ) and pore water samples from site specific  $K_d$  measurements ( $n=50$ ). Hence, the material includes pore water, near-surface groundwater, stream water, lake water and sea water. Saturation indices are presented for calcite, aragonite, strontianite, witherite, gypsum, celestite and barite. The modelling indicated that the barium concentrations in many water samples, primarily sea water and groundwater from certain Quaternary deposits, were controlled by barite. The modelling also indicated that many water samples were saturated with respect to calcite/aragonite, above all in the Forsmark area, which is in full accordance with the well-known abundance of  $\text{CaCO}_3$  in the Forsmark soils.

A thorough survey of the scientific literature demonstrated that the precipitation of barite in sea water is ubiquitous and well-known. The saturation with respect to barite that was modelled in the sea water samples therefore agrees well with the literature. Given the marine history of both the Forsmark and Simpevarp areas this also provides a possible explanation to the occurrence of barite in the soils, especially in old sedimentary deposits. Furthermore, barite may also occur as a primary mineral in the soils.

The potential occurrence of barite in the site investigation areas is important because Ra easily coprecipitates with barite. The literature survey showed that this process is well observed, especially in marine environments. In order to investigate the quantitative effects of barite on the  $K_d$  values for Ra another thermodynamic programme, PHREEQC, was used to model the coprecipitation of Ra with barite in the samples from the site investigation areas. The results demonstrate that barite would have a profound impact on the mobility of Ra in some soils – should it be present. There were, however, large uncertainties because one of the crucial parameters, the amount of barite in the solid phase, was unknown. The model was not capable of reproducing as high  $K_d$  values for Ra as those observed in the Forsmark area, possibly due to uncertainties in the parameterisation of the system.

Since the coprecipitation of Sr and Ca with barite is much weaker than for Ra, the occurrence of barite would provide an explanation to why the observed  $K_d$  values for Ba (and when available also those for Ra) often are much higher than those for Ca and Sr, although there may also be additional processes. The occurrence of barite would also explain various previous observations from Forsmark and Simpevarp, e.g. higher relative concentrations of particulate Ba in sea water and higher relative concentrations of Ba in the soil fraction, which is not soluble by aqua regia. The low solubility of barite in aqua regia also complicates the interpretation of the site specific  $K_d$  values, since some measurements were made using total digestion (including barite) and others using partial extraction by aqua regia (largely excluding barite). Some soils samples were also found to display suspiciously low  $K_d$  values for Ba due to anomalous Ba concentrations in the pore water.

All and all, the results suggest that there are good reasons to believe that barite is present in parts of the site investigation areas and that coprecipitation of Ra with barite potentially could be an important retention mechanism for Ra in these environments.

# Sammanfattning

Säkerhetsanalysen för slutförvaret av kärnbränsle har visat att  $^{226}\text{Ra}$  är en av de dominerande radionukliderna när det gäller de långsiktiga riskerna. Det är därför viktigt med en god, processbaserad kunskap om radiums beteende i miljön och att radionuklidtransportmodellerna kan parametreras på ett riktigt och tillförlitligt sätt. Ra ingår dock sällan i ordinära multielementanalyser på grund av de naturligt låga koncentrationerna av Ra i miljön. Biogeokemiskt antas radium ofta bete sig på liknande sätt som andra alkaliska jordartsmetaller som barium (Ba), strontium (Sr) och kalcium (Ca), vilka därför ofta används som naturliga analoger för radium. Tidigare mätningar av platsspecifika  $K_d$ -värden för ett flertal grundämnen i Forsmark och Simpevarp har dock i många fall visat på betydande skillnader mellan å ena sidan Ca och Sr och å andra sidan Ba.

För att förklara dessa skillnader undersöker denna rapport den möjliga förekomsten av baryt ( $\text{BaSO}_4$ ) i Forsmarks- och Simpevarpsområdet och vilken betydelse det i sådana fall skulle ha för mobiliteten för framför allt Ba och Ra. Termodynamisk modellering i Visual MINTEQ 3.0 användes för att studera lösligheten för de alkaliska jordartsmetallerna (Ca, Sr, Ba och Ra) i alla tillgängliga vattenprover från platsundersökningarna med tillräcklig bakgrundsinformation ( $n=424$ ) och i samtliga porvatten som användes för att bestämma de platsspecifika  $K_d$ -värdena ( $n=50$ ). Materialet omfattar således havsvatten, sjövattnet, bäckvattnet, yttnära grundvattnet och markvattnet. Mättnadsgraden redovisas för mineralerna kalcit ( $\text{CaCO}_3$ ), aragonit ( $\text{CaCO}_3$ ), strontianit ( $\text{SrCO}_3$ ), witherit ( $\text{BaCO}_3$ ), gips ( $\text{CaSO}_4 \cdot 2 \text{H}_2\text{O}$ ), celestit ( $\text{SrSO}_4$ ) och baryt ( $\text{BaSO}_4$ ). Modelleringen indikerade att bariumkoncentrationen i många prover kontrollerades av baryt, framför allt i havsvatten och i grundvattnet från vissa jordtyper. Modelleringen visade också att många vattenprover, speciellt i Forsmarksområdet, var mättade med avseende på kalcit/aragonit, vilket stämmer väl med de höga på  $\text{CaCO}_3$ -koncentrationer som tidigare har observerats i många jordprover från Forsmark.

En grundlig litteraturgenomgång visade att utfällning av baryt i havsvatten är vanligt förekommande och väl dokumenterat. Den mättnad med avseende på baryt som modelleringen visade på i havsvattenproverna stämmer därför väl överens med den vetenskapliga litteraturen. Givet att både Forsmarks- och Simpevarpsområdena båda har en marin historia erbjuder detta också en möjlig förklaring till den troliga förekomsten av baryt i delar av platsundersökningsområdena, inte minst i äldre sedimentjordar. Baryt kan dock även förekomma som primärt mineral i svenska jordar.

Den troliga förekomsten av baryt i platsundersökningsområdena är viktig, eftersom Ra lätt faller ut tillsammans med baryt (så kallad samfällning). Litteraturundersökningen visade att denna process är väldokumenterad, i synnerhet i marina miljöer. För att undersöka den kvantitativa effekten av baryt på  $K_d$ -värdena för Ra användes ett annat termodynamiskt modelleringsprogram, PHREEQC, för att modellera samfällning av Ra med baryt i proverna från platsundersökningen. Resultaten visade att baryt skulle ha en betydande inverkan på radiums mobilitet. Det faktum att en av de avgörande parametrarna, nämligen mängden baryt i den fasta fasen, var okänd innebär dock en stor osäkerhet i resultaten. Även om man antog att allt barium som uppmätts i den fasta fasen förekom i baryt hade modellen svårt att återskapa lika höga  $K_d$ -värden som de som observerats i Forsmarksområdet. Möjligen beror detta på osäkerheter i parametriseringen av systemet, eftersom fördelningkoefficienten inte är välbestämd.

Eftersom utfällningen av Sr och Ca med baryt är mycket svagare än för Ra, skulle förekomsten av baryt kunna ge en förklaring till varför de observerade  $K_d$ -värdena för Ba (och även de för Ra i de fall de var tillgängliga) ofta är mycket högre än motsvarande värden för Ca och Sr. Det kan dock inte uteslutas att även andra processer påverkar. Förekomsten av baryt skulle dock även förklara ett flertal tidigare observationer från Forsmark och Simpevarp, exempelvis avsevärt högre relativa koncentrationer av partikulärt Ba i havsvatten och avsevärt högre relativa koncentrationer av Ba i svårslösliga mineralfraktioner. Baryt är nämligen mycket svårslösligt i kungsvatten, vilket har varit den extraktionsmetod som har använts vid de flesta  $K_d$ -mätningar. Detta komplicerar också tolkningen av de platsspecifika  $K_d$ -värdena, eftersom vissa mätningar gjordes med totalupplösning (baryt löses upp) och andra med partiell extraktion med kungsvatten (baryt förblir till stora delar olöst). I de fall där barytfraktionen inte togs med i beräkningen finns en risk att man missar den viktigaste retentionsprocessen och således överskattar mobiliteten för såväl Ba som Ra. Några  $K_d$ -prover uppvisade även på märkligt låga och förmodligen missvisande  $K_d$ -värden för Ba på grund av anmärkningsvärt höga bariumkoncentrationer i porvattnet.

Sammantaget visar resultaten att det finns goda skäl att tro att baryt förekommer i delar av platsundersökningsområdena och att utfällning av Ra med baryt potentiellt kan vara avgörande för radiums mobilitet i dessa miljöer.

# Contents

<b>1</b>	<b>Background and purpose</b>	<b>7</b>
<b>2</b>	<b>Theory</b>	<b>9</b>
2.1	Radionuclide sorption in soils and the $K_d$ model	9
2.1.1	Precipitation and the $K_d$ approach	9
2.2	The alkaline earth metals	10
2.3	Coprecipitation and solid solutions	11
2.3.1	Coprecipitation with baryte	12
2.3.2	Coprecipitation with calcite and aragonite	12
2.3.3	Coprecipitation with other minerals	13
2.4	Marine biogeochemistry of Ba and Ra	13
2.4.1	Precipitation of barite in marine environments	13
2.4.2	Ra biogeochemistry in marine environments	15
<b>3</b>	<b>Material and methods</b>	<b>17</b>
3.1	Thermodynamic modelling in Visual MINTEQ 3.0	17
3.2	Thermodynamic modelling in PHREEQC	17
3.2.1	Modelling of solid solutions in PHREEQC	17
3.2.2	Kinetics of Ra coprecipitation with barite	17
3.2.3	Modelling of $K_d$ values for Ra in the presence of barite	18
3.3	Thermodynamical constants	18
3.4	Data used in the modelling	18
3.4.1	Dataset 1: Site investigation data	19
3.4.2	Dataset 2: Sediment $K_d$ data	19
3.4.3	Dataset 3: 2009 $K_d$ data	21
3.4.4	Dataset 4: 2011 $K_d$ data	21
<b>4</b>	<b>Solubility of alkaline earth metals in Forsmark and Simpevarp</b>	<b>23</b>
4.1	Saturation indices	23
4.1.1	Saturation indices in near surface ground water	23
4.1.2	Saturation indices in lakes	23
4.1.3	Saturation indices in stream waters	25
4.1.4	Saturation indices in marine waters	26
4.1.5	Saturation indices in the sediment $K_d$ samples	27
4.1.6	Saturation indices in the 2011 $K_d$ samples	28
4.2	Precipitation of pure $RaSO_4$ and $RaCO_3$	29
4.3	Sensitivity to pH	29
4.4	Speciation of sulphur in the sediment $K_d$ samples	30
4.5	Summary of the saturation with respect to barite	32
<b>5</b>	<b>Modelling of Ra coprecipitation and speciation</b>	<b>35</b>
5.1	The effects of barite on the $K_d$ for Ra	35
5.1.1	Modelled Ra $K_d$ values in lake sediments	35
5.1.2	Modelled Ra $K_d$ values in marine sediments	36
5.1.3	Modelled Ra $K_d$ values in 2011 soil samples	36
5.2	Ra speciation	38
5.3	Sensitivity for the Guggenheim parameter	39
<b>6</b>	<b>Discussion</b>	<b>41</b>
6.1	Solubility of alkaline earth metals	41
6.2	Effects of extraction method on the $K_d$ values for Ba and Ra	42
6.3	$K_d$ values in sediments	43
6.3.1	Sediment samples	43
6.3.2	Particulate Ba in the water column	44
6.4	$K_d$ values in soils	45
6.4.1	2009 Soil $K_d$ samples	45
6.4.2	2011 $K_d$ samples	46
6.5	Radium and uranium	51

6.6	Compilation of reported $K_d$ values	53
6.7	The mechanisms behind the $K_d$ values	55
6.7.1	Radium in soils	55
6.7.2	Radium and manganese	56
6.7.3	Dealing with barite in transport models	56
6.7.4	Barite in the future landscape	58
<b>7</b>	<b>Conclusions</b>	<b>59</b>
	<b>References</b>	<b>61</b>
<b>Appendix A</b>	Measured $K_d$ values	<b>65</b>
<b>Appendix B</b>	Basic theory of solubility products and saturation indices	<b>67</b>
<b>Appendix C</b>	Basic theory of solid solutions	<b>69</b>
<b>Appendix D</b>	Saturation indices	<b>71</b>
<b>Appendix E</b>	Ra speciation	<b>83</b>
<b>Appendix F</b>	Effects of barite on the $K_d$ for Ra	<b>85</b>

# 1 Background and purpose

In the safety analysis of a repository of spent nuclear fuel  $^{226}\text{Ra}$  dominates the long term risk. It is therefore important to find accurate and reliable  $K_d$  values for Ra in all relevant environments that can be used in radionuclide transport models. Site specific  $K_d$  measurements for Ra and a wide range of other elements for the Simpevarp and Forsmark areas have been presented by Sheppard et al. (2011). In order to strengthen the reliability of the results of the dose modelling and the  $K_d$  values, upon which the models are based, it is important to gain as much knowledge as possible about what processes the observed  $K_d$  values represent. Without such knowledge it is hard to assess how representative the observed  $K_d$  values are in space and in time – and whether a  $K_d$  approach is suitable at all.

Ra is often assumed to have large similarities with other alkaline earth elements, primarily Ba, Sr and Ca. However, throughout the site investigation areas the site specific  $K_d$  measurements have demonstrated substantial differences, mainly between Ca and Sr on one hand and Ra and Ba on the other (Sheppard et al. 2009, 2011). At many sites the Ba and Ra  $K_d$  values are considerably higher than the corresponding  $K_d$  values for Ca and Sr. It is already known that calcite is present above all in the Forsmark area, but the high  $K_d$  values for Ba may indicate that barite ( $\text{BaSO}_4$ ) also could be present. If so, barite would control the aqueous concentrations of Ba and lead to higher  $K_d$  values for Ba. More importantly, Ra would in that case be affected by coprecipitation with barite, since  $\text{BaSO}_4$  and  $\text{RaSO}_4$  easily form a solid solution. Therefore, barite could potentially be the major retention processes for Ra in parts of the site investigation areas.

The purpose of this study was therefore to investigate all available data from streams, lakes, seawater, near-surface groundwater and pore water of soils and sediments, which have been gathered within the frames of the site investigations and other projects. In total, the material comprises 474 observations. Thermodynamic equilibrium modelling was used to examine which waters are likely to be saturated with respect to important alkaline earth minerals, including calcite, aragonite, strontianite, witherite, gypsum, celestite and barite. Thermodynamic modelling was also used to quantify the potential impact of barite on the mobility of Ra. Information about controlling phases in the soils was then used to discuss the results of the site specific  $K_d$  measurements.

In brief, the aim of this study could be summarized in the following points:

- Are there reasons to believe that the mobility of alkaline earth metals, especially Ba and Ra, is controlled by precipitation or coprecipitation in parts of the site investigation areas?
- How would the presence of alkaline earth carbonates or sulphates affect the  $K_d$  values for Ra, Ba, Sr and Ca? Can it explain the patterns in the site specific  $K_d$  data?
- How would coprecipitation of Ra with barite affect the behaviour, transport and  $K_d$  value of Ra in different environments?

## 2 Theory

### 2.1 Radionuclide sorption in soils and the $K_d$ model

In order to model the transport of radionuclides in soils and sediments it is essential to know how it is distributed between the solid and the aqueous phase. A common way to solve this problem is to use a linear distribution (or partitioning) coefficient, often denoted as  $K_d$ .  $K_d$  relates the concentration of a certain substance in the solid phase to its respective concentration in the pore water (Equation 2-1)

$$Kd = \frac{[A]_s}{[A]_{aq}} \quad (2-1)$$

where A is an arbitrary substance.  $[A]_s$  denotes the concentration in the solid phase and  $[A]_{aq}$  the concentration in the aqueous phase.  $K_d$  is an apparent constant, used to describe the result of a large number of different processes in the interaction between the soil matrix and the pore water. For instance, there are several processes that could be important for binding Ra to the solid phase, e.g. sorption to illite (the most common clay mineral in Forsmark) and other clay minerals, sorption to organic matter, sorption to iron and manganese oxyhydroxides or coprecipitation with barite and aragonite. Given that many of these processes also vary with changing geochemical conditions, e.g. pH and temperature, it is clear that the  $K_d$  approach is an attempt to simplify a number of processes that sometimes can be highly complex. A discussion of the advantages and disadvantages of the  $K_d$  approach can be found in Siegel and Bryan (2007).

#### 2.1.1 Precipitation and the $K_d$ approach

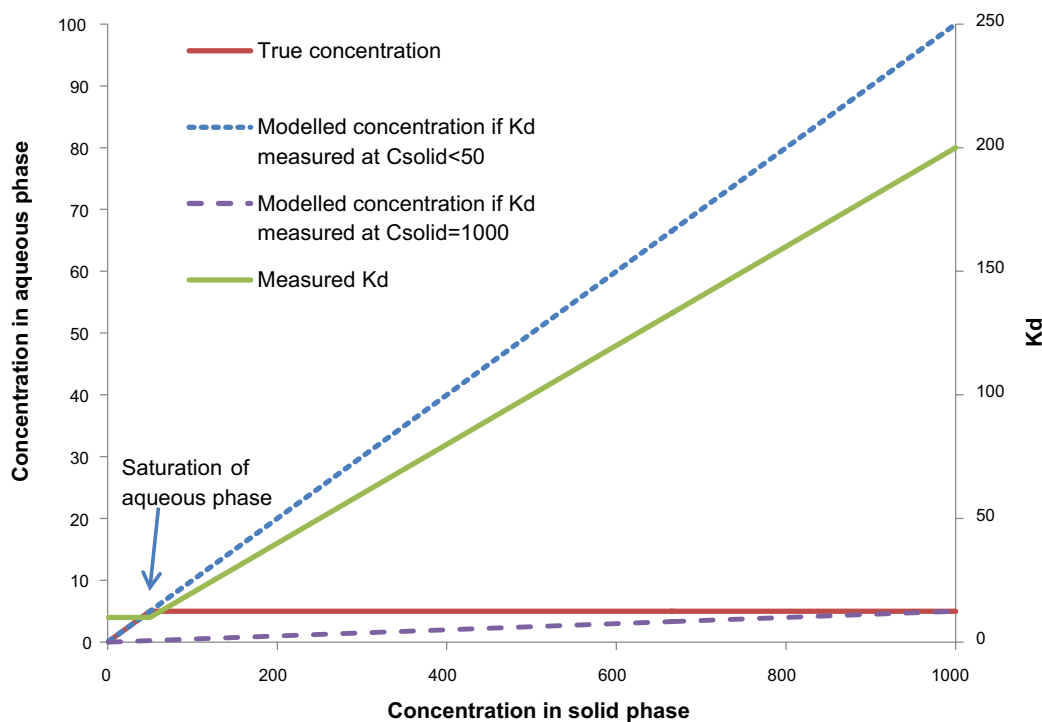
One situation, which is hard to handle using a  $K_d$  approach, is when the concentration of an element is controlled by the solubility of a pure (fixed composition) mineral. For instance, if the water is saturated with respect to barite, the product of the sulphate and Ba activities cannot increase further. Since sulphate usually occurs in much higher concentrations than Ba, any additional Ba that is added will tend to precipitate as barite. The result will be an increased amount of Ba in the solid phase, whereas the Ba concentration in the aqueous phase remains stable. This is not what a  $K_d$  model would predict, since it assumes a constant ratio between the amount of Ba in the solid phase and the aqueous phase, respectively. In principle, the amount of barite in the solid phase could increase to infinite levels without affecting the Ba concentrations in the aqueous phase. The problem is illustrated in Figure 2-1 below.

Figure 2-1 gives a hypothetical example of what might happen if the  $K_d$  approach is used in a situation where the element in question is controlled by the precipitation of a mineral. Below saturation the  $K_d$  value is 10 (arbitrary units) and the aqueous concentration will increase linearly with the solid concentration until saturation is reached. In this case precipitation will occur at an aqueous concentration of 5. The pore water is now saturated and the aqueous concentration will remain constant no matter how much the solid concentration increases, assuming that no changes in temperature, ionic strength or speciation occur.

The green line describes how the apparent  $K_d$  value changes as a function of the concentration in the solid phase, assuming that saturation and precipitation occurs at an aqueous concentration of 5. If a sample is taken at a site where the aqueous concentration is not controlled by solubility, a  $K_d$  of 10 will be measured that accurately will describe the sorption of the element in question as long as the aqueous concentration remains below 5. However, as soon as saturation is reached, the  $K_d$  approach will overestimate the concentration in the pore water. If the solid concentration at one site is 1,000, the model predicts an aqueous concentration of 100, i.e. a factor 20 higher than the true concentration. This situation is illustrated by the blue line.

On the other hand, if the  $K_d$  value is determined from a sample with a solid concentration of 1,000, we would conclude that the  $K_d$  value is 200. Using this value would lead to an underestimation of the aqueous concentration at all sites with lower concentrations in the solid phase. For instance, if the solid concentration is 50, the model would predict an aqueous concentration of 0.25, i.e. a factor 20 lower than the true concentration. Furthermore, a  $K_d$  value of 200 would lead to an underestimation in all samples where the solid concentration is higher than 1,000.





**Figure 2-1.** Hypothetical example of the change in  $K_d$  for an element that is limited by the precipitation of a mineral phase at aqueous concentrations  $>5$  (arbitrary unit). The red line displays the true aqueous concentration as a function of the amount present in the solid phase. The green line displays the  $K_d$  value that would be measured depending on the concentration in the solid phase. The blue and purple lines indicate the hypothetical aqueous concentrations that would be modelled depending on the conditions under which the  $K_d$  value was determined.

The example illustrates that the linear  $K_d$  approach is sensitive to the occurrence of controlling mineral phases. It is also evident that the  $K_d$  value in this example has very little to do with the properties of the soil, which the  $K_d$  value is meant to describe. The errors in the given examples were only a factor 20, but, as mentioned, there are no limits to how misleading the results the model can give under such circumstances.

## 2.2 The alkaline earth metals

Ca, Sr, Ba and Ra all belong to the group of alkaline earth metals in the periodic table of the elements. Biogeochemically the four elements are quite similar and share many important features. For instance, all elements only occur in the divalent oxidation state in natural waters, and they are not particularly prone to form strong complexes with other ions or organic matter. Therefore, the dominating species for alkaline earth metals in natural waters is often the free metal ion, e.g.  $Ba^{2+}$  or  $Ra^{2+}$ . This is a factor that makes their behaviour somewhat easier to predict.

Apart from the oxidation state an important prerequisite for the similarities between these elements is the relatively small differences in ionic radii between the four elements. The element that comes closest to Ra in this sense is Ba, and therefore Ba is expected to be the best analogue for Ra. The difference is biggest between Ca and Ra so generally speaking Ca could be expected to be least representative for Ra.

All four elements may form precipitates with sulphate and carbonate.  $BaSO_4$  forms the mineral barite. The corresponding Sr mineral,  $SrSO_4$ , is celestite (or celestine). The isomorphic counterpart of barite and celestite for Ca would be anhydrite, which is anhydrous  $CaSO_4$ . However, in the presence of water  $CaSO_4$  will absorb water molecules, and the resulting mineral is called gypsum ( $CaSO_4 \cdot 2H_2O$ ).  $RaSO_4$  shares the same crystal structure as barite, celestite and anhydrite, but since Ra is so rare,  $RaSO_4$  does not occur as a mineral in nature and, consequently, it does not have a mineral name.

Among the carbonates there is a similar pattern.  $\text{BaCO}_3$  forms the mineral witherite and  $\text{SrCO}_3$  forms the mineral strontianite. They both share the same orthorhombic crystal structure as  $\text{RaCO}_3$ , which, for the same reasons as  $\text{RaSO}_4$ , lacks a mineral name.  $\text{CaCO}_3$ , finally, may form three different minerals: vaterite, aragonite and calcite. They all have the same chemical composition, but different crystal structures. Vaterite is the least stable polymorph with a hexagonal crystal system. It is relatively easily transformed to calcite or aragonite. Calcite, on the other hand, is the most stable polymorph of Ca carbonate so over time aragonite can also be expected to transform into calcite. However, calcite has a trigonal (rhombohedral) crystal system, whereas aragonite has an orthorhombic lattice. This makes aragonite similar to the corresponding Sr, Ba and Ra compounds.

The distinction between calcite and aragonite is important because it affects how much Sr, Ba and Ra that can be coprecipitated along with the Ca. The trigonal crystal structure of calcite makes it harder for larger cations such as Sr, Ba and Ra ions to substitute Ca in the crystal lattice. This substitution is much easier in aragonite, which shares the orthorhombic crystal structure of strontianite, witherite and  $\text{RaSO}_4$ . Although calcite is the most stable form of  $\text{CaCO}_3$ , precipitation of aragonite is sometimes favoured. For instance, the precipitation of calcite is inhibited by high magnesium concentrations. If the Mg/Ca ratio in the water is higher than 0.5, parts of the Ca carbonate may start to precipitate as aragonite in abiotic systems (Tang et al. 2007). The Mg/Ca ratio in present-day seawater is c 2.5 so aragonite would be the preferred mineral. Hence, in recent marine sediments one should expect to find aragonite rather than calcite with the exception of biologically mediated precipitation as in diatoms, molluscs or shells.

In general, the solubility of alkaline earth sulphates decreases downwards in the periodic table. Hence,  $\text{RaSO}_4$  is the least soluble sulphate, followed by barite. For carbonates, calcite is the least soluble mineral, while strontianite is the most soluble. The solubility of  $\text{RaCO}_3$  is close to the solubility of witherite. Solubility products for all these minerals can be found in Table 3-1.

### 2.3 Coprecipitation and solid solutions

Coprecipitation is a process where an element is simultaneously precipitated along with some other element from the same solution. The environmental importance of coprecipitation hinges on the fact that it may control the solubility of a trace element that does not commonly occur in high enough concentration to achieve pure solid saturation. One such example is Ra, which is so rare that it hardly can be expected to precipitate as pure phase under natural conditions. Instead, Ra atoms may, for instance, substitute Ca atoms in calcite or Ba atoms in barite. This process is facilitated if the atoms have similar atomic radii, similar valence state and if the two involved minerals have similar crystal structure. In the case of Ra coprecipitation with barite, both Ra and Ba are divalent ions, although the Ra is slightly larger than Ba, and the solvent,  $\text{BaSO}_4$ , has the same crystal structure as the corresponding Ra mineral.

The result of coprecipitation is called a solid solution. It is referred to as a solution rather than a compound because the mixture will remain a single homogeneous phase. In nature, solid solutions are common. For instance, many mineral series of variable composition can be considered as solid solutions of two or more pure end-members, e.g. carbonates, plagioclases, amphiboles and pyroxenes (Appelo and Postma 2005).

Solid solutions may not only form by coprecipitation. For instance, if Ra is introduced in the pore water of a soil, where barite is present, some Ra will start to substitute Ba in the crystal lattice of barite. It has been suggested that such substitution of Ba by Ra in barite may be the dominating scavenging process for Ra in the near-field of a deep repository (Curti et al. 2010). Therefore, using a term like solid solution formation would be more general and more proper than speaking of coprecipitation only. In this report, however, the terms are used interchangeably unless clearly stated otherwise in special contexts where it is relevant to distinguish different formation processes.

The basic theory of solid solutions is presented in Appendix C. Basic theory of solid solutions.

### 2.3.1 Coprecipitation with baryte

Coprecipitation of Ra with barite has been known at least since 1925 (Doerner and Hoskins 1925). By now the phenomenon is well documented in literature, e.g. Paige et al. (1998), Zielinski et al. (2001), Zhu (2004a) and references therein. Hence, there is no doubt that Ra will be incorporated into barite, whenever barite is present. The question is only to what extent and at what rate. Two crucial parameters are temperature and the degree of non-ideality of the solid solution. For instance, Langmuir and Riese (1985) have suggested Equation 2-2 for the distribution factor,  $D$ , for Ra coprecipitation with barite:

$$\log_{10} D = \frac{428.2}{T} - 1.181 \quad (2-2)$$

where  $T$  is the absolute temperature in K. The exact definition of  $D$  can be found in Appendix C (Equation C-9). Hence, at 25°C the distribution factor would be about 1.8, while it would increase to almost 2.2 if the temperature decreased down to 10°C. With these assumptions there would be a preferential incorporation of Ra into barite in the sense that the Ra/Ba-ratio in the barite should be about twice higher than in the aqueous solution, from which it was formed (Zhu 2004a). Recent studies have indicated that there may be some degree of non-ideality in the  $\text{RaSO}_4$ - $\text{BaSO}_4$  solid solution series e.g. Bosbasch et al. (2010) and Curti et al. (2010). According to these results incorporation of Ra into barite is not preferential, i.e. the Ra/Ba ratio in the barite will be lower than in the aqueous solution. However, the possible existence of a miscibility gap is probably not crucial in this context, since the Ra concentrations are likely to remain low in comparison to the natural Ba concentrations. Bosbasch et al. (2010) demonstrated that aqueous Ra concentrations can be controlled by a  $\text{Ra}_x\text{Ba}_{1-x}\text{SO}_4$  solid solution at concentrations several orders of magnitude below the Ra solubility with respect to a pure  $\text{RaSO}_4$ . It is also demonstrated that the equilibration between aqueous  $\text{Ra}^{2+}$  and barite involves the replacement of a substantial fraction of the initial barite and proceeds significantly beyond pure surface adsorption processes. Hence, there is strong evidence supporting influence of barite on the mobility of Ra.

It can be noted that Sr and Ca also may coprecipitate with barite, but they are not expected to be incorporated to the same degree as Ra. See Grandia et al. (2008) for a more detailed of the (Ba,Sr)  $\text{SO}_4$  system. Moreover, since barite does not occur in very high amounts relative to Sr and Ca, it is not believed to affect the  $K_d$  values for these elements. Hence, coprecipitation of Sr and Ca with barite was not considered in the modelling.

### 2.3.2 Coprecipitation with calcite and aragonite

Initially, only barite was considered in this project and therefore only the effects of barite have been taken into account in the modelling. However, if calcite, and particularly aragonite, also are present in significant amounts, that does not only affect Ca, but also Sr, Ba and Ra by coprecipitation. Furthermore, it is not clear how the coprecipitation of Ra with barite is affected by other cations such as Sr. The affinity of Ra for calcite and aragonite is expected to be lower than for barite, but on the other hand calcite and aragonite commonly occur in much higher amounts. Elevated Ra activities have been shown in fresh calcite (Fairclough et al. 2006). Based on the thermodynamic estimates of Langmuir and Riese (1985) the distribution coefficient for Ra in calcite would be 0.82. Measurements from an area with rapid calcite precipitation in the French Massif Central have indicated that the distribution coefficient would be 0.4 (Sverjensky and Molling 1992). Further measurements in the French Massif Central show that the apparent calcite-water partition coefficients for Ra, Ba and uranium vary during precipitation, showing a general decrease as precipitation proceeds (Rihs et al. 2000). The apparent partition coefficient for Ra varies from 0.80 to 0.47 in the samples of water and calcite layers downstream from thermal springs. Rihs et al. (2000) argue that these apparent coefficients are much higher than equilibrium values, possibly due to the high precipitation rates. However, there are also measurements by Gnanapragasam and Lewis (1995) suggesting that the distribution coefficient would be as low as 0.013. Yoshida et al. (2008) present homogeneous partition coefficients determined from coprecipitation experiments of Ra in calcite of  $0.15 \pm 0.06$ . These results were derived at slow precipitation rates in solutions that were oversaturated with respect to calcite. It is noticeable that the partition coefficient for Ra is an order of magnitude larger than for Ba in calcite ( $0.016 \pm 0.011$ ). Curti (1999), finally, suggests that the partition coefficients for Ra in calcite are in the range 0.003–0.053. Hence, there is a considerable variation. However, given the high calcite concentrations in some samples, it is possible that the  $K_d$  for Ra also would be affected by calcite and aragonite.

On the other hand, Ra is probably not the element that would be most affected by calcite, since Sr has an ionic radius that fits much better into the calcite and, particularly, the aragonite crystals. Tang et al. (2007) presented a partition coefficient of 0.1 for Sr in calcite, and Curti (1999) proposed that the partition coefficient is in the range 0.02–0.4. These values are considerably higher than most presented values for Ra. Dietzel et al. (2004) presented partition coefficients for Sr in aragonite of 1.3. If the  $K_d$  values for Ca are affected by calcite and aragonite precipitation, it would be necessary to have a substantial coprecipitation of Sr in order to explain the correlation between the  $K_d$  values for Ca and Sr respectively.

### 2.3.3 Coprecipitation with other minerals

Ra may also coprecipitate with other minerals, although the distribution factor varies considerably. For instance, the distribution coefficient for Ra into celestite is 280, so the presence of celestite would strongly affect the transport of Ra (Langmuir and Riese 1985). Acantharian skeletons (a type of plankton) are made of celestite, but acantharia are thought to be scarce in cold and temperate sea water (Caron and Swanberg 1990). Precipitation of celestite has also been observed in deep-sea carbonate sediments, where it forms a solid solution with barite (4.3–7.8 mole %  $\text{BaSO}_4$ ) (Baker and Bloomer 1988). It can also be noted that anglesite ( $\text{PbSO}_4$ ) is isomorphic with barite so  $\text{Pb}^{2+}$  may also easily coprecipitate with barite. Conversely, Ra and Ba may also coprecipitate with anglesite. The mineral hokutolite is a solid solution of  $\text{BaSO}_4$  and  $\text{PbSO}_4$ , which has been encountered in thermal springs. It is known to contain fair amounts of Ra (Lin et al. 2012). Ra has also been observed to show signs of phase formation, presumably coprecipitation, in the presence of rhodochrosite ( $\text{MnCO}_3$ ), dolomite ( $\text{CaMg}(\text{CO}_3)_2$ ) and witherite ( $\text{BaCO}_3$ ). However, together with other carbonate minerals such as siderite ( $\text{FeCO}_3$ ), ankerite ( $\text{Ca}(\text{Fe},\text{Mg},\text{Mn})(\text{CO}_3)_2$ ) and magnesite ( $\text{MgCO}_3$ ) Ra seems to be retained by a simple sorption process (Jones et al. 2011).

## 2.4 Marine biogeochemistry of Ba and Ra

### 2.4.1 Precipitation of barite in marine environments

It is a well-established fact that barite is formed in seawater and present in marine sediments (e.g. Church and Wolgemuth 1972, Dehairs et al. 1980, Bishop 1988, Monnin et al. 1999, Gonneea and Paytan 2006, van Beek et al. 2009). The formation of barite in seawater has attracted considerable interest due its many applications, e.g. tracing fluxes of particulate organic carbon (POC), estimating historical oceanic productivity and dating marine sediments (Pierret et al. 2012, Dymond et al. 1992, Paytan et al. 1996, Tribovillard et al. 2006 and references therein). Due to the similarity between Ra and Ba, Ra isotopes have also been used to study the behaviour of marine barite (Bishop 1988). It has been suggested that marine barite has the potential to record seawater Sr isotopic compositions or rare earth element patterns (Church and Wolgemuth 1972).

Analyses indicate that marine barite constitutes 50–100% of the total nondetrital, solid-phase Ba both in the water column and in pelagic sediments (Pierret et al. 2012, Dymond et al. 1992, Gingele and Dahmke 1994, Bishop 1988, Church and Wolgemuth 1972 and references therein). Dehairs et al. (1980) argued that the Ba in the water column is mostly recycled and that the marine Ba cycle is dominated by the precipitation of dissolved Ba as barite within the upper water column. This is followed by a partial remobilization in the sediments (McManus et al. 1994).

The behaviour of Ba and other trace elements in anoxic sediments of the Achterwasser, a shallow lagoon in the southeast Baltic Sea, was investigated by Scholz and Neumann (2007). The authors argue that the Ba distribution is controlled by reductive dissolution of authigenic barite in the sulfate reduction zone, coupled with upward diffusion and re-precipitation. They used PHREEQC to calculate saturation indices from the chemical analysis of 50 cm cores of the sediment. The measurements indicated that Ba starts to accumulate in pore water at 13 cm depth, which coincides with the depth where sulphate reduction becomes significant. Calculations of saturation indices indicate that barite remain close to equilibrium down to 25 cm depth, which in turn, coincides with maximum measured concentrations of dissolved Ba in pore water. At 25 cm depth the cores become undersaturated with respect to barite.

Yet, the mechanisms for barite precipitation in the world's oceans remains poorly understood. A fundamental paradox is that most of the world's seawater does not appear to be saturated with respect to barite. Calculations by Monnin and Cividini (2006) on 1,400 seawater samples from all over the world have shown that only about 25% of the samples were saturated or supersaturated with respect to barite. Some examples where saturation is reached are places such as surface waters of the Southern Ocean, deep waters of the Bay of Bengal and intermediate waters of the Pacific (Monnin et al. 1999). Nevertheless, it is clear that barite is present in the water column even at places where the waters seem to be undersaturated with respect to barite and that the barite – at least partly – must be precipitated *in situ* (Monnin and Cividini 2006). One explanation might be that the thermodynamic models are not sufficiently accurate to capture all aspects of barite saturation and precipitation. However, it has also been suggested that barite could be formed in microenvironments that are supersaturated with respect to barite. Such microenvironments could for instance arise from the decomposition of organic matter (Paytan et al. 2002, van Beek et al. 2009). Paytan et al. (2002) also argue that barite can precipitate from supersaturated pore fluids at the oxic-anoxic boundary within marine sediments and where Ba-rich pore fluids are expelled and come into contact with sulphate-rich seawater or from hydrothermal solutions. It has also been shown that acantharian skeletons, which are made up of Ba-enriched celestite (a Ba/Sr molar ratio of approximately 0.003), can contribute to precipitation of barite (Bernstein and Byrne 2004). Furthermore, it has been shown that some organisms are able to form barite within their cells (Gooday and Nott 1982). van Beek and Reyss (2001) argue that the most important factors for controlling Ba and Ra in the world's oceans are biological uptake by substitution of Ca in calcareous skeletons and precipitation of barite (and coprecipitation of Ra). Laboratory experiments have also indicated that bacteria may play a crucial role in mediating the precipitation of barite in seawater (Gonzalez-Muñoz et al. 2012).

Barite has been found at considerable depths in reducing sediments from the Baltic Sea (Böttcher and Lepland 2000). A long (> 4 m) core was sampled from the Landsort Deep between Gotland and Småland. At two depths, one corresponding to the Ancyclus Lake and the other to the Yoldia Sea, authigenic barite was observed coexisting with iron monosulphides. Hence, even if the sediment are sulphate-reducing, precipitation of sulphides does not necessarily imply that barite cannot be present too. On the other hand, it is of course possible that the dissolution of barite in other environments could be faster than in the investigated cores. The Ba concentrations in these samples (1,900 and 1,070 ppm respectively) were significantly higher than in the marine sediments that have been sampled in Forsmark and Simpevarp. Outside the areas of anomalous Ba concentration the concentrations ranged from 128 to 432 ppm. The authors speculate whether barite could have been accumulated as a result of sulphur diffusing downwards from brackish water sediments and Ba being desorbed from freshwater sediments as a result of co-diffusing cations. Although the concentrations of Ba in Forsmark and Simpevarp are considerably lower than in the core investigated by Böttcher and Lepland (2000), this does not imply that barite cannot be present. It is important to realise that the mechanisms for barite accumulation in sediments are different from the formation of sulphides in reducing sediments. In strongly reducing environments, sulphide will continuously be produced by reduction of sulphate, which is the dominating sulphur species in oxic seawater and occur in high concentrations. Since the solubility of sulphides is low, sulphide minerals may be formed, which will keep the sulphide concentration in the pore water at relatively low levels. In this manner, there will be a continuous accumulation in the sediments as long as there is sulphate left that can be reduced and some metal ions in sufficiently high concentrations to cause precipitation. However, since the reduction of sulphate will lower the concentration of sulphur and the precipitation will lower the concentrations of iron, lead and other metals that may precipitate with sulphide, there can be a diffusion of more sulphate, iron and other elements from more oxic seawater, where the concentration of such substances is higher. Therefore, there may be a considerable accumulation of sulphides if the conditions are favourable. Barite, on the other hand, is not dependent on the production of some substance in the sediments. Instead, seawater appears to be close to saturation with respect to barite and barite may just as well be produced in the water column as in the sediments. Hence, the processes governing the accumulation of barite in sediments is fundamentally different from those governing the accumulation of sulphides, and low amounts of Ba in the sediments are not necessarily an indication that barite is not present.

## 2.4.2 Ra biogeochemistry in marine environments

Because Ra easily coprecipitates with barite, it is believed that the marine biogeochemistry of Ra is strongly influenced by the presence of barite in seawater. van Beek and Reyss (2001) isolated barite from marine sediments and measured its content of  $^{226}\text{Ra}$  and its immediate parent  $^{230}\text{Th}$ . Their procedure for chemical separation of barite appears to have been successful, yielding barite concentrations that in most cases exceed 95%. The  $^{226}\text{Ra}$  activity of the barite decreased with depth due to radioactive decay, but in fresh barite activities close to  $20,000 \text{ Bq kg}^{-1}$  were detected. The  $^{230}\text{Th}$  activities were not in secular equilibrium with  $^{226}\text{Ra}$  in any of the samples so the measurements confirm that Ra indeed has a strong affinity for marine barite.

Similar results have been presented by Paytan et al. (1996). They found that the  $^{226}\text{Ra}$  activity in recently formed marine barite, separated from two equatorial Pacific sediment cores, exceeds that of its parent  $^{230}\text{Th}$  by at least an order of magnitude, indicating Ra uptake during barite precipitation. Furthermore, Paytan et al. (1996) suggest that  $^{226}\text{Ra}$  activity in marine barite could be used to determine sedimentation rates. In sediments, the  $^{226}\text{Ra}$  activities decrease exponentially with depth, implying that little exchange of Ra between the barite crystal and the pore water occurs after burial. Thus, Paytan et al. (1996) argue that barite behaves as a closed system below the sediment mixing layer. This would indicate that old barite would have a limited effect on the  $K_d$  for Ra. Probably, the reason is that it is hard for Ra ions to diffuse through the barite crystal. On the other hand, Bosbach et al. (2010) demonstrated that the Ra incorporation in barite proceeds beyond pure surface adsorption so the situation is not entirely clear concerning this matter. Possibly, the differences are related to the extent to which recrystallisation of the barite crystals takes place.

Our main conclusions regarding the marine biogeochemistry of Ba and Ra are:

- Barite is ubiquitous in marine environments. As much as 50–100% of the non-detrital, solid-phase Ba in marine environments can be expected to be barite.
- The mechanism behind the formation of barite is not fully understood, but it seems that biologically mediated precipitation of barite may occur even in places where the seawater is not saturated with respect to barite.
- Ra has a strong affinity for marine barite and its biogeochemistry in marine environments is strongly influenced by the presence of barite. The effect is particularly obvious as the barite is formed, whereas the interaction between Ra and old barite is more complex.

## 3 Material and methods

### 3.1 Thermodynamic modelling in Visual MINTEQ 3.0

Thermodynamic modelling in the chemical equilibrium programme Visual MINTEQ 3.0 was used to calculate saturation indices and investigate the possibility for different minerals containing alkaline earth metals to precipitate (Gustafsson 2012). The theory behind solubility products and saturation indices is given in Appendix B. Visual MINTEQ 3.0 was used for all water samples from the monitoring programme in SKB's site investigation areas. In Visual MINTEQ 3.0 the default parameters from the inherent MINTEQ database were used without exception. Some of the most important thermodynamic constants are summarised in Section 3.3.

### 3.2 Thermodynamic modelling in PHREEQC

The software used in the modelling of coprecipitation was PHREEQC for Windows version 2. The main reason for choosing PHREEQC for this task is that PHREEQC can be used to model solid solutions. One of the databases included in PHREEQC, wateq4f.dat, was used in the modelling.

#### 3.2.1 Modelling of solid solutions in PHREEQC

PHREEQC is capable of handling both ideal and non-ideal solid solutions. It may also be used for multicomponent solid solutions, i.e. more than two components, but then it is limited to ideal solid solutions only. For non-ideal solid solutions PHREEQC uses a Guggenheim approach (as described in Appendix C. Basic theory of solid solutions) for calculating the activities of the components.

Both the similar ionic radii of Ba and Ra and the similar solubility products for  $\text{RaSO}_4$  and  $\text{BaSO}_4$ , respectively, would suggest that the solid solution would be nearly ideal. This was for instance assumed by Grandia et al. (2008). However, recent experiments by Curti et al. (2010) indicate that there may be some degree of non-ideality in  $\text{RaSO}_4$ - $\text{BaSO}_4$  solid solutions. This is also supported by the observations of Bosbach et al. (2010). Based on these recent results the  $\text{RaSO}_4$ - $\text{BaSO}_4$  solid solution was treated as a regular solid solution, i.e. with a non-zero first Guggenheim parameter and all the following Guggenheim parameters being zero. Based on the experiments of Curti et al. (2010) and Bosbach et al. (2010) the first Guggenheim parameter was set to 1.5. The effects of varying this value are discussed in Section 5.3. However, since the Ra/Ba ratios under all realistic assumptions will be very low in the Forsmark and Simpevarp areas, the possible existence of a miscibility gap in the  $\text{RaSO}_4$ - $\text{BaSO}_4$  solid solution should have no practical implications and the effects of non-ideality should be small.

#### 3.2.2 Kinetics of Ra coprecipitation with barite

There are a few studies that have investigated the kinetics of Ra coprecipitation with barite. Bosbach et al. (2010) studied the uptake of Ra by barite for a period of 435 days. After this time the solid solution was not yet in equilibrium with the aqueous phase, but it could not be concluded whether this was due to slow kinetics or the fact that parts of the barite crystals may not be available so that equilibrium will not be reached for the system as a whole. However, observations by Curti et al. (2010) indicate that Ra rapidly may form solid solutions with barite. They also showed that the resulting solid solution will be in thermodynamic equilibrium with the aqueous solution. Hence, the situation regarding the kinetics of Ra coprecipitation and recrystallisation with barite is still unclear. Therefore, no kinetic reactions have been considered in the modelling. If the reactions proceed rapidly, as Curti et al. (2010) suggest, this should not be a problem. If the reactions, on the other hand, proceed more slowly, as Bosbach et al. (2010) suggests, it might possibly be of some importance when modelling the transport of Ra, depending on the flow velocity of the groundwater. However, since there is clear evidence that there is a considerable uptake of Ra in both experiments, assuming no kinetic effects should be a fair approximation in any case.

### 3.2.3 Modelling of $K_d$ values for Ra in the presence of barite

PHREEQC was used to model  $K_d$  values for Ra in the presence of barite, assuming coprecipitation of Ra with barite. PHREEQC is a process-based model working with chemical equilibria, which is fundamentally different from the linear  $K_d$  model that is used in SKB's safety analyses. As a consequence, there is no way to strictly implement a linear  $K_d$  model in PHREEQC. However, by specifying an imaginary surface with a very large number of binding sites it is possible to make the model behave linearly as long as the soil chemistry stays within reasonable limits.

It is obvious that this approach is not realistic in the sense that the number of binding sites in the model actually should represent the reality. Therefore, it is not expected that the model would produce reliable results if the water chemistry changed too much. However, in the case of Ra the concentrations will under all circumstances be so low that it seems unreasonable that it would affect the sorption properties of the soils appreciably. This does not imply that the sorption behaviour of Ra is not affected by, for instance, increased competition by Ca ions. Moreover, the objective of this modelling has been to elucidate the effects of barite on the  $K_d$  of Ra. Therefore, a semi-linear adsorption model for Ra was implemented in order to mimic the  $K_d$  approach used in SKB's safety models.

The  $K_d$  value for the linear sorption model was assumed to be equal to the measured  $K_d$  value for Sr in each sample, assuming that Ra would behave as Sr in the absence of barite. Hence, the  $K_d$  value for Ra was initially equal to the determined  $K_d$  value for Sr. Based on the measured Ba concentrations in the solid phase, the maximum amount of barite that could be present in each sample was calculated. The pore water was then saturated with respect to barite (so that the added barite would not dissolve), and barite was added to the model stepwise until the amount of barite in the model equalled the maximum amount of barite that could be present in the sample based on the observed concentrations of Ba. For each step, the  $K_d$  value for Ra was calculated by adding the effects of the linear sorption model and the barite, yielding the  $K_d$  for Ra as a function of the amount of barite.

The effects of organic carbon have been neglected in this model because there are no known thermodynamic parameters describing the affinity of Ra for organic matter. However, if the affinity of Ra for organic matter is assumed to be similar to that of Ba, the effects of neglecting organic carbon should even out because the coprecipitation into barite is governed by the Ra/Ba free ion ratio in the pore water.

## 3.3 Thermodynamical constants

The most important thermodynamic constants used in the modelling in Visual MINTEQ and PHREEQC are given in Table 3-1. In most cases, the constants from the Visual MINTEQ database have been used, but since Ra is not included in these databases, thermodynamic constants were selected from the scientific literature (see references below).

## 3.4 Data used in the modelling

The hydrochemical data presented in this report derive from four different datasets: (1) hydrochemical data from the site investigations, (2) sediment  $K_d$  data, (3) 2009  $K_d$  data and (4) 2011  $K_d$  data. The first set comprises 401 samples from lakes, streams, seawater and near-surface groundwater in the site investigations in Forsmark and Simpevarp. These samples were selected from SKB's database based on the criterion that all necessary parameters for the modelling had been analysed. These samples will henceforth be referred to as the site investigation data. The second dataset comprises pore water from 16 lake and marine sediments samples (Tröjbom et al. 2007, 2008, Engdahl et al. 2008). These samples will be referred to as the sediment  $K_d$  data. The third and fourth datasets comprise pore water from 57 soil and wetland samples, where  $K_d$  measurements have been made. The third dataset comprises seven samples from Forsmark and Simpevarp, and will be referred to as the 2009  $K_d$  data based on the report, in which they are presented (Sheppard et al. 2009). The fourth dataset comprises 50 pore water samples from soils and wetlands. These measurements were presented by Sheppard et al. (2011) and will therefore be referred to as the 2011  $K_d$  data. Since there are differences in how the measurements were conducted and which parameters that were analysed, the four datasets were partly treated differently in the modelling.



**Table 3-1. Compilation of thermodynamical constants used in the simulations.**

	log $K_s$	$\Delta H^\circ$ (kJ/mol)	Reference
<b>Solid phases</b>			
Barite (BaSO <sub>4</sub> )	-9.98	23	Smith et al. 2003
Celestite (SrSO <sub>4</sub> )	-6.62	2.0	Smith et al. 2003
Gypsum (CaSO <sub>4</sub> ·2H <sub>2</sub> O)	-4.61	1.0	Smith et al. 2003
Witherite (BaCO <sub>3</sub> )	-8.57	2.0	Smith et al. 2003
Calcite (CaCO <sub>3</sub> )	-8.48	-8.0	Plummer and Busenberg 1982
Aragonite (CaCO <sub>3</sub> )	-8.34	-8.0	Plummer and Busenberg 1982
Strontianite (SrCO <sub>3</sub> )	-9.27	-1.0	
RaCO <sub>3</sub>	-8.30	-9.6	Langmuir and Riese 1985
RaSO <sub>4</sub>	-10.38 <sup>a</sup>	-39 <sup>b</sup>	<sup>a</sup> Zhu 2004a and references therein <sup>b</sup> Langmuir and Riese 1985
<b>Solution species</b>			
RaSO <sub>4</sub> (aq)	2.75	5.40	Langmuir and Riese 1985
RaCO <sub>3</sub> (aq)	2.50	4.50	Langmuir and Riese 1985
RaOH <sup>+</sup>	0.50	4.60	Langmuir and Riese 1985
RaCl <sup>+</sup>	-0.10	2.10	Langmuir and Riese 1985

### 3.4.1 Dataset 1: Site investigation data

243 out of the 401 water samples included in this study were taken from the Forsmark area and the remaining 158 samples were taken from the Simpevarp area. There are 33 near surface ground water samples representing five different sites in Forsmark. The lake samples included in the study comprise 102 observations representing eight lake sites in Forsmark and 28 samples taken at one lake site in Simpevarp. The dataset includes 47 stream water samples representing eight sites in Forsmark and 70 samples representing 12 sites in Simpevarp. The dataset also includes 61 marine samples representing six sites in Forsmark and 60 marine samples representing five sites in Simpevarp (Tröjbom et al. 2007, 2008).

#### **Saturation indices modelling for site investigation samples**

Saturation indexes for barite (BaSO<sub>4</sub>), celestite (SrSO<sub>4</sub>), gypsum (CaSO<sub>4</sub>·2H<sub>2</sub>O), witherite (BaCO<sub>3</sub>), calcite (CaCO<sub>3</sub>) and strontianite (SrCO<sub>3</sub>) have been modelled in Visual MINTEQ 3.0. All major ions were included in the model plus a number of trace elements: Al, Ba, Br, Ca, Cl, F, Fe, I, K, Mg, Na and Sr. In addition, measurements of CO<sub>3</sub>, NO<sub>3</sub>, PO<sub>4</sub>, SO<sub>4</sub>, DOC and pH were added to the model. Si was added as silicic acid. The temperature was set to 10°C. All ions were allowed to equilibrate with respect to the measured pH. DOC was modelled using the Stockholm Humic Model (SHM) (Gustafsson 2012).

### 3.4.2 Dataset 2: Sediment K<sub>d</sub> data

The 16 sediment K<sub>d</sub> samples were taken at four sites in Forsmark and four sites in Simpevarp (Table 3-2). At each site samples from two different depths have been analysed. Three of the eight sites are marine sites, while the remaining five sites are located in lakes. See Table 3-2 for an overview of the sediment samples used to measure the K<sub>d</sub>. A thorough description of the samples and sampling procedure is given by Engdahl et al. (2008). In order to separate samples from the same site the depth has been added to the ID code. For instance, PFM000074 2530 should be understood as site PFM000074, depth 25–30 cm. Figures displaying the relationships between the K<sub>d</sub> values are shown in Appendix A. Measured K<sub>d</sub> values.

**Table 3-2. Overview of the sediment  $K_d$  samples. Two samples at different depths were collected at each site.**

ID code	Type	Site	Depth 1 [cm]	Depth 2 [cm]
PFM000074	Lake	Forsmark	0–5	25–30
PFM000107	Lake	Forsmark	0–5	25–31
PFM000117	Lake	Forsmark	0–5	25–32
PSM002065	Lake	Simpevarp	0–5	20–25
PSM002067	Lake	Simpevarp	0–5	15–20
PFM000063	Marine	Forsmark	0–5	20–25
PSM002064	Marine	Simpevarp	0–5	25–30
PSM007090	Marine	Simpevarp	0–5	25–30

Both the sediments and the pore water of the sediment sampling were analysed with respect to trace elements using AFS, ICP-AES and ICP-SFMS. For the analyses of Ba in the sediments, a microwave-assisted digestion with a nitric/hydrochloric/hydrofluoric acid mixture was used. Ca and Sr was analysed after  $\text{LiBO}_2$  fusion. A detailed description of the analysis procedure is given by Engdahl et al. (2008). These techniques imply that the concentrations in the solid phase should correspond to the total concentration, which is important to keep in mind when comparing  $K_d$  values.

#### **Saturation indices modelling of sediment $K_d$ samples**

The saturation indices for the alkaline earth sulphate (barite, celestite and gypsum) and carbonate (calcite, aragonite, strontianite and witherite) minerals were modelled for the sediment samples using Visual MINTEQ 3.0.

All major ions were included in the model, plus a number of selected trace elements: Al, Ba, Br, Ca, Cl, F, Fe, I, K, Mg, Na, Sr and U. In addition, C, N, P, S, Si and pH were added to the model. It was assumed that inorganic C was present as carbonate, that all N was present as nitrate, all P as phosphate and Si as silicic acid. All detected sulphur in the samples was assumed to exist as sulphate (this assumption is discussed in Section 4.4.). All ions were allowed to equilibrate with respect to pH. DOC was modelled using the Stockholm Humic Model (SHM) using the SHMgeneric08 database. The measured TOC levels were assumed to represent DOC. The temperature was kept at  $10^\circ\text{C}$  and pH was assumed to be 8 in all samples, based on earlier groundwater measurements from the Forsmark and Simpevarp areas.

#### **Coprecipitation modelling of sediment $K_d$ samples**

Input data in the coprecipitation modelling in PHREEQC was pH, temperature, Al, Ba, Ca, Cl,  $\text{HCO}_3$ , Fe, K, Mg, Mn, N, Na, Pb, Ra, S, Si, Sr and U. Temperature was set to  $10^\circ\text{C}$ . It was assumed that inorganic C was present as carbonate. All N was assumed to be present as nitrate and all S was assumed to be present as sulphate. See Section 4.4 for a discussion of the speciation of sulphur.

Concentrations of Ra in the sediment  $K_d$  samples have been set to mean values of previous measurements at the sites. In two sites, PSM002067 and PSM007090, no measurements of Ra concentration are available. In these cases a mean value of the Ra measurements at the  $K_d$  sites included in this study were used ( $1.9 \cdot 10^{-14}$  M). Although there are some uncertainties regarding the true Ra concentrations in the samples, it is not believed to affect the general behaviour of Ra, since the concentrations under all circumstances must be very low.

#### **Modelling aqueous Ra speciation in the sediment $K_d$ samples**

The calculation of the aqueous speciation of Ra was made in PHREEQC using the constants presented in Table 3-1. However, no thermodynamic constants for the binding of Ra to organic matter are available. Therefore, it was assumed that the affinity for DOC was the same as for Ra as for Ba. Judging from the observed  $K_d$  values in the wetland samples this may possibly lead to an underestimation of the association of Ra with DOC, since these measurements indicate that Ra may have a slightly higher affinity than Ba for organic matter (Sheppard et al. 2011).

### 3.4.3 Dataset 3: 2009 $K_d$ data

The 2009  $K_d$  samples represent water from seven soils where  $K_d$  values for Ba, Ca and Sr have been determined. An overview of the samples can be found in Table 3-3. Description of the 2009  $K_d$  samples used in this study and further details are presented by Sheppard et al. (2009). Four of the sites are located in Simpevarp, and three sites are located in Forsmark. In this dataset there are 2–6 duplicates for each site. A mean value for each site has been used in the  $K_d$  calculations and the thermodynamic modelling. Figures illustrating the relationships between the  $K_d$  values in this dataset are shown in Appendix A. Measured  $K_d$  values.

The 2009  $K_d$  samples in dataset 3 were centrifuged to separate the pore water from the soil. The pore water was then filtered through a 0.45- $\mu\text{m}$  syringe filter and acidified to  $\text{pH} < 2$  for ICP-MS analyses. The centrifuged soil was also analysed by ICP-MS. The extraction method used was partial extraction with aqua regia. Consequently, the observed concentrations do not correspond to total concentrations in the solid phase. The methods for analyses of elements in the soil samples are further described and discussed by Sheppard et al. (2009).

The 2009  $K_d$  samples lack some of the chemical parameters, which are important for the ion balance and, therefore, for the modelling, e.g. DOC, S and  $\text{CO}_3$ . For calculating the saturation indices for carbonate minerals the  $\text{CO}_3$  is absolutely crucial so no reliable estimation could be made in these cases. Likewise, sulphate is crucial for the sulphate minerals, and since S was not measured it is not possible to make any reliable estimation of the sulphate concentrations in the analysed samples. Hence, the saturation indices for the sulphate minerals are impossible to calculate as well. As a result, no saturation indices are presented for this dataset.

Contrary to the sediment samples, the 2009  $K_d$  samples have higher  $K_d$  values for Ca and Sr than for Ba. As discussed in Section 6.4.1, we believe that this is due to some problem with the measurement of Ba in the pore water. Therefore, no simulation of the coprecipitation of Ra with barite was made for this dataset.

### 3.4.4 Dataset 4: 2011 $K_d$ data

The fourth dataset includes 50 soil samples from agricultural land and wetlands, for which  $K_d$  values have been determined for 69 elements, including Ba, Ca, Ra, Sr and U. The samples represent the five major types of Quaternary deposits, which can be used for agriculture: clay till, glacial clay, clay gyttja, cultivated peat and wetland peat. Each site was sampled at two different depths: 0.2 m and 0.5 m.

Elemental analyses of elements in the pore water were carried out using ICP-SFMS. Recovery of  $^{226}\text{Ra}$  was tested using CRM IAEA-428 and CRM IAEA-430 and was found to be in the range of 92–97 percent. Solid samples were analysed following digestion by aqua regia leaching of 0.5 g solid for two hours in a heating block held at  $90^\circ\text{C}$ . Leachates were diluted and analysed by ICP-SFMS. The methods for sampling and analyses are described in detail in by Sheppard et al. (2011).

The 2011  $K_d$  samples were not analysed for DOC/TOC, carbonate and pH. Without accurate pH and carbonate concentrations it is not possible to make reliable calculations of the saturation with respect to carbonate minerals. Therefore, only the saturation indices for barite are presented for these samples.

**Table 3-3. Description of the 2009  $K_d$  samples used in this study. Note that the  $K_d$  values for Ba are questionable for reasons explained in Section 6.4.1.**

SITE	IDCODE	Min. depth (cm)	Max. depth (cm)	Soil type	$K_d$ Ba (l/kg)	$K_d$ Ca (l/kg)	$K_d$ Sr (l/kg)	$\text{CaCO}_3$ (% dw)
Forsmark	AFM001076	0.3	0.35	Clayey silty till	34	452	324	25
Forsmark	PFM006024	0.3	0.35	Peat	15	400	311	
Simpevarp	ASM001426	0.3	0.35	Sandy till	30	230	1,317	0.6
Simpevarp	ASM001434	0.3	0.35	Clay gyttja	22	39	62	0.3
Simpevarp	ASM001440	0.3	0.35	Peat	16	41	70	
Simpevarp	PSM000277	0.3	0.35	Clay gyttja	51	13	33	0.3
Forsmark	PFM002670	0.3	0.35	Clayey silty till	92	244	192	5.3

### **Saturation indices modelling for the 2011 $K_d$ samples**

Saturation indices for barite were modelled in Visual MINTEQ 3.0. The chemical species included in the calculations were: Al, Ba, Br, Ca, Cl, Fe, I, K, Mg, Na, Si, Sr and  $\text{SO}_4$ . The temperature was set to 10°C and an assumption of pH 8 was made for all samples. Si was included assuming that all Si was present as silicic acid.

The saturation index of barite is not expected to change much with pH. (See Section 4.3 for a discussion of the variation of the solubility for alkaline earth sulphates and carbonates with pH.) Since DOC was not analysed in the pore water, the amount of Ba bound to DOC could not be assessed. This is probably most problematic in the peat samples, where high concentrations of DOC should be expected. Based on the modelling of the Ba speciation at other sites in the Forsmark area it seems likely that up to 20% of the Ba could be bound to DOC. In that case, the saturation indices may have been exaggerated by up to 0.1 log units.

### **Coprecipitation modelling in the 2011 $K_d$ samples**

Coprecipitation of Ra with barite was calculated using the modelling program PHREEQC. Input data for these calculations was pH, temperature, Al, Ba, Ca, Cl, Fe, K, Mg, Mn, Na, Pb, Ra, S, Si, Sr and U. Temperature was set to 10°C. No analyses of pH were made on the pore water of the 2011  $K_d$  samples. Instead the pH in the soil (after water was added) was used in the PHREEQC calculations. The uncertainties in the pH values together with the fact that there are no data available on alkalinity and DOC makes these calculations more uncertain than the calculations using the site investigation data, but these uncertainties should not be large enough to disable an assessment of the barite saturation at the different sites.

When modelling the effect of barite on the  $K_d$  for Ra, it was assumed that  $K_d$  values for Ba under unsaturated conditions have the same correlation with  $K_d$  for Sr as for the wetland peat samples (Figure 6-6. Relationships between  $K_d$  for Ba and  $K_d$  for Sr in the five types of soils sampled. Based on the observations this seems to represent a minimum level for the Ba  $K_d$  value. Using this assumption and the observed concentrations of Ba in the pore water, the minimum amount of Ba in the solid phase *not* present as barite was estimated. This amount was subtracted from the total extracted concentration of Ba to determine the amount of labile barite, i.e. the maximum amount of barite that could have been dissolved in the aqua regia extraction. Note that the true content of barite in the saturated samples could be substantially higher, but since the total concentration of Ba in the solid phase was not determined, it is not possible to calculate the total potential amount of barite in each sample. Barite has a low solubility in aqua regia, but the possibility that barite has contributed to the observed concentrations of Ba in the solid phase cannot be excluded.

Based on the measurements of the peat samples the initial  $K_d$  value for Ra in unsaturated conditions was assumed to have the same correlation with  $K_d$  for Sr values as in the wetland peat samples (Figure 6-7). As for Ba, this represents an apparent minimum  $K_d$  value for Ra. In the subsequent modelling the pore was then saturated with respect to barite and the estimated maximum amount of barite was added in 20 steps. It is important to realize that the maximum amount of barite in this context does not refer to the total concentration of barite in the solid phase, but to the fraction that was dissolved by aqua regia.

## 4 Solubility of alkaline earth metals in Forsmark and Simpevarp

### 4.1 Saturation indices

Saturation indices for the most abundant sulphate and carbonate minerals of Ba, Sr and Ca were calculated and the complete results are found in Appendix D. Saturation indices. The saturation indices for gypsum, celestite, witherite and strontianite were in all samples well below saturation ( $< -1$ ). It is therefore concluded that the precipitation of these minerals is not likely to occur in either Forsmark or Simpevarp under the current conditions.

The results also show that many samples are saturated with respect to barite, aragonite and calcite. Figure 4-1 and Figure 4-7 show the saturation indices for barite and calcite, respectively. The saturation index for aragonite will always be 0.16 log units lower than the saturation index for calcite at 25°C because the precipitation/dissolution of aragonite involves the same species as calcite with the only exception that the solubility constant for aragonite is 0.16 log units lower than that of calcite. Whether calcite or aragonite will precipitate at a specific site is determined by local conditions. For instance, the precipitation of calcite is inhibited by high magnesium concentrations. If Mg/Ca exceeds 0.5, some of the  $\text{CaCO}_3$  could precipitate as aragonite instead. In seawater, for instance, where the Mg/Ca-ratio is roughly 2.5, all precipitating  $\text{CaCO}_3$  is expected to be aragonite (Tang et al. 2007).

In principle, saturation indices greater than zero indicate supersaturation, values below zero indicate undersaturation and values close to zero indicate equilibrium with a mineral phase. Theoretically, supersaturation should not be possible, but this kind of modelling is associated with some degree of uncertainty both due to uncertainties in the measured concentrations and uncertainties in the thermodynamic constants that are used. Moreover, natural soil/water systems may not always behave ideally. Therefore, samples with saturation indices between  $-0.5$  and  $0.5$  could be considered as close to equilibrium. This corresponds to an error of approximately a factor 3 in the measured concentrations and constants, which allows for some natural variation in the measured concentrations. Supersaturation with respect to barite within this range may not necessarily imply that barite must be precipitated, although the chances increase with higher saturation index. Likewise, a saturation index slightly below zero does not necessarily imply that barite cannot be present.

#### 4.1.1 Saturation indices in near surface ground water

Saturation indices have been calculated for five near surface ground waters in Forsmark. The results show that barite and calcite are in many cases close to saturation. Figure 4-1 shows the mean values of the calculated saturation indices for barite and calcite at the five modelled ground water sites. Maximum and minimum values are also included in the graph.

Figure 4-1 indicates that SFM0002, SFM0008, SFM0057 and, possibly, also SFM0005 are saturated with respect to both barite and calcite. These data are in agreement with sediment composition. All these samples are from sandy till sediments (Table 4-1), which contain high concentrations of  $\text{CaCO}_3$  ( $> 12.5\%$ ), except for SFM0057 where no information was available (Hedenström and Sohlenius 2008). According to these results calcite is likely to occur also at SFM0057.

Sample SFM0049, which represents clayey sandy till, should also contain significant amounts of  $\text{CaCO}_3$  (12%). With such high calcite concentrations in the solid phase, one would expect the pore water to be saturated, contrary to what the modelling suggests, but it could possibly be related to the low permeability of the clay or uncertainties in the pH measurements.

#### 4.1.2 Saturation indices in lakes

Most lakes in the Forsmark area are in equilibrium with calcite/aragonite (Figure 4-2). Among the investigated lakes, PFM102270 appears to be the only exception. In addition, the site in the Simpevarp area, PSM002065, is clearly not controlled by calcite. This is not surprising, since the calcite concentrations of the soils in Simpevarp tend to be lower than in Forsmark.

**Table 4-1. CaCO<sub>3</sub> concentrations and soil type in some of the near surface ground water sites (from Hedenström and Sohlenius 2008). No data were available for SFM0057.**

ID	Type	CaCO <sub>3</sub> (%)
SFM0002	Sandy till	12.5–17
SFM0005	Sandy till	25
SFM0008	Sandy till	19–31
SFM0049	Clayey sandy till	12

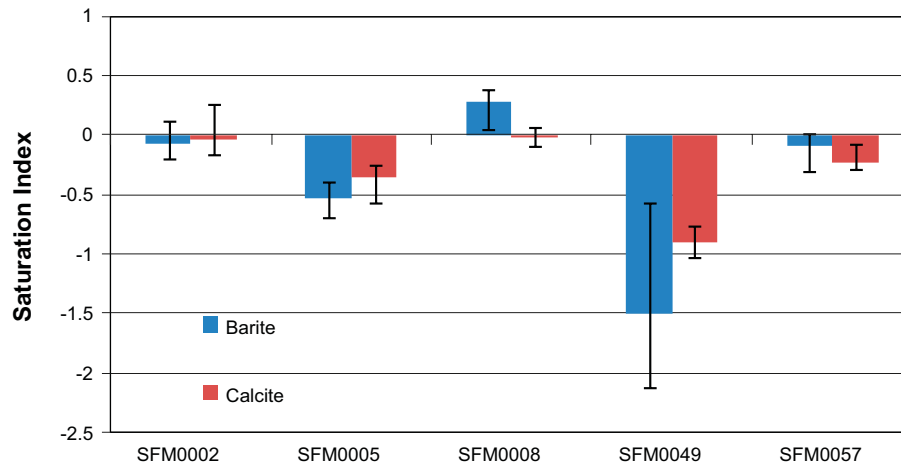


**Figure 4-1.** Modelled saturation indices for near surface ground waters at Forsmark. The bars represent the maximum and minimum modelled saturation indices at each site.

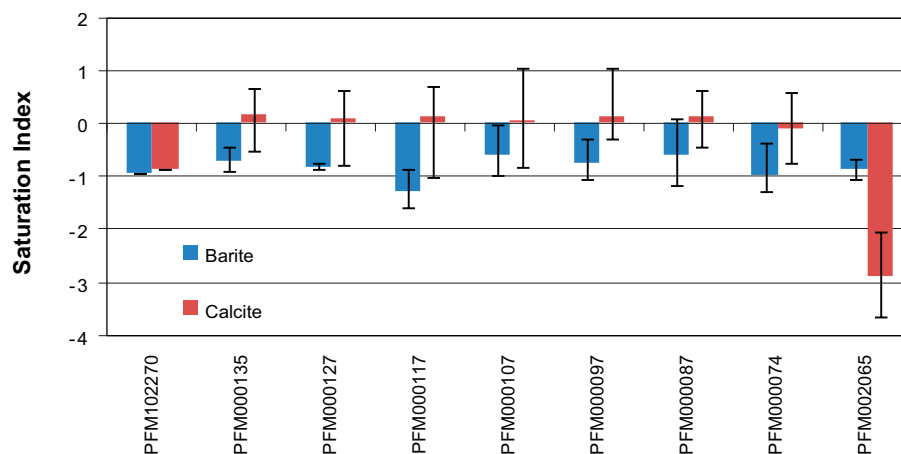


**Figure 4-2.** Modelled saturation indices in lake water. The bars represent the maximum and minimum modelled saturation indices at each site.

For barite the results are more ambiguous. The saturation indices are in most cases greater than -1 and may in some cases approach saturation (PFM000107) or even exceed saturation (PFM000087). The variation is considerable in some of the lakes, which could be related to inflow of various types of water during different time periods. This could indicate that barite is present in parts of the catchments. Sample PFM000107 is from Bolundsfjärden, which is known to be occasionally affected by inflow of seawater, since the lake was isolated from the Baltic Sea only recently. This would explain the large variations in this case, as seawater tends to have high saturation indices for barite – see Figure 4-5. Generally, it cannot be excluded that barite sometimes is present in some of the lakes.

For calcite there is also a large variation over time. However, this variation is easier to explain, since the carbonate concentrations in the lakes may vary considerably. The carbonate concentrations are not only affected by the inflow of water to the lake, but also by biological processes such as primary

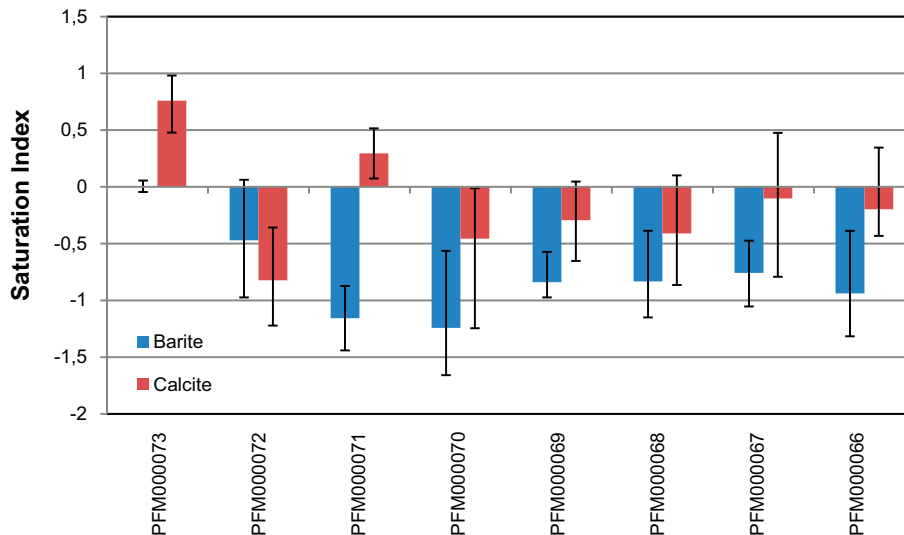


**Figure 4-3.** Modelled saturation indices for stream water sites in Forsmark. The bars represent the maximum and minimum modelled saturation indices at each site.

production, which consumes carbon dioxide, and decomposition of organic matter, which produces carbon dioxide. Moreover, in the wintertime, when the lakes are covered by ice, the exchange with the atmosphere is limited. In combination with decomposition, this may also lead to higher carbonate concentrations in the lake and, in turn, precipitation of calcite or aragonite depending on what the Mg/Ca-ratio is in each lake.

#### 4.1.3 Saturation indices in stream waters

Figure 4-3 shows that most of the streams in Forsmark are influenced by calcite, at least during parts of the year. This is expected given that soils in the Forsmark area often have high calcite concentrations. As for the lakes, variations may partly depend on varying groundwater sources or biologically induced changes in the carbonate concentrations.

The results for barite are also similar to observations for the lakes in Forsmark. Most streams appear to be undersaturated with respect to barite with saturation indices close to  $-0.5$  or slightly lower. However, at site PFM000073 all observations fall close to zero and indicate saturation with respect to barite. It is possible that this stream runs through barite bearing soils, supplying the stream with groundwater that is saturated with respect to barite. PFM000072 also shows saturation for some observations, which may indicate that parts of its catchment may contain significant amounts of barite.

Figure 4-4 indicates that calcite is not present to the same extent in the Simpevarp area as in the Forsmark area. This is consistent with what is known about the mineralogy of these two sites. Most of the monitored streams in the Simpevarp area have saturation indices that clearly indicate that these waters are not saturated with respect to calcite. PSM002085 could possibly be an exception from this pattern.

The results for barite are more variable. Some sites, such as PSM002072, are clearly not saturated with respect to barite, whereas others, e.g. PSM002085, PSM002086 and PSM002087, appear to be saturated. The results suggest that barite may be present in some of the soils in the Simpevarp area.

For both lakes and streams it is suggested that further spatial analyses are carried out to investigate whether the high saturation indices for barite and calcite in some samples can be linked to some specific type of Quaternary deposits in their respective catchments. Given that both Forsmark and Simpevarp are affected by land rise, it could, for instance, be hypothesised that areas with old marine sediments could contain barite. However, it is also possible that barite is present as a primary mineral in some of the Quaternary deposits. A similar approach could also be used for the groundwater samples.

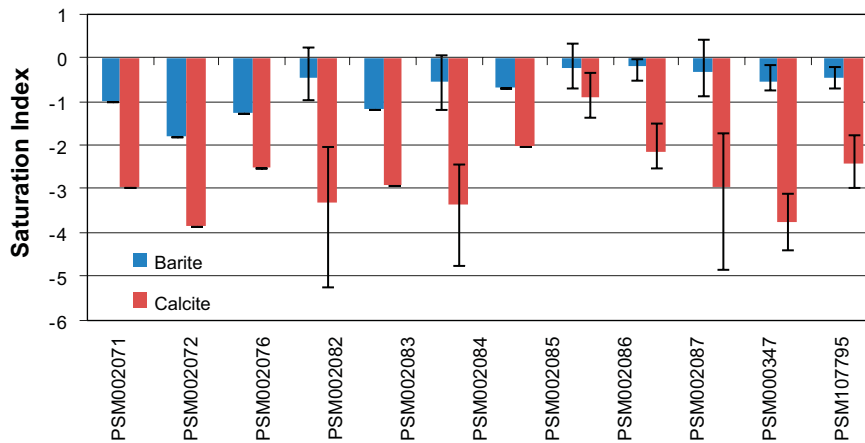


**Figure 4-4.** Modelled saturation indices for stream water sites in Simpevarp. The bars represent the maximum and minimum modelled saturation indices at each site.

#### 4.1.4 Saturation indices in marine waters

The calculated saturation indices for barite are close to zero in all marine samples, which indicates that barite probably is present in sediments from both Forsmark and Simpevarp. This is consistent with the scientific literature, where it is well-established that barite microcrystals are present both in seawater and in marine sediments – see Section 2.4.1. There are no obvious differences between Forsmark (Figure 4-5) and Simpevarp (Figure 4-6) in this respect, which is logical given that both areas border the Baltic Sea.

The saturation indices for calcite are, with a few exceptions, below zero with averages around  $-0.5$ . Again, there is a considerable variation between different samples from the same site, which is probably caused by the same processes that were discussed in the lakes – primary production, decomposition of organic matter etc. It is likely that saturation is reached during parts of the year at some of the sites. However, given the high Mg/Ca-ratios, it is predicted that aragonite rather than calcite will be precipitated. This is important because Sr, Ba and Ra will coprecipitate more easily with aragonite than with calcite. Since the ionic radius of Sr is closest to that of Ca, coprecipitation is expected to affect Sr the most.

The variation is also considerable at some of the sites in Simpevarp, most notably PSM002064 and PSM00797 (Figure 4-6). The possibility that aragonite is precipitated during certain periods cannot be excluded in any of the cases.

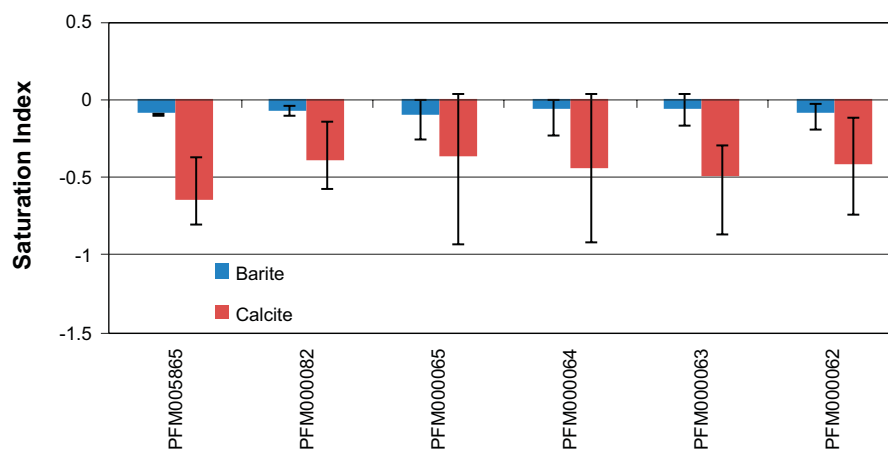


**Figure 4-5.** Modelled saturation indices for marine waters in Forsmark. The bars represent the maximum and minimum modelled saturation indices at each sampling site.



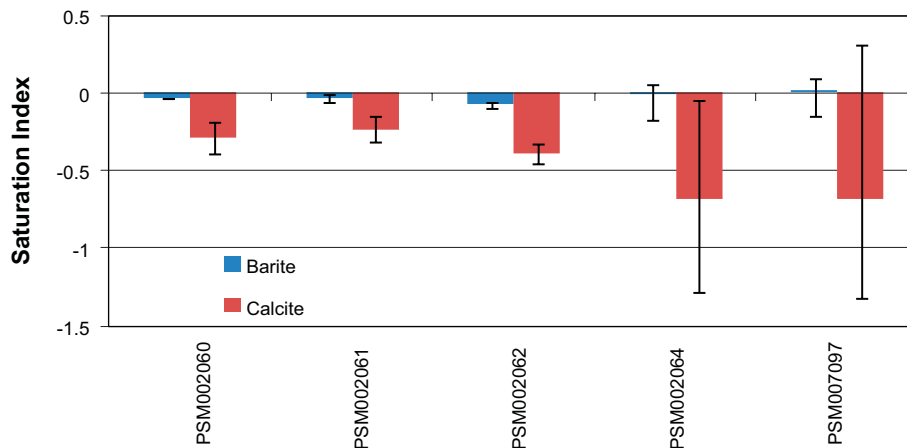


**Figure 4-6.** Saturation indices for marine waters in Simpevarp. The bars represent the maximum and minimum modelled saturation indices at each site.

#### 4.1.5 Saturation indices in the sediment $K_d$ samples

The saturation indices for barite and calcite for the sediment  $K_d$  samples are given in Figure 4-7. The results are also presented in Table 4-2 along with saturation indices for calcite and aragonite. For all modelled samples, the saturation indices with respect to barite are between  $-1$  and  $1$ . This indicates that barite should be present in many of the samples, above all in the marine sediments. Based on the saturation indices the presence of barite cannot be excluded at any of the sites, although the results are not conclusive at sites like PFM000074 and PFM000117. The indication that barite is present in the marine sediments is consistent with the scientific literature (Section 2.4.1.) and modeling of the sea water (Section 4.1.4).

It is worth noticing the considerable differences between the analysed depths at some of the sites. At all marine sites (PFM000063, PSM002064 and PSM007090), the saturation index for barite decreases with depth, which suggests that barite could be precipitated in the water column or near the sediment surface. However, it is possible that sulphate is being reduced further down in the sediments, which would lead to a decrease in the saturation index and, possibly, to dissolution of the barite. The same pattern is also valid for one of the lakes in Forsmark, namely Bolundsfjärden (PFM000107). This lake was isolated from the sea recently and still occasionally is affected by inflow of seawater. Theoretically, low saturation indices should lead to dissolution of the barite, but it does not necessarily imply that all barite is dissolved. Barite has been found deep in reducing sediments from the Baltic Sea (Böttcher and Lepland 2000).

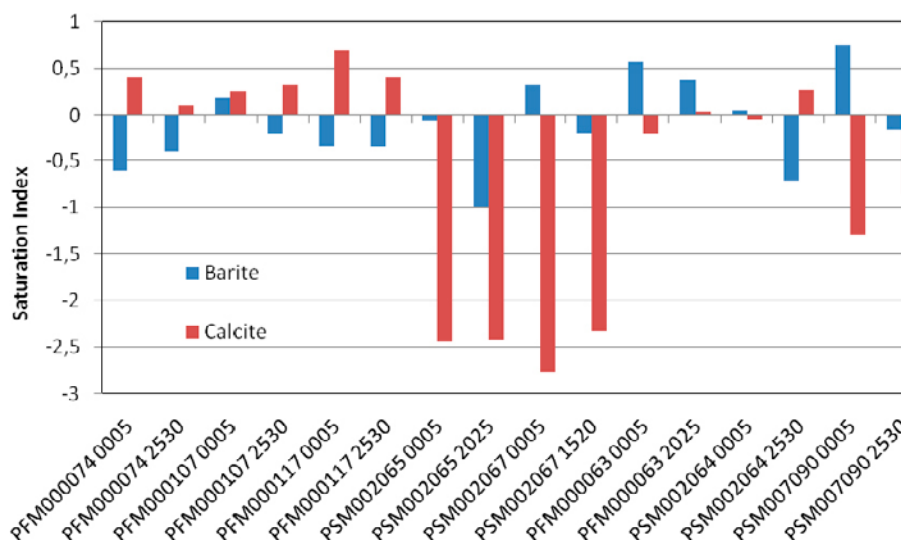


**Figure 4-7.** Saturation indices for barite and calcite in the sediment  $K_d$  samples.

In general, the results for these samples agree well with the conclusions from the analysis of the site investigation data presented in the previous sections. As in the samples from site investigations, no celestite or gypsum is expected to be present (Hedenström and Sohlenius 2008).

A more detailed discussion of the saturation indices and their relation to the measured  $K_d$  values at the different sites is found in Section 6.3.

Many of the sediment samples are also saturated with respect to calcite/aragonite (Table 4-2). At least in the marine sediments, aragonite should be the most stable Ca carbonate mineral. For all marine samples except PSM007090, the saturation indices indicate that aragonite should be present in the sediments. Additionally, all included lake sites in Forsmark indicate saturation with respect to calcite/aragonite. The conclusion is supported by the fact that almost all measurements in Forsmark have shown that  $\text{CaCO}_3$  is present in the soils – most sites have values of  $\text{CaCO}_3$  content between 1 and 63% (Hedenström and Sohlenius 2008).

In Simpevarp, all but one site (PSM002064) have saturation indices that indicate undersaturation with respect to calcite and aragonite. These results also agree well with the fact that almost all measurements in soils from Simpevarp show  $\text{CaCO}_3$  concentrations below 1% (Hedenström and Sohlenius 2008).

#### 4.1.6 Saturation indices in the 2011 $K_d$ samples

The saturation indices for barite in the 2011 soil  $K_d$  samples are shown in Figure 4-8. The results can also be found in Appendix D. Saturation indices along with the measured  $K_d$  values. Most of the 2011 soil  $K_d$  samples are saturated or close to saturation with respect to barite according to the calculations. Clay gyttja is the regolith type that most consistently indicates saturation. This could reflect the fact the material was deposited in brackish water (Sheppard et al. 2011), containing marine barite. All of the cultivated peat samples and half of the wetland peat samples were saturated or close to saturation with respect to barite, indicating the barite possibly could be present also in some of the peat samples. In a Polish wetland, Smieja-Król et al. (2010) have for example observed precipitation of 0.2–0.3 mm long barite aggregates inside plant cells.

**Table 4-2. Saturation indices for the sediment  $K_d$  samples. Red areas indicate that the samples are near saturation.**

SITE	IDCODE	Min depth (cm)	SI Barite	SI Celestite	SI Gypsum	SI Calcite	SI Aragonite	Name
Forsmark	PFM000074	0	-0.6	-3.6	-2.5	0.4	0.3	Labboträsket
Forsmark	PFM000074	25	-0.4	-3.4	-2.3	0.1	-0.1	
Forsmark	PFM000107	0	0.2	-2.9	-2.4	0.3	0.1	Bolunds-fjärden
Forsmark	PFM000107	25	-0.2	-2.7	-2.1	0.3	0.2	
Forsmark	PFM000117	0	-0.3	-3.4	-2.3	0.7	0.5	Eckarfjärden
Forsmark	PFM000117	25	-0.4	-3.4	-2.2	0.4	0.3	
Simpevarp	PSM002065	0	-0.1	-3.1	-2.5	-2.4	-2.6	Frisksjön
Simpevarp	PSM002065	20	-1.0	-4.0	-3.5	-2.4	-2.6	
Simpevarp	PSM002067	0	0.3	-2.9	-2.4	-2.8	-2.9	Jämsen
Simpevarp	PSM002067	15	-0.2	-3.5	-2.9	-2.3	-2.5	
Forsmark	PFM000063	0	0.6	-1.2	-1.1	-0.2	-0.4	Tixelfjärden
Forsmark	PFM000063	20	0.4	-1.4	-1.3	0.0	-0.1	
Simpevarp	PSM002064	0	0.0	-1.5	-1.4	-0.1	-0.2	Granholms-fjärden
Simpevarp	PSM002064	25	-0.7	-2.4	-2.2	0.3	0.1	
Simpevarp	PSM007090	0	0.8	-1.1	-1.0	-1.3	-1.5	Kräkelund
Simpevarp	PSM007090	25	-0.2	-2.2	-2.1	-0.9	-1.0	

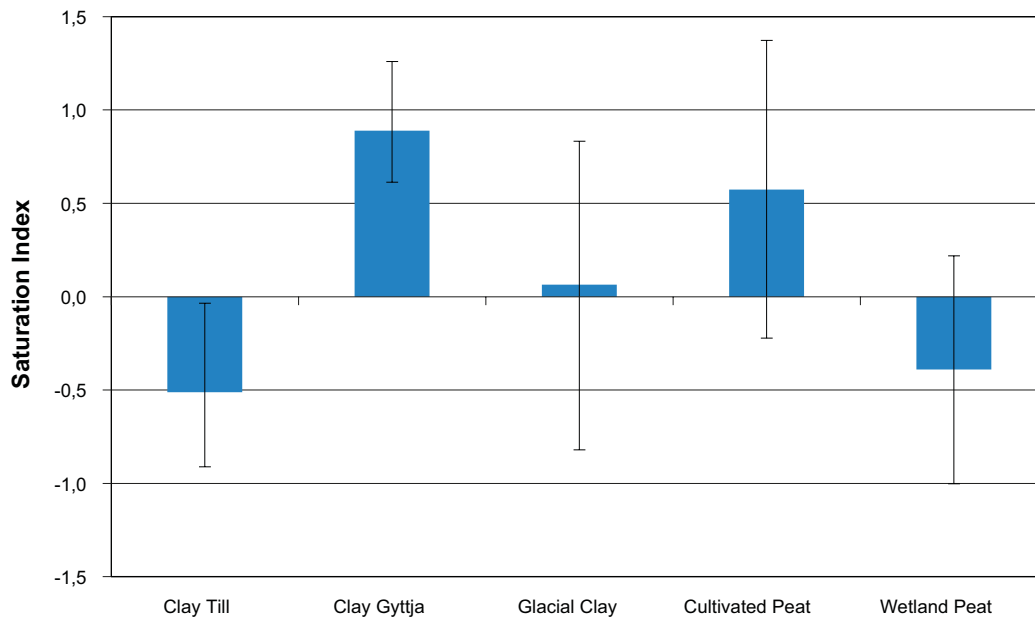


**Figure 4-8.** Saturation indices for 2011  $K_d$  samples. The bars represent the maximum and minimum modelled saturation indices of each soil type.

## 4.2 Precipitation of pure $\text{RaSO}_4$ and $\text{RaCO}_3$

At standard conditions (25°C and 1 atm) the solubility product for barite is  $10^{-9.99}$  (Helgeson et al. 1978). This is in close agreement with the value in Visual MINTEQ, which is  $10^{-9.98}$  (Smith et al. 2003). For  $\text{RaSO}_4$ , Zhu (2004b) uses a value of  $10^{-10.38}$  based on data from Sverjensky and Molling (1992). This value is also close to what was suggested by Paige et al. (1998) ( $10^{-10.21}$ ) and Langmuir and Riese (1985) ( $10^{-10.26}$ ). Using either of these values,  $\text{RaSO}_4$  is undoubtedly less soluble than  $\text{BaSO}_4$ . However, since the solubility products for barite and  $\text{RaSO}_4$  are so similar, precipitation of  $\text{RaSO}_4$  would require Ra concentrations that are in the same order of magnitude as the natural Ba concentrations. As an example, this would correspond to a Ra concentration of  $10 \mu\text{g l}^{-1}$  in sample PFM000063 (0–5) cm. This corresponds to a  $^{226}\text{Ra}$  activity of approximately  $400 \text{ kBq l}^{-1}$ , which is approximately a million times higher than the natural Ra levels. The  $^{226}\text{Ra}$  activities in the Forsmark area are probably already comparatively high due to the high U concentrations in the local soils and waters. Therefore, it seems unlikely that naturally occurring levels of Ra ever would lead to precipitation of  $\text{RaSO}_4$ . Even in the case of a canister failure it is doubtful that so high activities ever will be reached in the biosphere (Grandia et al. 2008). Since the modelling has shown that many types of water in the site investigation areas are saturated with respect to barite, any  $\text{RaSO}_4$  in these areas is likely to occur in trace amounts in a  $\text{RaSO}_4$ – $\text{BaSO}_4$  solid solution.

For  $\text{RaCO}_3$  the solubility product is estimated to be  $10^{-8.3}$  (Langmuir and Riese 1985). This is close to the solubility product for witherite, which is  $10^{-8.57}$ . As shown by the solubility modelling, witherite is not likely to occur either in Forsmark or in Simpevarp. Again, given that the Ra concentrations are several orders of magnitude lower than the Ba concentrations, it follows that Ra will not precipitate as  $\text{RaCO}_3$  either.

## 4.3 Sensitivity to pH

The sensitivity of the saturation indices for variations in pH has been tested for a number of samples. This is both because pH was not measured in all samples and because pH can be expected to vary in the future, which could lead to precipitation or dissolution of different minerals. In the simulations pH was allowed to vary between 6 and 9. One example of the variation in solubility for different alkaline earth minerals with pH is shown in Figure 4-9. However, the trends were similar in all investigated samples.

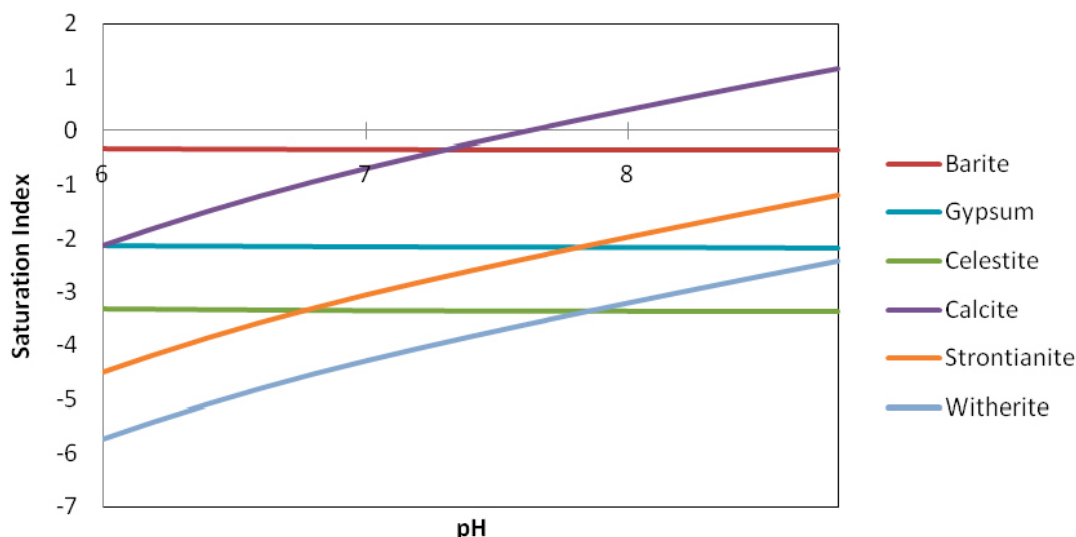


**Figure 4-9.** Variation of the solubility for alkaline earth sulphates and carbonates with pH in PFM000117 25–30 cm.

It is clear that the solubility of barite does not change much with pH. The fact that barite precipitation is quite independent of pH is expected, since the reaction does not involve transfer of hydrogen atoms or any species that are particularly sensitive to changes of the pH. Much lower pH is needed before sulphate is protonated and the Ba speciation is dominated by free Ba ions throughout the whole modelled pH range. There is only a weak tendency for the solubility of the alkaline earth sulphates to increase with pH.

As a contrast, the solubility of calcite ( $\text{CaCO}_3$ ) is highly dependent on pH. This is because increasing pH will lead to increased deprotonation of bicarbonate and, as a consequence, higher carbonate concentrations. As pH approaches the second  $\text{pK}_a$  value of carbonic acid (10.33) more and more bicarbonate will transform into carbonate. At pH above 10.33, carbonate will be the dominating species in the carbonate system. Hence, pH will directly affect the concentration of one of the ions forming calcite. The same is true for strontianite ( $\text{SrCO}_3$ ) and witherite ( $\text{BaCO}_3$ ). Accordingly, future changes in the pH would affect the stability of the carbonate minerals appreciably.

#### 4.4 Speciation of sulphur in the sediment $K_d$ samples

When modelling the solubility of barite and other sulphate minerals, the sulphate concentration is a key parameter, since it is a part of the ion activity product of all sulphate minerals. In nature, sulphur (S) exists in at least five different oxidation states: sulphide (–II), elemental sulphur (0), hyposulphite (+II), sulphite (+IV) and sulphate (+VI). Sulphate is the dominating form of sulphur in surface waters and many groundwaters. In strongly reducing environments (with no  $\text{O}_2$ ,  $\text{Fe}^{3+}$  or  $\text{NO}_3^-$ ) sulphate may be reduced to elemental sulphur or sulphide by microbial activity. The solubility of these sulphur species is considerably lower than for sulphate. An example of the behaviour of some redox pairs at site PSM000063 is shown in Figure 4-10.

In the site investigation data sulphate concentrations were measured, but for the sediment  $K_d$  samples only the total sulphur concentrations are available. Therefore, it is necessary to make some assumption about the speciation of sulphur in these samples. As mentioned in Section 3.4.2, it was assumed that all sulphur is present as sulphate – an assumption that taken literally obviously cannot be true.

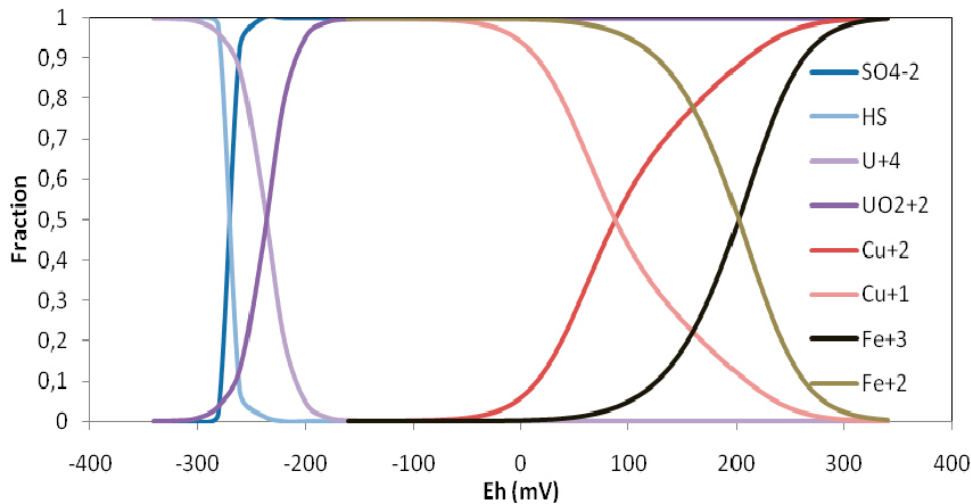


**Figure 4-10.** Modelled fractions for four different redox-pairs in sample PFM000063 (0–5 cm) as a function of the redox potential.

At least some sulphur should be present in dissolved organic matter and – if the conditions are reducing enough – as sulphide or elemental sulphur. However, the saturation indices presented in this report are logarithmic values, more precisely the difference between the logarithm of the ion activity product and the logarithm of the solubility constant. This means that although the saturation index is directly dependent on the sulphate activity, the dependence is not proportional. Just as a decrease in pH by one unit requires a decrease by an order of magnitude in the hydrogen activity, a decrease in the sulphate activity by an order of magnitude would result in a decrease of the saturation index for a sulphate mineral by approximately 1. Therefore, the results are not too sensitive to the assumption that all sulphur is present as sulphate. As long a sulphate is the major sulphur species in the aqueous phase, the results should be reliable. The crucial question is therefore: is it reasonable to assume that the aqueous sulphur in these samples is dominated by sulphate?

Both sulphate and sulphide concentrations are available for 77 samples in the dataset of surface and near surface groundwater used in this report. Among these samples sulphate was without exception the dominating sulphur species. There was only one site where less than 99% of the sulphur was sulphate (SFM000049). At this site the portion of sulphate varied between 69.9 and 99.5%. Even with that variation the assumption that 100% is sulphate could be justified from a modelling perspective and should give a decent result as argued above.

It is important to note the even if sulphate may be the dominating sulphur species in the aqueous phase, this does not imply that there cannot be production of sulphide and precipitation of sulphide minerals in that environment. SFM000049 is one example, but a distinct smell of H<sub>2</sub>S was also noted as sediments were sampled at site PSM007090. This is a clear sign that sulphide is present in those sediments.

If the reduction of sulphate in the sediments (or elsewhere) proceeds without exchange with sulphate-rich waters, e.g. diffusing sea water, it is unavoidable that the sulphate sooner or later will decrease and that sulphide will become the dominating S species. This has for instance been observed in sediments from the estuary of Oder in the Baltic Sea (Scholz and Neumann 2007). Approximately 15 cm down in the sediments sulphate concentrations started to decrease from typical sea water concentrations to below detection limit, at around 30 cm. Simultaneously, there was an increase in sulphide concentration, but it coincided with a decrease in total sulphur so sulphide never reached the same concentrations as the initial sulphate concentration.

It is unknown how widespread sulphate reduction may be in the site investigation areas, but there are some samples in the sediment K<sub>d</sub> dataset that represent a depth of 25–30 cm. In this case the total S concentrations remain high, suggesting that the sulphate supply has not yet been depleted. However, in order to see what might happen if there was a reduction of sulphate at one of the sites (PSM000063) Visual MINTEQ 3.0 was used to vary the redox potential. Note that the only sulphur

species accounted for in the simulations were sulphate and sulphide. The reduction of sulphate rapidly lead to strong supersaturation with respect to many sulphide minerals, e.g. FeS, galena (PbS), mackinawite (iron-nickel sulphide), NiS, wurtzite (ZnS) and chalcopyrite (copper-iron sulphide). Saturation indices as high as 28 were observed, which indicates that the measured levels of metals like nickel, copper, zinc and lead hardly could be present in the pore water if sulphur was present mainly as sulphide. The comparatively high concentrations of many of the mentioned metals in the sediments indicate that at least some of those sulphide minerals indeed could be precipitating in the sediments, but it is clear that such accumulation is not dependent on sulphide being the dominating sulphur species. The precipitation will proceed at much lower sulphide concentrations so it does not violate the assumption that sulphate is the dominating sulphur species. It can also be noted that whereas Ba sulphate has low solubility, Ba sulphide is highly soluble. Therefore, precipitation of sulphides cannot explain why the  $K_d$  for Ba deviates from that of Ca and Sr.

It is also important to point out that the presence of noticeable amounts of sulphide does not indicate that barite cannot be present. In the cases where barite was found in the bedrock in Forsmark it was found together with pyrite, i.e. iron sulphide (Drake and Tullborg 2007). Barite has also been found at depths of several meters in reducing sediments from the Baltic Sea where extensive precipitation of sulphide minerals has occurred (Böttcher and Lepland 2000). It is unclear, however, whether this barite still was in equilibrium with the pore water or not.

#### 4.5 Summary of the saturation with respect to barite

Figure 4-11 summarizes the results of modelling of surface water, pore water and groundwater with respect to barite. Note that the distributions are representative for these types of samples in Forsmark and Simpevarp only in so far as the samples themselves are representative for water chemistry in these areas. In many cases a varying number of observations have been made at the different sites, and the sites themselves may not be representative for each sample type as a whole. In any case, it is clear that there are differences between different types of water and that it is common that the water in Forsmark and Simpevarp is saturated or close to saturation with respect to barite. In many cases there is even a clear supersaturation, e.g. in the peat pore water, but it must be emphasized that the fact that the water is saturated or even supersaturated does not prove that barite is present in the solid phase. Likewise, the fact that a certain water sample is not saturated with respect to barite does not necessarily imply that barite cannot be present in the soil.

All and all, there are good reasons to believe that barite indeed is present in many environments in both Simpevarp and Forsmark. The precipitation of barite in marine environments is well-known, and Figure 4-11 shows that all sea water samples are either saturated or close to saturation with respect to barite. Consequently, it is not surprising that the marine sediments in Forsmark are saturated with respect to barite (although there are only two observations). In Simpevarp one out of four sediment pore water samples was not close to saturation with respect to barite. The marine influences are also obvious in the clay gyttja, where all analyzed pore water samples were saturated with respect to barite. The general impression is therefore that water in Forsmark and Simpevarp often is saturated or close to saturation with respect to barite, which is a strong indication that barite should be a commonly occurring mineral in these systems. For instance, in near surface groundwater as much as half of the analyzed samples may be affected by barite.

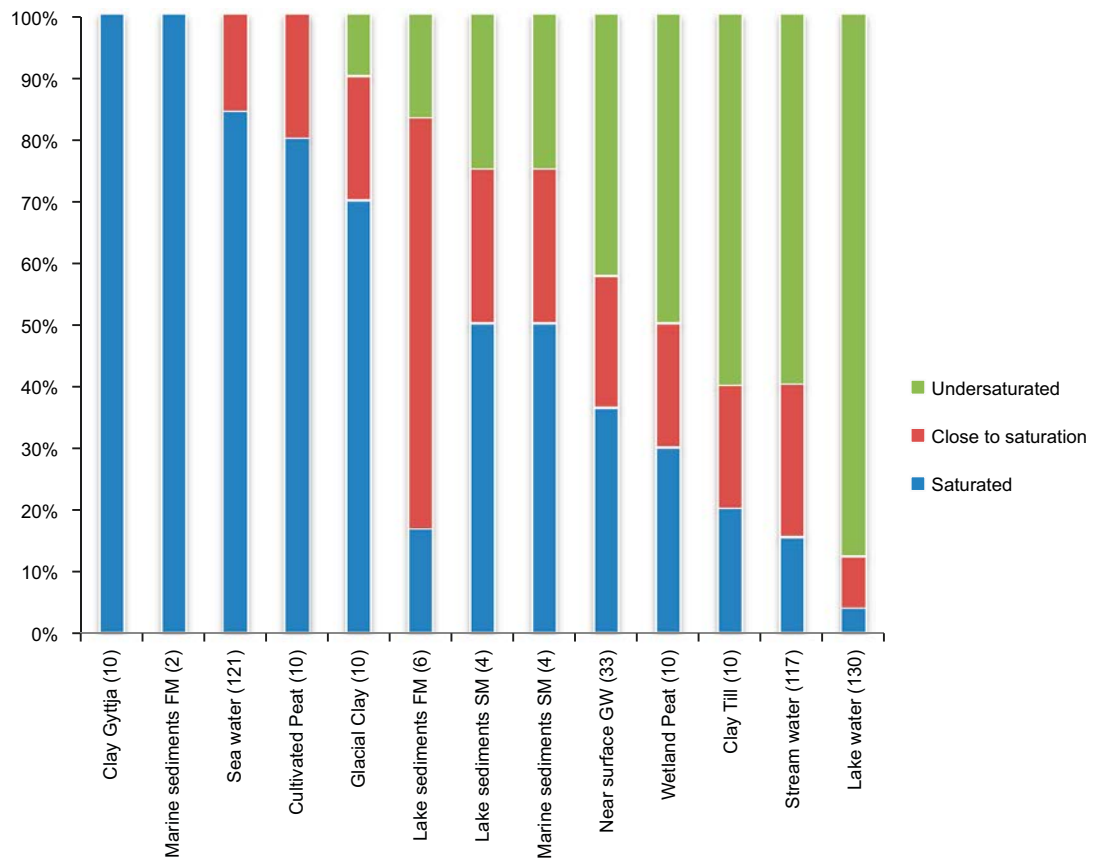


**Figure 4-11.** Saturation with respect to barite for the investigated sample types. Descriptions such as “clay gyttja” refer to the pore water. The numbers in parentheses denote the number of observations. Blue shows the percent of the observations with SI greater than  $-0.1$ , red shows where SI is in the interval  $[-0.5, -0.1]$  and green shows the clearly undersaturated samples with  $SI < -0.5$ . FM=Forsmark; SM=Simpevarp; GW=groundwater.

## 5 Modelling of Ra coprecipitation and speciation

### 5.1 The effects of barite on the $K_d$ for Ra

There are two key factors that control the contribution of barite to the  $K_d$  value for Ra. The first factor is the amount of barite present in the soil. The more barite that is present, the more Ra is needed to saturate it. Hence, more barite will lead to increasing  $K_d$  values. The second factor is the sulphate concentration. The more sulphate that is present in the pore water, the more Ra is forced into the barite. Hence, more sulphate will also lead to increasing  $K_d$  values. Table 5-1 presents the result of the simulations of the effects of barite on the  $K_d$  for Ra in the sediment  $K_d$  samples. The minimum Ra  $K_d$  value is set by the Sr  $K_d$  for the sediment  $K_d$  samples. Detailed graphs of the simulated changes in  $K_d$  for each sample are provided in Appendix F. Chapter 3.2 gives an overview of the method for the modelling of coprecipitation and chapters 3.4.2 and 3.4.4 gives detailed descriptions of how the modelling have been done in each dataset. The results are further discussed in Sections 5.1.1 and 5.1.2.

#### 5.1.1 Modelled Ra $K_d$ values in lake sediments

Figure 5-1 shows an example (site PFM000117) of the result of the modelling of barite influence on Ra  $K_d$  values in lakes. Similar results were found for all modelled lake sites in both Forsmark and Simpevarp (Appendix F). At these sites the modelled effect of adding barite is relatively small, less than 35% compared to the minimum value set by the  $K_d$  for Sr. Hence, the amounts of Ba present in the lake sediments, even if all of it is assumed to be barite, seem to be too low to substantially affect the  $K_d$  for Ra. This is logical given that the lake water generally is not saturated with respect to barite (Figure 4-11). It would therefore seem that the higher  $K_d$  values for Ba as compared to Sr and Ca in lake sediments has some other explanation.

**Table 5-1. Compilation of calculated  $K_d$  values for Ba, Ca and Sr (Tröjbom et al. 2007, 2008, Engdahl et al. 2008) and modelled  $K_d$  values for Ra. The last column gives the percent increase in the Ra  $K_d$  value when adding barite in the simulations.**

SITE	IDCODE	Min depth (cm)	Max depth (cm)	$K_d$ Ba (l/kg)	$K_d$ Ca (l/kg)	$K_d$ Sr (l/kg)	Max mod. Kd Ra (l/kg)	Sediment type	Diff. in $K_d$ Ra (%)
Forsmark	PFM000074	0	5	790	860	390	400	Lake	1
Forsmark	PFM000074	25	30	1,100	260	270	320	Lake	19
Forsmark	PFM000107	0	5	1,600	140	210	280	Lake	32
Forsmark	PFM000107	25	30	5,500	150	250	330	Lake	35
Forsmark	PFM000117	0	5	770	360	280	330	Lake	16
Forsmark	PFM000117	25	30	1,200	370	360	370	Lake	3
Simpevarp	PSM002065	0	5	5,100	410	720	810	Lake	13
Simpevarp	PSM002065	20	25	5,800	550	840	850	Lake	2
Simpevarp	PSM002067	0	5	3,300	410	650	800	Lake	24
Simpevarp	PSM002067	15	20	3,200	350	600	650	Lake	8
Forsmark	PFMN000063	0	5	12,000	95	92	2,300	Marine	2,300
Forsmark	PFM000063	20	25	11,000	70	77	1,500	Marine	1,900
Simpevarp	PSM002064	0	5	5,700	82	100	400	Marine	300
Simpevarp	PSM002064	25	30	3,500	46	65	95	Marine	47
Simpevarp	PSM007090	0	5	3,300	67	68	1,000	Marine	1,400
Simpevarp	PSM007090	25	30	2,600	68	68	150	Marine	120



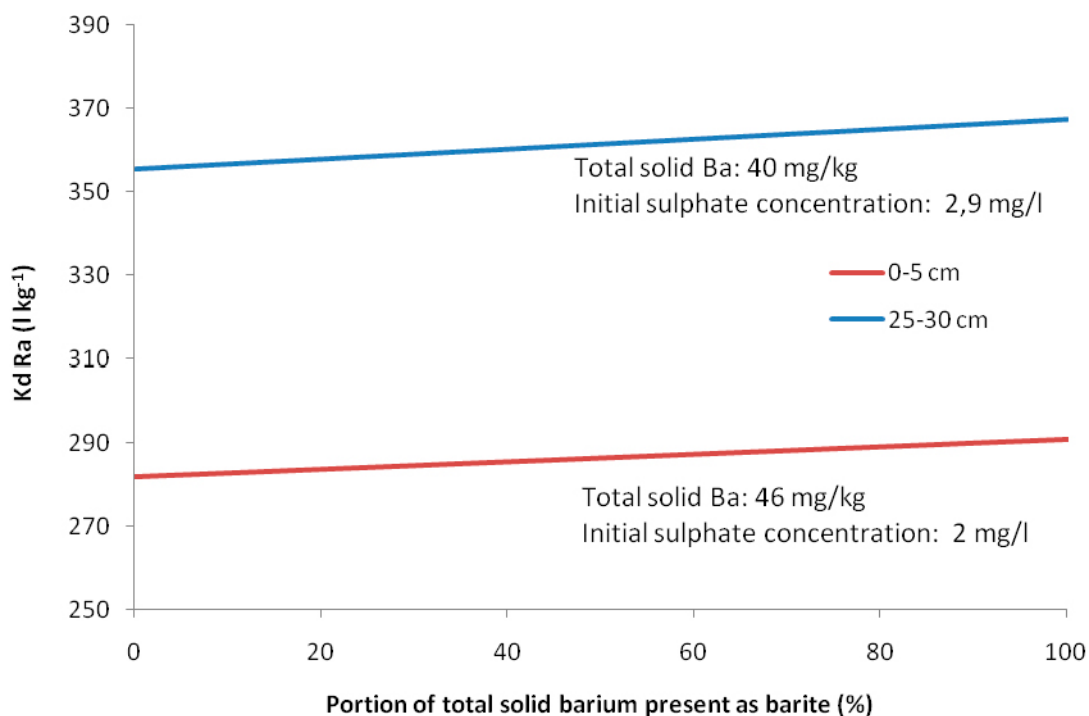


Figure 5-1. Modelled effect of barite on Ra  $K_d$  -values at lake site PFM000117, depth 0–5 cm and 25–30 cm.

### 5.1.2 Modelled Ra $K_d$ values in marine sediments

One example (PFM000063) of the results of the modelling of the marine sites is presented in Figure 5-2. The results from the other marine sites show similar patterns and are presented in Appendix F. Effects of barite on the  $K_d$  for Ra is clear that barite has a pronounced influence on the Ra  $K_d$  at the marine site, especially in the surface samples. The differences between the minimum and the maximum modelled  $K_d$  values are generally relatively high (47–2,300%). Minimum values of Ra  $K_d$  for the marine environments in both Forsmark and Simpevarp were set by the measured Sr  $K_d$  values, between 65 and 100 l kg<sup>-1</sup>. The modelled maximum Ra  $K_d$  values vary considerably between sites and depth within the same sites showing a total range of 95–2,300 l kg<sup>-1</sup>. These results can be compared to the Ra  $K_d$  values of 1,000 l kg<sup>-1</sup> and 4,530 l kg<sup>-1</sup>, which were observed in two marine sediment samples (Sheppard et al. 2011).

### 5.1.3 Modelled Ra $K_d$ values in 2011 soil samples

Figure 5-3 shows the modelled effect of barite on Ra  $K_d$  in the clay gyttja sample AFM001368. The modelling indicates an increase in the Ra  $K_d$  values by a factor 4–9 times the values under unsaturated conditions. However, although the modelling indicates a strong influence of barite on the Ra  $K_d$ , barite by itself cannot explain the high measured  $K_d$  values under the assumptions made in the calculations. The measured  $K_d$  values for Ra at this site are 4,300 l kg<sup>-1</sup> at depth 20–25 cm and 6,400 l kg<sup>-1</sup> at depth 50–55 cm. These results are further discussed in Section 6.4.2. The results from calculations in clay till and glacial clay show similar patterns. Examples of the result from other sites are given in Appendix F. Effects of barite on the  $K_d$  for Ra.

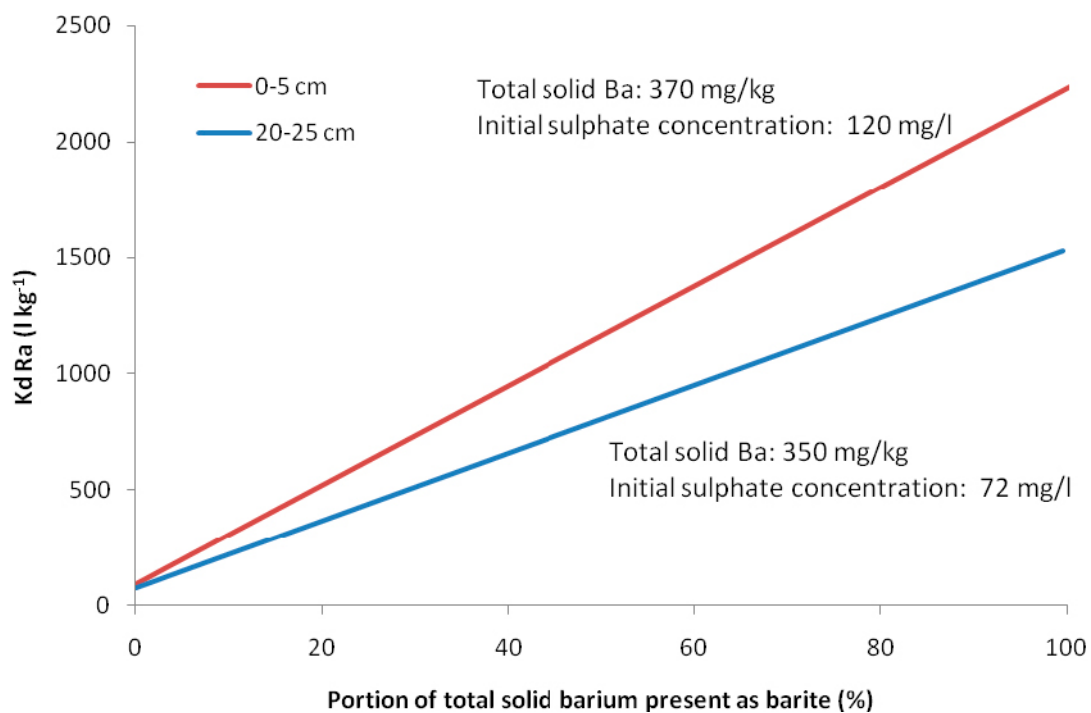


**Figure 5-2.** Modelled effect of barite on Ra  $K_d$  values at the marine site PFM000063, depth 0–5 cm and 20–25 cm.

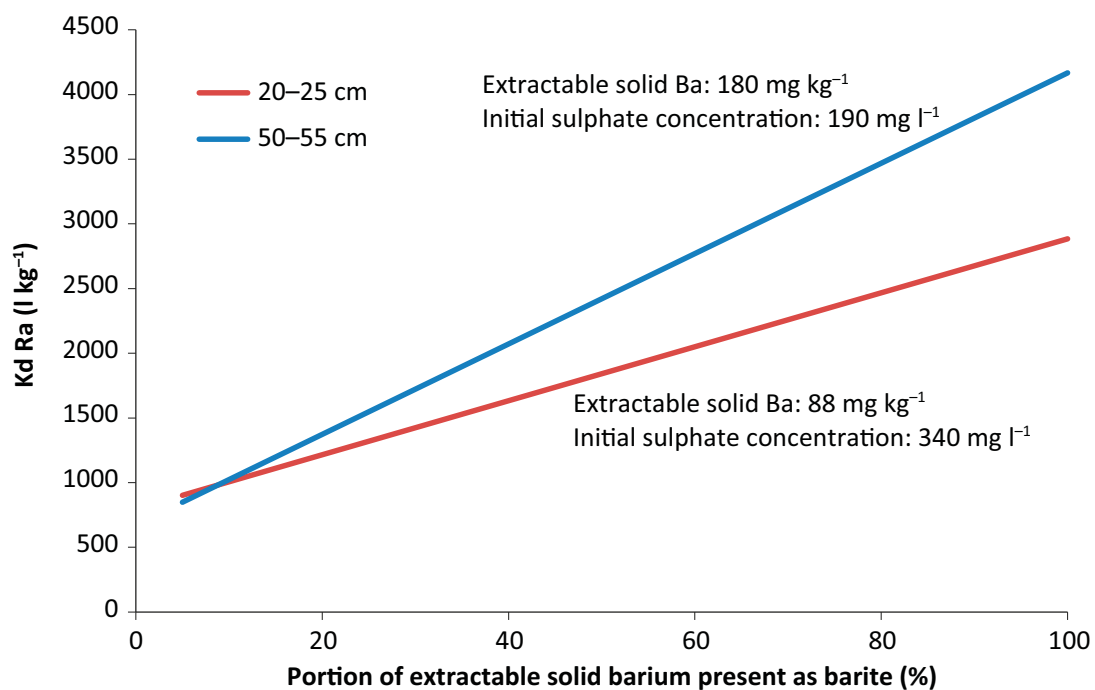


**Figure 5-3.** Modelled effect of barite on Ra  $K_d$  -values at 2011 soil site AFM001368, depth 20–25 cm and 50–55 cm.

## 5.2 Ra speciation

The Ra speciation was calculated using the sediment  $K_d$  dataset. The results of the Ra speciation calculations are shown in Figure 5-4. In all 16 sediment samples,  $\text{Ra}^{2+}$  is the by far most common Ra species. Not in any of the samples was the percentage of free Ra ions predicted to fall below 90%. See Appendix E for a full compilation of the result of the speciation calculations. The dominating role of  $\text{Ra}^{2+}$  is in agreement with previous attempts to model the Ra speciation in other environments, e.g. the French Massif Central (Rihs and Condomines 2002) and Brazilian groundwater (Lauria et al. 2004).

Besides  $\text{Ra}^{2+}$  the dominating Ra species are  $\text{RaCl}^+$  and  $\text{RaSO}_4(\text{aq})$  (above all in marine environments where the concentrations of chloride and sulphate are high) and organically bound Ra. Based on the analogy with Ba, complexation to organic matter is more important in the lakes, above all in Simpevarp. Assuming that the accumulation of Ba and Ra in wetlands is dominated by sorption to organic matter, the observations of Sheppard et al. (2011) suggest that Ra may have higher affinity for organic matter than Ba. In that case, the organically bound fraction in Figure 5-4 is probably underestimated.  $\text{RaOH}^+$  and  $\text{RaCO}_3(\text{aq})$  were also included in the database, but none of them exceeded 0.3% in any of the samples so they were not included in the graph. Accordingly, the local chemistry seems to have only limited impact on the speciation of Ra. Free Ra ions can be expected to be the dominating Ra species throughout the Simpevarp and Forsmark areas.

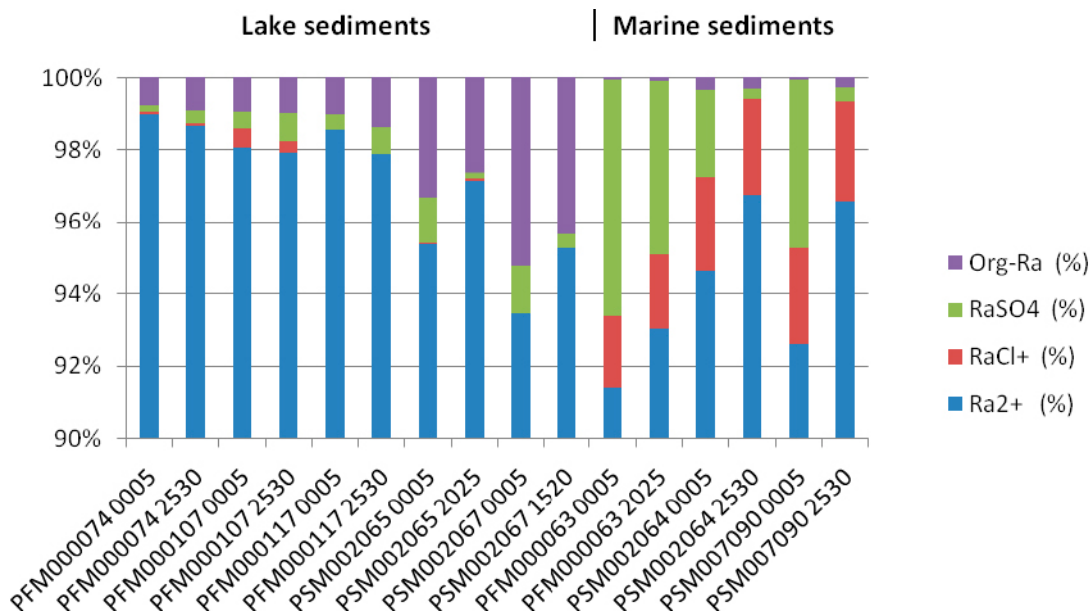


**Figure 5-4.** Ra speciation in the porewater of the sediment  $K_d$  samples. Note that the scale of the y-axis start at 90% so  $\text{Ra}^{2+}$  is always the dominating species.

### 5.3 Sensitivity for the Guggenheim parameter

A crucial part of the modelling of the uptake of Ra in barite is the parametrisation. More specifically, an important issue is whether the  $\text{Ra}_x\text{Ba}_{1-x}\text{SO}_4$  solid solution behaves ideally or not and – in the latter case – how large the degree of non-ideality is. The variation of the partitioning coefficient,  $D$  (see Appendix C for details), and the first Guggenheim parameter in a regular model is shown in Figure 5-5. The affinity of barite for Ba and Ra will be equal if the Guggenheim parameter is set to approximately 0.8. For lower values there will be a preferential inclusion of Ra; for higher values there will be a preferential inclusion of Ba into the barite.

Based on semi-empirical calculations, Zhu (2004a) has suggested a value of 0.36 for the first Guggenheim parameter. However, recent experiments have indicated that the value may be higher. For example, Bosbach et al. (2010) tried to evaluate their experiment using 0.36, but they seem inclined to believe that the actual value of the interaction parameter should be greater. Measurements by Curti et al. (2010) suggest that the Guggenheim parameter should be in the range 1.5–2.5. It is clear from Figure 5-5 that choosing a value in that range will produce very different results than 0.36. For 0.36 the partitioning coefficient would be approximately two, which would imply that the  $K_d$  value for Ra could reach twice as high as the  $K_d$  value for Ba. Currently, there are no explanations to the deviations between the different studies. However, given that two recent studies on Ra coprecipitation with barite indicate that there is some degree of nonideality, a value of 1.5 was chosen in the PHREEQC modelling of the sediment samples. For the 2011 soil  $K_d$  samples Ra  $K_d$  measurements were available. A comparison of measured Ra  $K_d$  values and modelling results using a Guggenheim parameter of 1.5 showed that measured Ra  $K_d$  values could not be reached using this assumption. Therefore, a value of 0.36 (Zhu 2004a) was chosen for the modelling of the 2011  $K_d$  samples in order to capture the likely maximum potential of coprecipitation with barite.

As discussed above, setting the Guggenheim parameter to 1.5 the model predicts that the Ra/Ba ratio in the barite will be lower than in the aqueous phase. Hence, there will be a preferential incorporation of Ba over Ra into the barite. This implies that the apparent  $K_d$  value for Ra will be less affected by barite than the  $K_d$  values for Ba. For instance, if 50% of the Ba in the solid phase is present in barite, this will increase the Ba  $K_d$  by 50%. Since Ra is disfavoured in barite, assuming a Guggenheim parameter of 1.5, the increase in the Ra  $K_d$  due to coprecipitation with barite will be approximately 25%. However, since there are still uncertainties in how the Guggenheim parameter should be chosen, there remains a considerable uncertainty in the modelling of the Ra coprecipitation with barite. If one instead chooses a Guggenheim parameter of 0.36, as suggested by Zhu (2004a), there will be a preferential incorporation of Ra into the barite, causing the Ra  $K_d$  to increase by approximately 80% in the example above. Evidently, the uncertainty in the Guggenheim parameter contributes significantly to the uncertainty of modelling results.

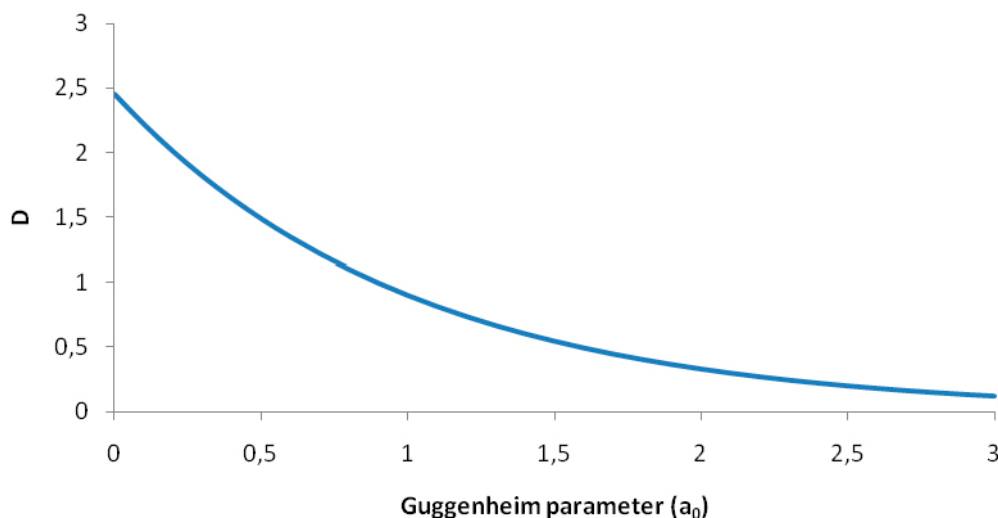


**Figure 5-5.** Dependence of the partitioning coefficient,  $D$ , on the Guggenheim parameter for a regular  $\text{Ra}_x\text{Ba}_{1-x}\text{SO}_4$  solid solution at 25°C.

## 6 Discussion

### 6.1 Solubility of alkaline earth metals

The SI calculations showed that many water samples in both Forsmark and Simpevarp appear to be saturated with respect to barite and calcite/aragonite. These results are consistent with previous measurements of high Ca carbonate concentrations in soils from the Forsmark area, presumably mainly calcite, but also the fact that aragonite can precipitate in seawater. As for barite, there are no measurements yet that can confirm its occurrence in the biosphere, but at least in the marine samples there is strong evidence from the scientific literature that barite should be present. Furthermore, the thermodynamic modelling suggests that saturation with respect to barite may occur both in different types of environments in both Forsmark and Simpevaro, especially in sea water Figure 6-1. Given the marine history of both the Simpevarp and Forsmark areas due to the isostatic uplift, this could also explain the occurrence of barite in the soils. In that case, one would expect saturation with respect to barite above all in previous marine sediments, which could be investigated by further spatial analysis of the data. However, barite may also occur as a primary mineral in the soils.

Accordingly, there are strong reasons to believe that the solubility of Ca and Ba locally is limited by the occurrence of calcite/aragonite and barite, respectively, in the site investigation areas. As was discussed initially,  $K_d$  values may give misleading information if the aqueous concentrations are controlled by a mineral phase. Due to coprecipitation one should expect that the occurrence of these minerals also has consequences for the mobility of Sr and Ra.

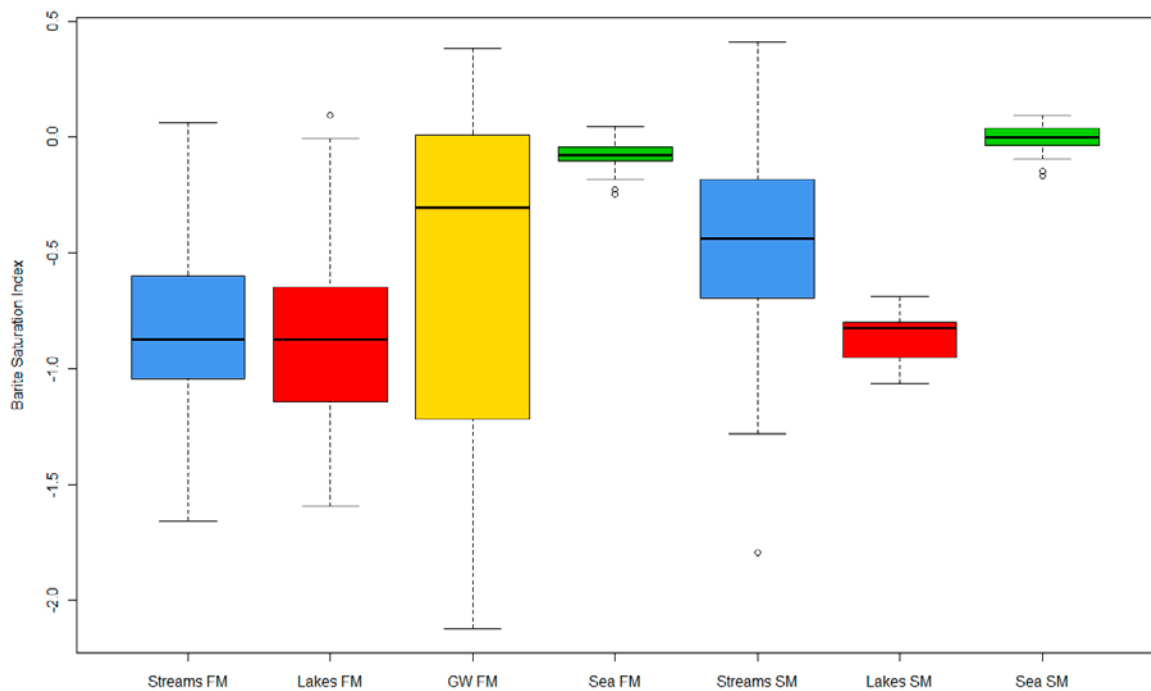


**Figure 6-1.** Saturation indices with respect to barite in different types of water in Forsmark (FM) and Simpevarp (SM). GW denotes near-surface groundwater.

## 6.2 Effects of extraction method on the $K_d$ values for Ba and Ra

When determining element concentrations in the solid phase, a total digestion method was used for the sediment samples, while a partial digestion method (aqua regia) was used for the 2009 and 2011 soil samples. The argument for choosing a partial digestion method is often that one wants to quantify only the active part of the soil matrix. For example, the inside of resistant mineral grains such as silicates is not in direct contact with the pore water, and its influence over the pore water chemistry should therefore be nil. Accordingly, it is argued that the inclusion of this material would inflate the  $K_d$  values. Therefore, a partial extraction method such as aqua regia is sometimes preferred when measuring  $K_d$  values (e.g. Sheppard et al. 2011).

The solubility of Ba in aqua regia is approximately  $1 \text{ mg L}^{-1}$  (Ansari et al. 2001) so barite is not easily dissolved by the digestion method that was used for the soil  $K_d$  data (both the 2009 and 2011 datasets). The pronounced differences between total digestion and aqua regia digestion, which were observed in some marine sediments where both methods were applied (Sheppard et al. 2011), demonstrate that a considerable amount of Ba is present in some insoluble mineral. Since barite is precipitated in sea water and the pore water of the sediments was saturated with respect to barite, it seems plausible that this insoluble form of Ba largely may be barite. Apart from barite, Ba can also substitute K and Ca in silicate minerals, e.g. K feldspar. Ba and K, for instance, have similar ionic radii. K feldspar is also resistant to aqua regia, and K also exhibits a clear difference between total digestion and aqua regia extraction, suggesting an alternative explanation to the high amount of insoluble Ba. However, the difference between total digestion and partial extraction by aqua regia is smaller for K than for Ba, and it is doubtful whether there could be preferential substitution of K by Ba in K feldspar. Since the pore water is saturated with respect to barite, barite does appear as the most likely explanation.

However, if the barite is not completely resistant to aqua regia, there may be a dissolution of barite that is significant enough to affect the  $K_d$  measurements. Hence, it cannot be uncritically assumed that the observed  $K_d$  values for Ba are unaffected by the presence of barite. On the contrary, the differences in Ba/Sr and Ba/Ca  $K_d$  ratios between saturated and unsaturated samples suggest that there may be an artifact in the measurements due to partial dissolution of barite.

Data on Ba in various types of soils in the site investigation areas have previously been published in a number of SKB reports: Tröjbom and Söderbäck (2006), Sheppard et al. (2009, 2011) and Hannu and Karlsson (2006). In the first three of these datasets aqua regia extraction was used to analyse the Ba content. In these datasets the measurements of extracted Ba gives average values of approximately  $50 \text{ mg kgdw}^{-1}$  (Table 6-1). In the dataset presented by Hannu and Karlsson (2006), on the other hand, the samples were digested using a mixture of nitric/hydrochloric/hydrofluoric acids followed by  $\text{LiBO}_3$  melting. In this case, the average Ba concentration was close to  $500 \text{ mg kgdw}^{-1}$ . Combined these investigations comprise various types of soil types in the site investigation areas. If the 19 samples presented by Hannu and Karlsson (2006) are assumed to represent a reasonably similar selection of soils as the 83 samples investigated by Tröjbom and Söderbäck (2006) and Sheppard et al. (2009, 2011), it would appear as if extraction by aqua regia on average would dissolve approximately 10% of the barium that is present in the soils, leaving c 90% for barite or other insoluble minerals. However, since different samples were used no certain conclusion can be drawn. Yet, Table 6-1 demonstrates that Ca and Sr do not show this pattern of large differences of measured concentrations depending on extraction method, indicating that the differences between the samples is not general for the alkaline earth metals.

Since the solubility of barite in aqua regia is low, it must be considered that all  $K_d$  measurements using this extraction method do not fully account for the potential effects of barite on the  $K_d$  values of Ba and Ra. Yet, the possibility that the observed  $K_d$  values for Ba and Ra partially are affected by barite cannot be excluded, since small amounts of barite can be dissolved in aqua regia. If a large share of the Ba and Ra in a soil sample is present in barite, it is possible that even a small portion of the barite could contribute significantly to the measured Ba and Ra concentrations in the solid phase, thereby leading to higher  $K_d$  values. Therefore, it remains uncertain to whether the  $K_d$  values based on partial extraction are affected by barite and – if so – to what extent.

**Table 6-1. Comparison of measurements of Ca, Sr and Ba in various types of soils from different SKB reports.**

SKB-Report	Matrix	Ca mean [mg kg <sub>dw</sub> <sup>-1</sup> ]	Sr mean [mg kg <sub>dw</sub> <sup>-1</sup> ]	Ba mean [mg kg <sub>dw</sub> <sup>-1</sup> ]	Ba Min	Ba Max	Number of samples	Digestion method
R-06-19 <sup>a</sup>	Till	71,112	72	39	19	84	43	Aqua regia extraction
R-09-27 <sup>b</sup>	Clay gyttja, sandy till, peat etc.	45,800	56	59	48	66	7	Aqua regia extraction
R-11-24 <sup>c</sup>	Clay gyttja, clay till, peat etc.	39,399	41	65	15	190	33	Aqua regia extraction
P-06-220 <sup>d</sup>	Till, peat etc.	36,777	147	480	320	640	19	Digested with acids and LiBO <sub>3</sub> melting

a) (Tröjbom and Söderbäck 2006).

b) (Sheppard et al. 2009).

c) (Sheppard et al. 2011).

d) (Hannu and Karlsson 2006).

In any case, it is clear that the choice of extraction method will have a profound impact on the observed  $K_d$  values if barite is present. Based on the knowledge that barite should be present in marine environments and that the modelled seawater and sediment pore water samples are saturated with respect to barite the differences between total extraction and aqua regia extraction in the sediment  $K_d$  samples can probably largely be attributed to the presence of barite (Table 5-1). As demonstrated by Sheppard et al. (2011), the  $K_d$  values for Ba increase by approximately one order of magnitude in the  $K_d$  sediment samples, if total extraction is used instead of aqua regia. What the effects would be in the soil  $K_d$  samples depends on whether barite is present at all and – if it is – what amounts of barite there are. The differences between the measured Ba concentrations in soils of Hannu and Karlsson (2006) on one hand and Tröjbom and Söderbäck (2006) and Sheppard et al. (2009, 2011) on the other indicate that it could be approximately an order of magnitude in the soils too.

## 6.3 $K_d$ values in sediments

### 6.3.1 Sediment samples

In the sediment samples there is a good agreement between Ca and Sr, while Ba exhibits considerably higher  $K_d$  values – sometimes more than 100 times higher than those of Ca and Sr. The similar geochemical similarities between these three elements therefore suggest that the  $K_d$  values not only reflect ion exchange or other sorption/desorption processes. Accordingly, there are good reasons to believe that the  $K_d$  values for Ba are inflated by the presence of barite. The literature review has shown that barite is present in sea water, which also is supported by the observation that the relative abundance of Ba in suspended particles is much higher than for Ca and Sr (see below). Moreover, the thermodynamic modelling consistently shows that the sediment pore waters are saturated with respect to barite. In addition, Sheppard et al. (2011) found that a large fraction of the Ba in marine sediment samples could not be extracted using aqua regia. This fraction was much larger than for Ca and Sr, indicating that Ba must be present in some mineral that is resistant to aqua regia and does not contain large amounts of Ca and Sr. Barite is one likely candidate.

Figure 6-2 shows the saturation index for barite plotted against the logarithm of the  $K_d$  value for Ba divided by the  $K_d$  value for Ca. Hence, this ratio expresses how much higher (or lower) the  $K_d$  value for Ba is in comparison with the  $K_d$  value for Ca. For instance, where the log ratio is 2, it means that the  $K_d$  value for Ba is 100 times higher than for Ca.

Figure 6-2 shows that Ba has much higher  $K_d$  values than Ca primarily in the marine samples. The marine sites also exhibit higher saturation indices in the newly deposited sediments than in older sediments. This can be caused by reduction of sulphate in the deeper sediments, if the samples were collected in such environments. However, the measured  $K_d$  values do not change considerably with depth, which suggests that the barite may not dissolve very rapidly.

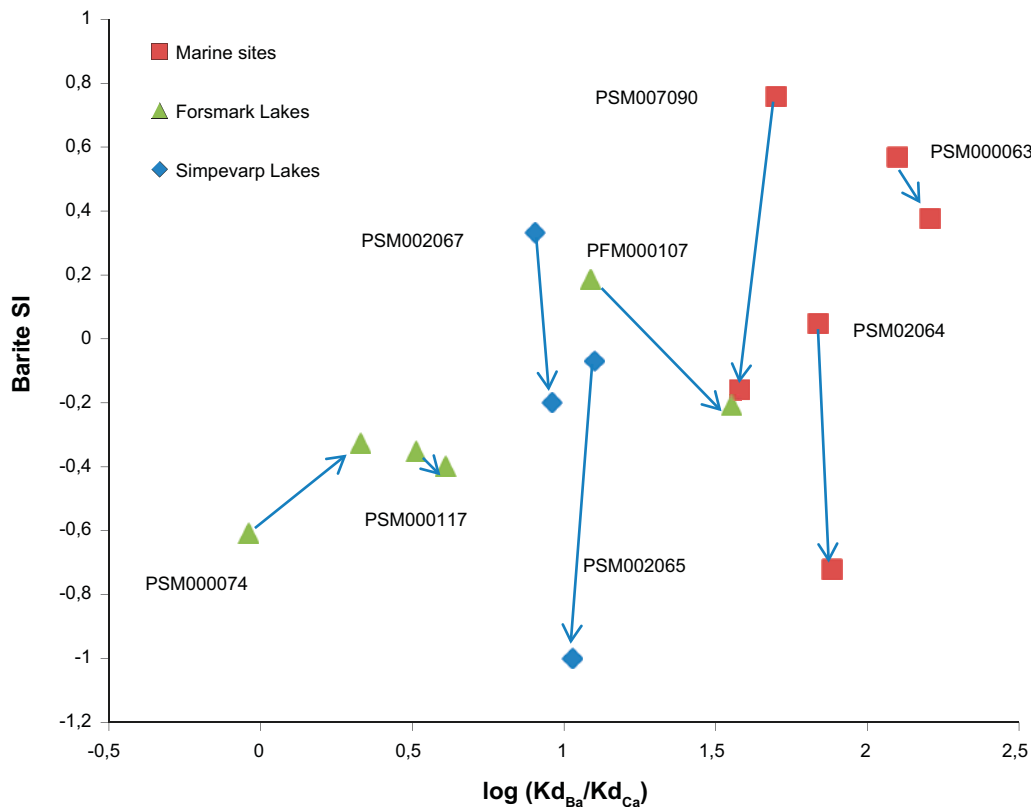


**Figure 6-2.** Barite saturation index for all sediment samples vs. the logarithm of the ratio between the  $K_d$  value for Ba and the  $K_d$  value for Ca. The arrows connect the samples from the same site and indicate how the saturation index and  $K_d$  values change with depth. The ID code of the site is shown next to the more superficial sample and the arrows point towards the deeper sample.

It can also be noted that in PFM000107 (Bolundsfjärden) there is significant increase in the log ratio with depth. Possibly, this is due to the fact that Bolundsfjärden is a young lake. It is therefore likely that the deeper sediments represent marine conditions, which accordingly could be expected to contain higher amounts of barite. If so, this would illustrate an important change for the mobility of Ba and Ra in the landscape evolution of the Forsmark and Simpevarp areas.

### 6.3.2 Particulate Ba in the water column

Measurements on suspended and dissolved fractions of Ca, Sr and Ba from the sampling sites for sediment  $K_d$  also reveal differences between Ca and Sr on one hand and Ba on the other. These samples were collected in connection with the sampling of the sediment cores used to determine the  $K_d$  values (Engdahl et al. 2008). These measurements provide further indications that barite is present in at least some of the samples. In connection with the sampling of the sediment cores, water samples from the water column at each site were collected and analysed for several chemical parameters. In addition, large volumes of water were filtered through 0.22  $\mu\text{m}$  filters and the content of the filters were later determined in order to quantify the amount of suspended material. In a pilot study from Borholmsfjärden (PSM007097) in the Simpevarp area, it can be estimated from the presented data that almost 1% of the Ba in the water column is present in the size fraction  $> 0.22 \mu\text{m}$ , whereas the corresponding figure is 0.01% for Ca and 0.02% for Sr. This indicates that Ba to a higher degree is present in some kind of particles, whereas Ca and Sr to a higher degree are present as dissolved ions (or colloids). This difference is important because it is the suspended material that will sink and form the sediments. For the sediment  $K_d$  sites investigated in this report only a relative quantification is possible, but yet it unambiguously shows that more Ba than Sr and Ca is caught in the filter relative to the amount that passes through it. This is especially apparent for the marine samples. (Engdahl et al. 2008).



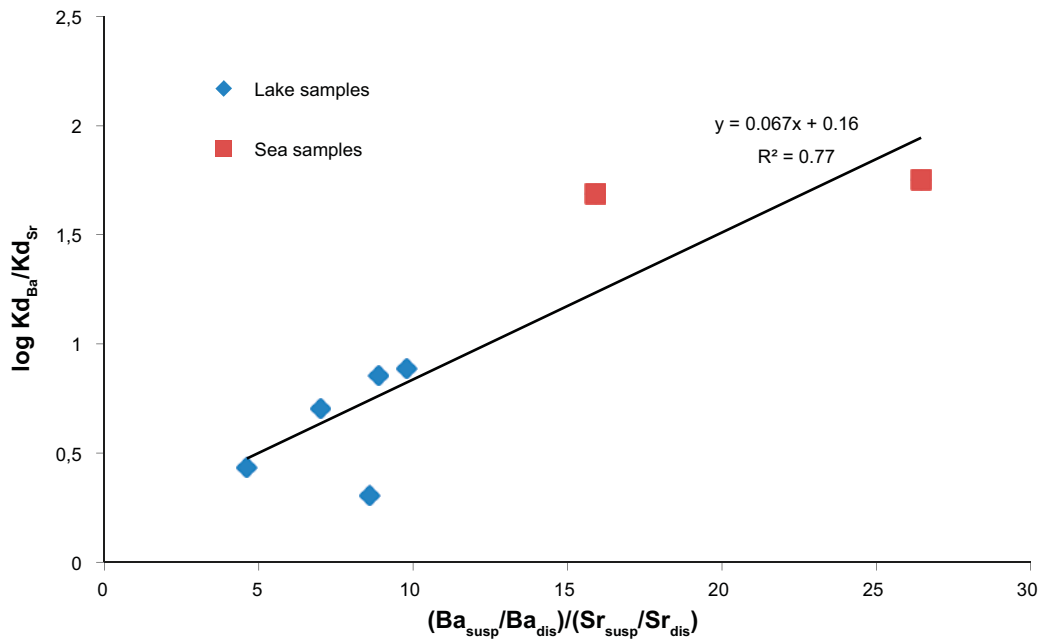


**Figure 6-3.** Difference in  $K_d$  between Ba and Sr in the sediment samples as a function of the relative occurrence in suspended material at each site.

It is possible that Ba has a higher affinity for suspended matter in general, e.g. iron and manganese oxyhydroxide particles or particulate organic matter. However, it is hard to envisage that the differences would be so large that they could cause such fractionation between Ba on one hand and Sr and Ca on the other. Instead, it seems more likely that these suspended particles are barite microcrystals. Measurements of barite from seawater has shown that marine barite tends to precipitate as small crystals or aggregates ranging in size from approximately 0.5 to 5  $\mu\text{m}$  (Dehairs et al. 1980, Bishop 1988). If these observations are representative also for the Baltic Sea, it would imply that barite crystals would not be able to pass through the filter. Hence, the presence of barite microcrystals would explain why Ba deviates from Sr and Ca. If these barite crystals eventually would settle on the sea floor, it would also explain why the  $K_d$  for Ba appears to be so much higher than for Sr and Ca when using total digestion. Indeed, Figure 6-3 shows that the more Ba that is suspended in the water compared to Sr, the more pronounced will the difference in  $K_d$  values be.

Thus, these measurements suggest that barite is present already in the water column. At least in the seawater it suggests that barite is precipitated in the water column. The origin and the age of the barite is probably important for how much Ra it will carry, since the possibility for Ra to substitute Ba in the crystal structure is much better as the crystal is being formed. As was mentioned, it has been observed that the  $^{226}\text{Ra}$  activity in barite decreases exponentially with depth in sediments, which suggests that the exchange with the pore water is limited (van Beek and Reyss 2001). A plausible explanation is that it is difficult for Ra to substitute Ba in the innermost parts of the barite crystals that are not directly exposed to the pore water.

## 6.4 $K_d$ values in soils

### 6.4.1 2009 Soil $K_d$ samples

The 2009  $K_d$  samples stand out because with one exception (PSM000277) the  $K_d$  values for Ba are lower than for Ca and Sr (Sheppard et al. 2009). This is contrary to what was observed in the 2011  $K_d$  samples, where the  $K_d$  values for Ba generally are substantially higher than those for Ca and Sr (Sheppard et al. 2011). However, Figure 6-4 demonstrates that the aqueous Ba concentrations used to calculate the 2009 soil  $K_d$  values are appreciably higher than any other observations that have been made in the Forsmark and Simpevarp areas. The concentrations are likewise much higher than the aqueous Ba concentrations in the 2011 soil  $K_d$  data. While the seven samples in the 2009 soil  $K_d$  dataset displayed Ba concentrations ranging from 706  $\mu\text{g L}^{-1}$  to 2480  $\mu\text{g L}^{-1}$ , the 401 samples from

the Forsmark and Simpevarp site investigations, representing all types of water in the biosphere, all had Ba concentrations between  $7.93 \mu\text{g L}^{-1}$  and  $135 \mu\text{g L}^{-1}$ . The 2011 soil  $K_d$  data, however, agreed well with the site investigation data, displaying a similar range in Ba concentrations:  $7.60\text{--}147 \mu\text{g L}^{-1}$ .

Based on the anomalously high concentrations of Ba in the pore water of the 2009  $K_d$  data the reliability of the 2009  $K_d$  values is questionable. It appears highly unlikely that the Ba concentrations in all of the investigated pore waters from this dataset would be substantially higher than any other observations that have been made in the site investigation areas. This suggests that there is some problem with these analyses. Accordingly, we recommend that the 2009  $K_d$  values for Ba be disregarded.

#### 6.4.2 2011 $K_d$ samples

A compilation of the measured  $K_d$  values for the alkaline earth metals Ca, Sr, Ba and Ra in the 2011  $K_d$  samples can be found in Table 6-2. When comparing  $K_d$  values for the alkaline earth metals in the 2011 soil  $K_d$  samples there are distinct differences between the samples, in which equilibrium with barite is indicated, and the samples, in which it is not. In samples, where the saturation index for barite is below  $-0.5$ , the  $K_d$  values for Ba are on average 5 times higher than for Ca and Sr. However, in samples, where the saturation index for barite is  $-0.1$  or higher, the  $K_d$  values for Ba are on average 10–20 times higher than for Ca and Sr. There is a similar difference between Ra on one hand and Ca and Sr on the other. In unsaturated samples the  $K_d$  value for Ra is approximately 20 times higher than for Ca and Sr, whereas it is on average 30–50 times higher in saturated samples. As a consequence, there are no relative differences between the  $K_d$  value for Ba and Ra, respectively, in saturated and unsaturated samples – the  $K_d$  value for Ra remains on average 3.5 times higher than that for Ba in both types of samples. With one exception (clay gyttja, AMF001367 55 cm) the observed  $K_d$  values are always higher for Ra than for Ba.

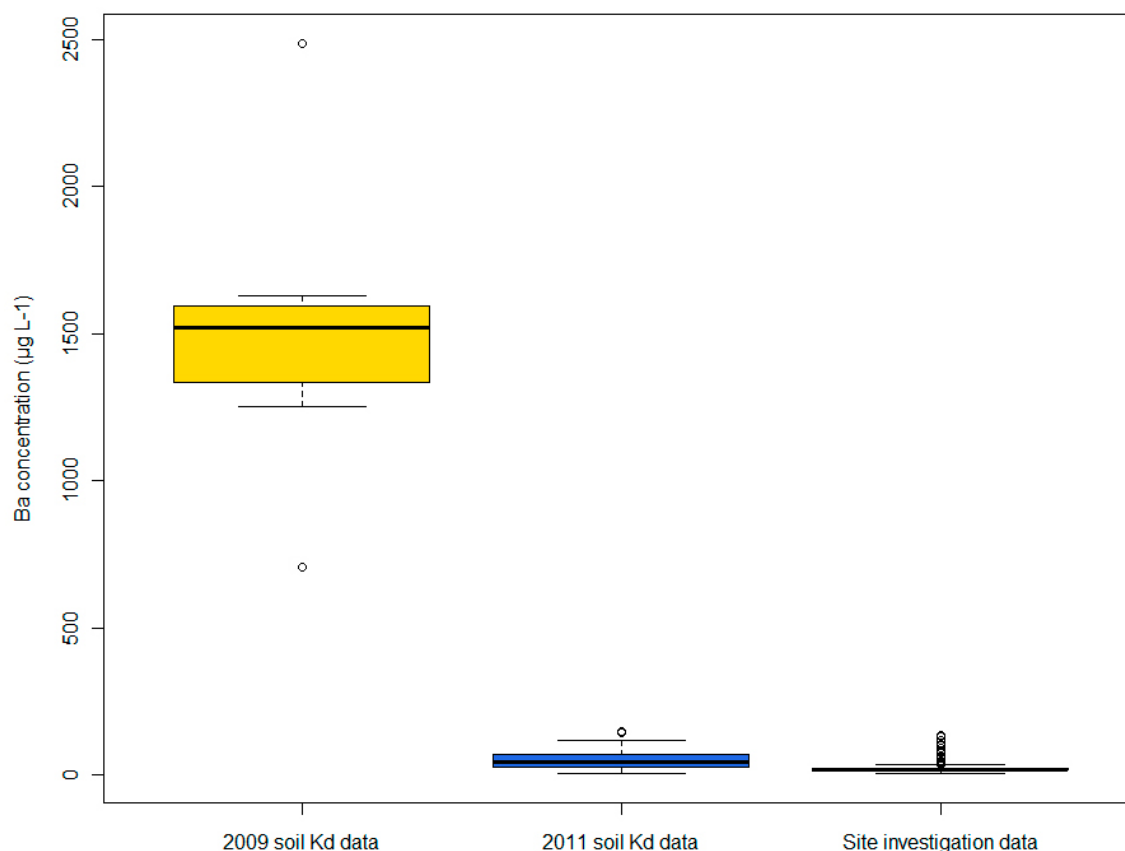


**Figure 6-4.** Aqueous Ba concentrations in the 2009  $K_d$  data ( $n=7$ ), the 2011 soil  $K_d$  data ( $n=50$ ) and the Forsmark and Simpevarp site investigation data ( $n=401$ ), respectively. Clearly, all aqueous Ba concentrations in the 2009  $K_d$  data are substantially higher than any other observations that have been made in Forsmark and Simpevarp.

**Table 6-2. Geometric means (GM) of  $K_d$  ( $L\ kg^{-1}$ ) of sampled wetland and agricultural soils in dataset 4. Geometric standard deviation (GSD) is given in brackets.**

Regolith type	Ba GM (GSD)	Ca GM (GSD)	$^{226}Ra$ GM (GSD)	Sr GM (GSD)
All	1,300 (2,100)	109 (2,800)	3,600 (2,600)	210 (2,400)
Clay till	1,600 (1,600)	260 (2,500)	8,700 (2,300)	200 (2,100)
Clay gyttja	1,300 (2,500)	44 (1,700)	2,600 (1,900)	78 (1,700)
Glacial clay	1,900 (2,300)	180 (3,200)	5,500 (2,200)	250 (2,900)
Cultivated peat	910 (1,800)	240 (2,000)	2,000 (2,200)	270 (2,000)
Wetland peat	950 (1,800)	340 (1,700)	2,100 (2,000)	350 (1,800)

As shown in Figure 6-5, there is generally a good agreement between the  $K_d$  values for Ca and Sr, respectively, especially in the peat samples. As the graph illustrates, there is almost a 1:1 ratio between Ca and Sr in these samples. The chemical resemblance between Ca and Sr and the similar  $K_d$  values suggest that the sorption of Ca and Sr largely is controlled by the same processes. Pronounced differences between Ca and Sr occur mainly in the glacial clay.

When comparing Sr and Ba (Figure 6-6), the picture becomes more complicated. The strong relationship between the  $K_d$  values in cultivated peat and wetland peat remains, but the slope of the regression line has increased, suggesting that there is stronger sorption of Ba in these soils. The  $K_d$  value of Ba is consistently approximately 3 times higher than the corresponding  $K_d$  value of Sr in the peat samples. When comparing to Figure 6-7, where Ra and Sr are shown, the slope of the regression line has increased even further so that the  $K_d$  values for Ra in peat are approximately 5–10 times higher than the  $K_d$  values for Sr.

When comparing the measured  $K_d$  values in the different types of samples, it is clear that the  $K_d$  values for Ba are particularly high in relation to those of Ca and Sr in the clay gyttja – see Table 6-2 for geometric means and Table D-12 in Appendix D. Saturation indices for the  $K_d$  values for each sample. Clay gyttja is the regolith type, in which the thermodynamic modelling most clearly and consistently indicates saturation with respect to barite.

In relation to Ra there seems to be no preferential sorption of Ba in the clay gyttja. On average, the  $K_d$  values for Ra are c 2–3 times higher than for Ba in the clay gyttja, the glacial clay, the cultivated peat and the wetland peat (Figure 6-8). The only exception is the clay till, where the sorption of Ra is approximately eight times higher than for Ba.

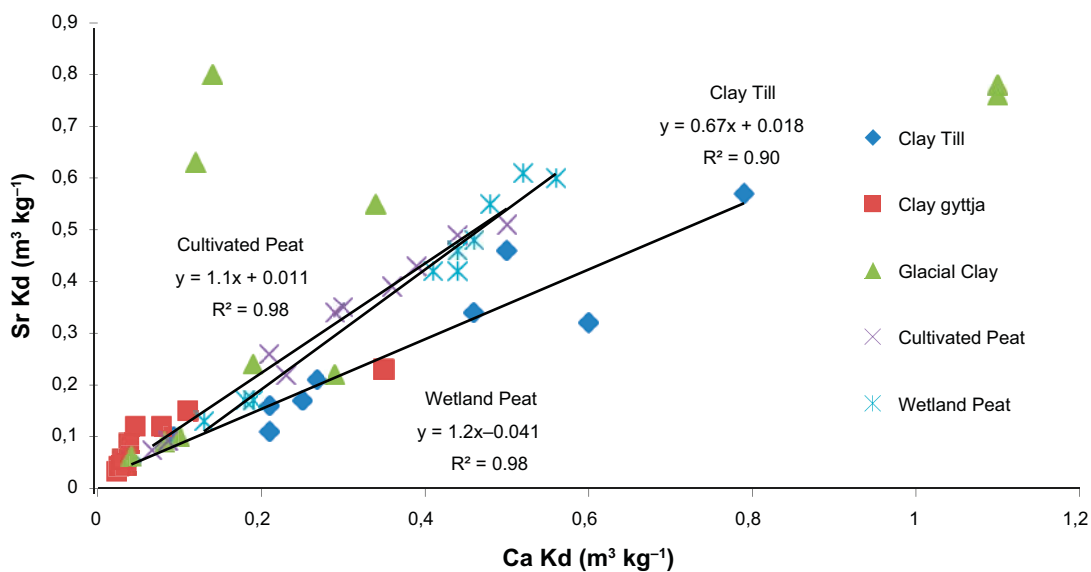


**Figure 6-5. Relationship between the  $K_d$  values for Ca and Sr, respectively, in different types of soils.**

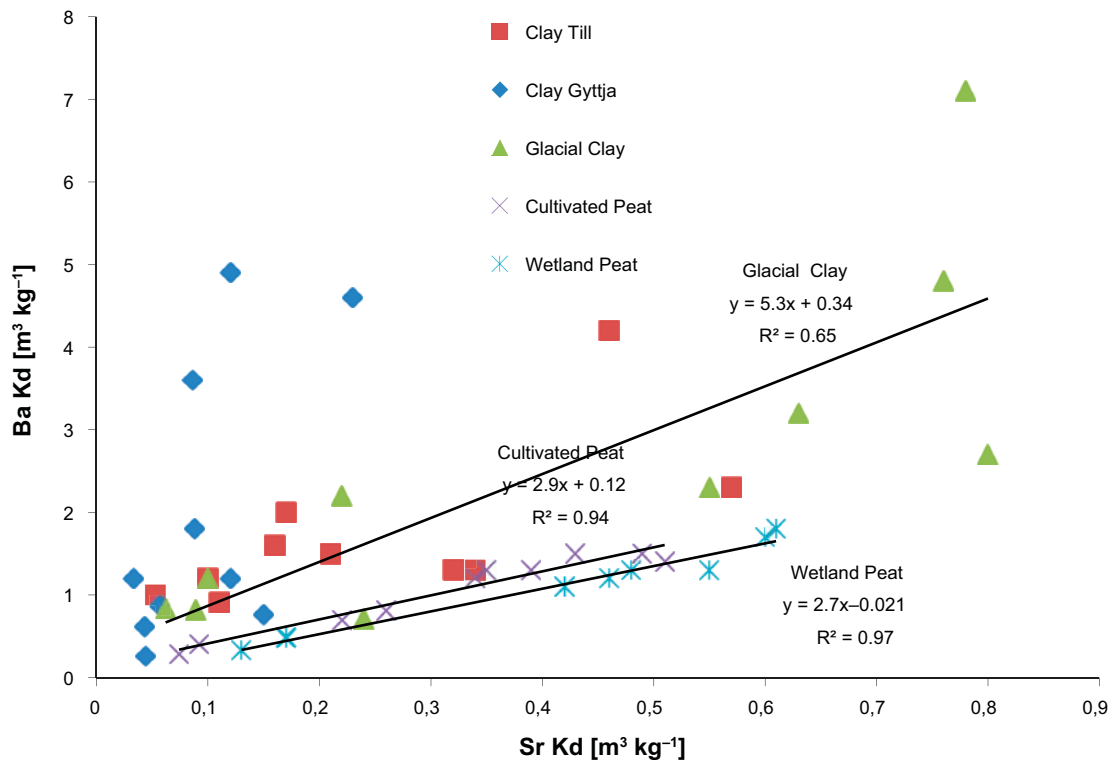


Figure 6-6. Relationships between  $K_d$  for Ba and  $K_d$  for Sr in the five types of soils sampled.

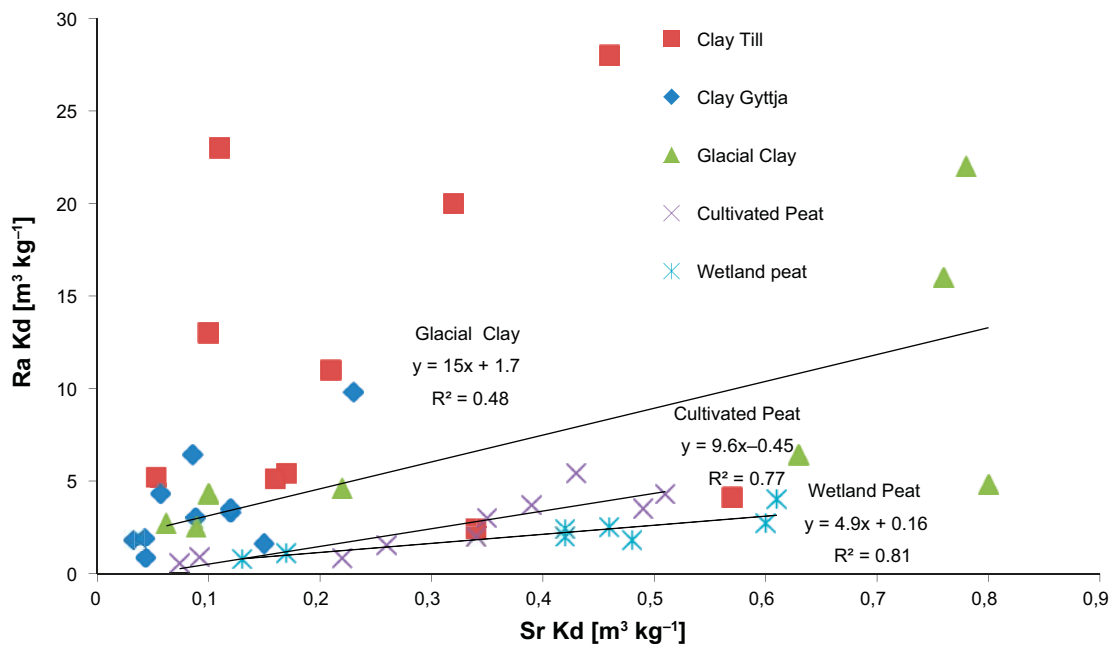


Figure 6-7. Relationships between  $Ra K_d$  och  $Sr K_d$  in the five types of soils sampled 2011.

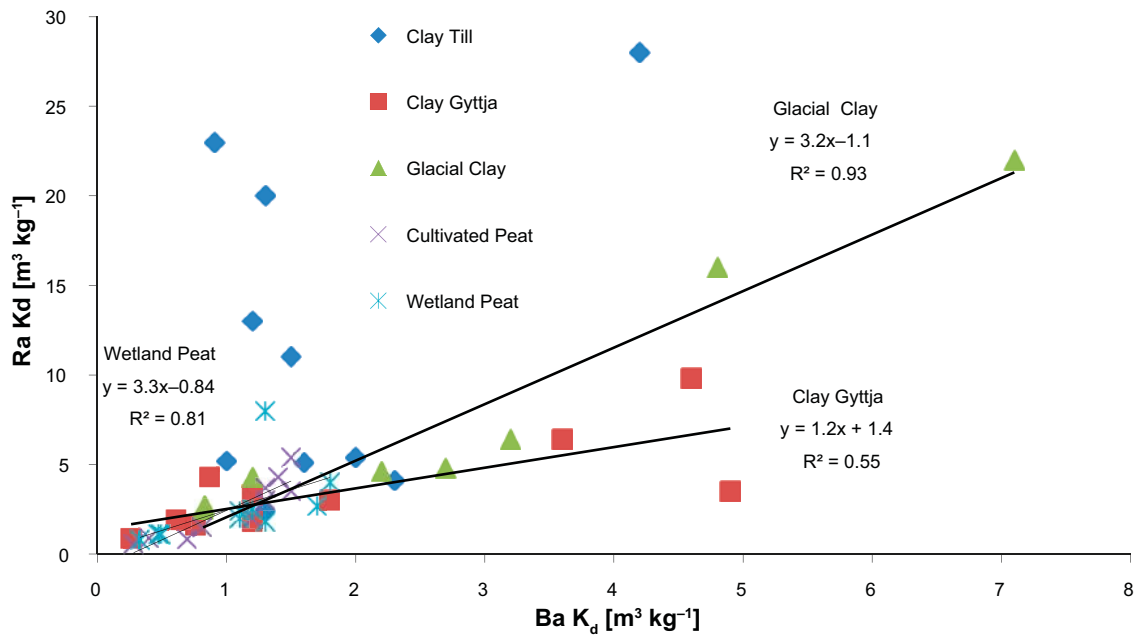


Figure 6-8. Relationship between  $Ra K_d$  and  $Ba K_d$  in the five types of soils sampled 2011.

All of the cultivated peat samples and half of the wetland peat samples were saturated or close to saturation with respect to barite (Table D-12 in Appendix D. Saturation indices), indicating that barite could be present in some of the peat samples. Barite crystals have previously been found in wetlands elsewhere so precipitation of barite in wetlands can obviously occur (Smieja-Król et al. 2010). However, there are no direct indications that this potential presence of barite would influence the  $K_d$  values of Ba appreciably. Firstly, there is no clear difference between samples, where the pore water is saturated with respect to barite, and samples, where the pore water is not. Secondly, the difference in  $K_d$  between Sr and Ba is less than a factor three, which does not seem unreasonable even in the absence of barite. Hence, there is no need to assume the presence of barite in these samples in order to explain the observed  $K_d$  values. Presumably, the sorption of both Sr and Ba in the peat is dominated by the organic material regardless of whether small amounts of barite may be present or not. However, since the  $K_d$  values in question are based on partial extraction by aqua regia, the possibility that significant amounts of barite were present in the residual fraction cannot be excluded.

Figure 6-3 demonstrates that in the clay till the relationship between the  $K_d$  values for Ra and Ba, respectively, vary as a function of the Ra/Ba ratio in the aqueous phase. The samples with large differences between the  $K_d$  values for Ra and Ba, respectively, are mainly found in the clay till. As Figure 6-10 suggests, most of the deviation seems to be caused by low Ra concentrations in the aqueous phase. In terms of the concentrations of Ba, Ra and U in the solid phase and Ba and U in the aqueous phase there is nothing special about these samples. From a chemical perspective it is not obvious why these samples should have particularly low Ra concentrations. It is possible that the low Ra concentrations have induced larger uncertainties or measurements errors. It should be noted that these samples contain the lowest concentrations of  $^{226}\text{Ra}$  that were measured in the 2011  $K_d$  set. The cultivated peat sample with the highest differences between Ra and Ba was also characterized by conspicuously low Ra concentrations in the aqueous phase (Figure 6-10).

Figure 6-11 shows the ratio between the  $K_d$  values for Ba and Sr, respectively, versus the modelled saturation indices for barite. The general impression is that there is no strong tendency of saturated soils, i.e. soils that may be likely to contain barite, to exhibit higher  $K_d$  values for Ba relative to Sr. There are differences between different soil types such as the generally higher  $K_d$  values for Ba in the clay gytja samples, which all show strong supersaturation with respect to barite. However, since measurement of Ba in the solid phase was made using partial extraction by aqua regia, one should not expect that barite – should it indeed be present – would dissolve to any higher degree.

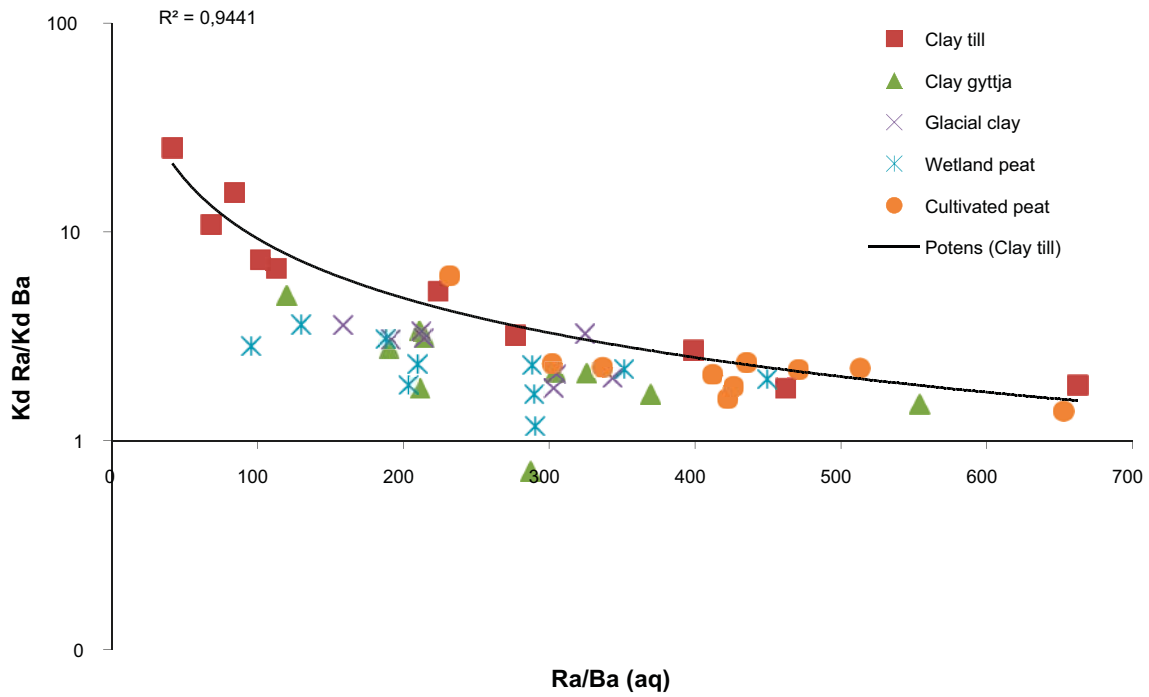


Figure 6-9. The ratio between the  $K_d$  values for Ra and Ba, respectively, vs. the Ra/Ba ratio in the pore water.

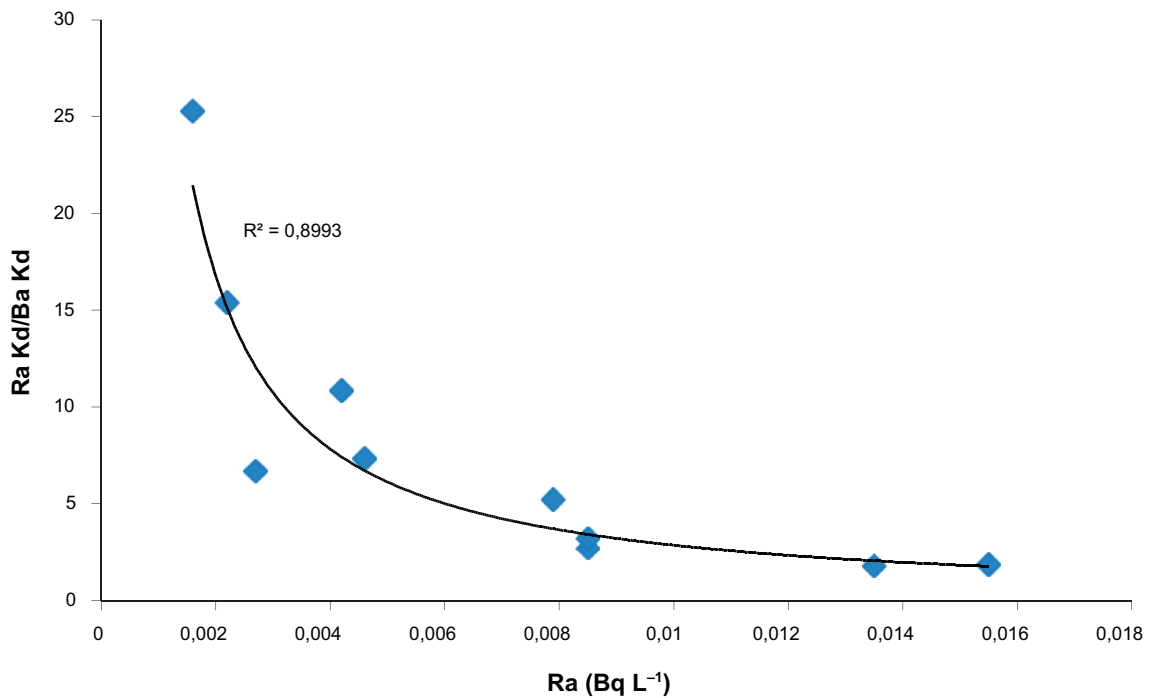
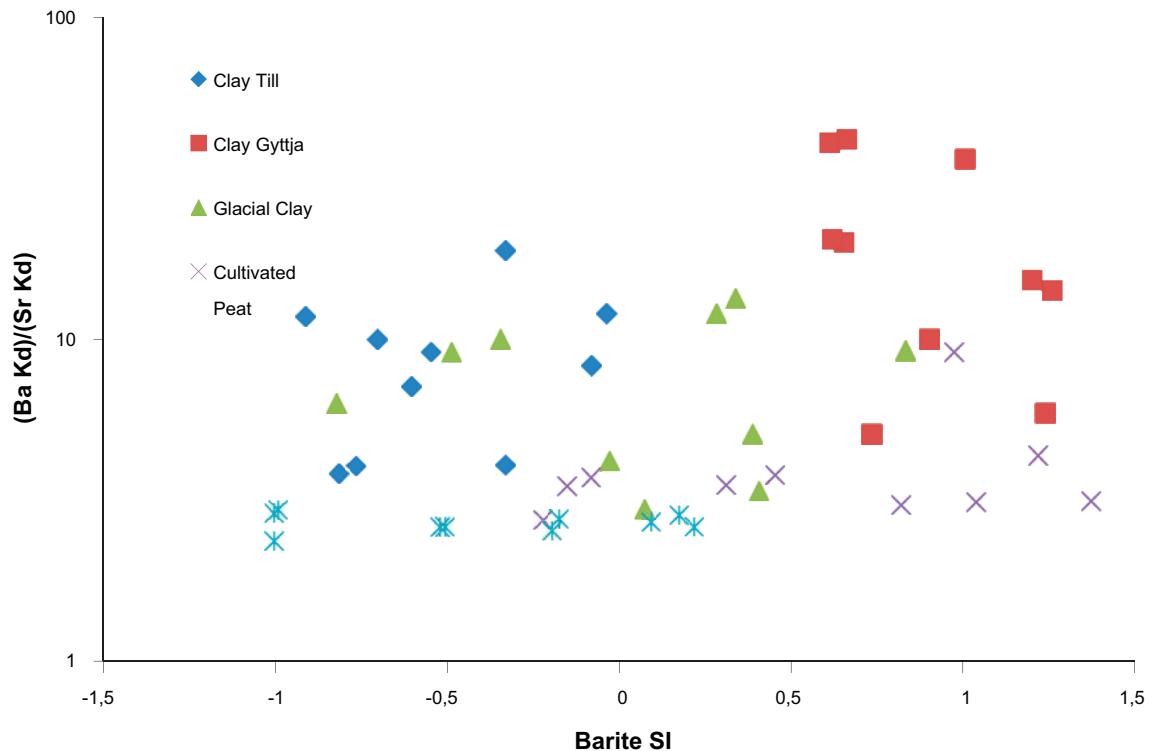


Figure 6-10. The ratio between the  $K_d$  values for Ra and Ba, respectively, in clay till samples as a function of the Ra concentration in the pore water.

Hence, Figure 6-11 provides no clues as to whether any of the samples contain significant amounts of barite or not, but it suggests that barite should have limited influence on the measured  $K_d$  values in the 2011  $K_d$  dataset. This is good in the sense that measurements should provide a more adequate quantification of the sorption of Ba and Ra in these environments, but by using them one also runs the risk of missing the effects of the potentially most important retention mechanism for Ba and Ra in barite-bearing soils. The fact that the  $K_d$  values for Ba are higher than those for Sr even in soils, which cannot be expected to contain barite, indicates that there also are other mechanisms that cause Ba to be less mobile than Sr.



**Figure 6-11.** The ratio between the  $K_d$  values for Ba and Sr, respectively, as a function of the modelled SI for barite in different types of soils in the 2011  $K_d$  data.

## 6.5 Radium and uranium

The analysed Ra isotope,  $^{226}\text{Ra}$ , belongs to the uranium decay chain. This means that it  $^{226}\text{Ra}$  is derived from the decay of  $^{238}\text{U}$  through a series of radionuclides, including  $^{234}\text{U}$  and  $^{230}\text{Th}$ . With a half-life of 1,600 years the occurrence of Ra in the environment is only partly a result of its biogeochemical properties – a fact that makes it different from most other elements. Due to the relatively short half-life of Ra its abundance in the environment is also strongly affected by the presence of  $^{238}\text{U}$  and its daughter radionuclides. In isolated systems  $^{226}\text{Ra}$  will normally reach secular equilibrium with its predecessors in approximately 10,000 years. Hence, there is a limitation to how far from the source  $^{226}\text{Ra}$  can be transported.

At equilibrium the activity ration between  $^{226}\text{Ra}$  and  $^{238}\text{U}$  is unity. Fractionation of  $^{234}\text{U}$  and  $^{230}\text{Th}$  can alter this equilibrium, but since  $^{226}\text{Ra}$  and  $^{238}\text{U}$  are the only radionuclides of the uranium decay chain that have been measured in the 2011  $K_d$  dataset, only these two radionuclides can be compared. Since  $^{234}\text{U}$  and  $^{238}\text{U}$  are isotopes of the same element, their fractionation is usually limited, especially in the solid phase, although it is well-known that there often is a preferential mobilization of  $^{234}\text{U}$ . Th is generally known have low mobility in many environments, and it has a high affinity for organic matter, just like U. However, Th is not redox sensitive like U and, occurring exclusively as a tetravalent ion, does not form as mobile carbonate complexes as the uranyl ion. Therefore, one might expect considerable fractionation between  $^{230}\text{Th}$  and the U isotopes particularly in calcite-rich areas like Forsmark. Accordingly, one cannot relate all differences between  $^{226}\text{Ra}$  and  $^{238}\text{U}$  to differences in the mobility of these two elements only.

Due to the extraction technique that was used for the 2011  $K_d$  samples (aqua regia) the measured activities of  $^{226}\text{Ra}$  and  $^{238}\text{U}$ , respectively, do not correspond to the total activities in the solid phase. Therefore, the activity ratios refer only to the situation in the extractable fraction of the soil. Nevertheless, the activities should still be comparable, since the radionuclides were extracted using the same technique. It is just that the ratios refer not to the total soil matrix, but only to the fraction, which can be dissolved by aqua regia. Given the low solubility of barite in aqua regia this should accordingly exclude most of the barite – should any be present. Hence, one cannot expect to see any pronounced effects of coprecipitation of Ra in the  $^{226}\text{Ra}/^{238}\text{U}$  ratios.

When comparing  $^{226}\text{Ra}$  and  $^{238}\text{U}$  in the solid phase, there are distinct differences between different soil types. These differences are displayed in Figure 6-12. All samples to the right of the vertical axis represent environments where Ra is more mobile than U. Conversely, samples to the left of the vertical axis represent environments where Ra is less mobile than U. All samples above the horizontal axis represent environments where there is an excess of Ra, either due to preferential leaching of U or preferential sorption of Ra. Conversely, samples below the horizontal axis represent environments where there is a Ra deficit, which could be either due to preferential leaching of Ra or preferential sorption of U.

For instance, almost all peat samples (both cultivated peat and wetland peat) are characterised by an excess of U. Since peat naturally contains only minute amounts of U and Ra, it is clear that there has been a preferential accumulation of U rather than a loss of Ra. This is consistent with U having high affinity for organic matter and alkaline earth metals have only modest ditto. Thus, the activity ratios in the peat clearly demonstrate that there is an accumulation of U in peat. The pore waters of the peat can carry an excess of U or – somewhat more frequently – an excess of Ra. Neither of these cases contradicts the conclusion that there is a preferential accumulation U in the peat, but whenever there is an excess of U in the pore waters of the peat, there must also be a higher inflow of U to the system. In two cases there is an excess of Ra in the peat, but both these samples are close to unity.

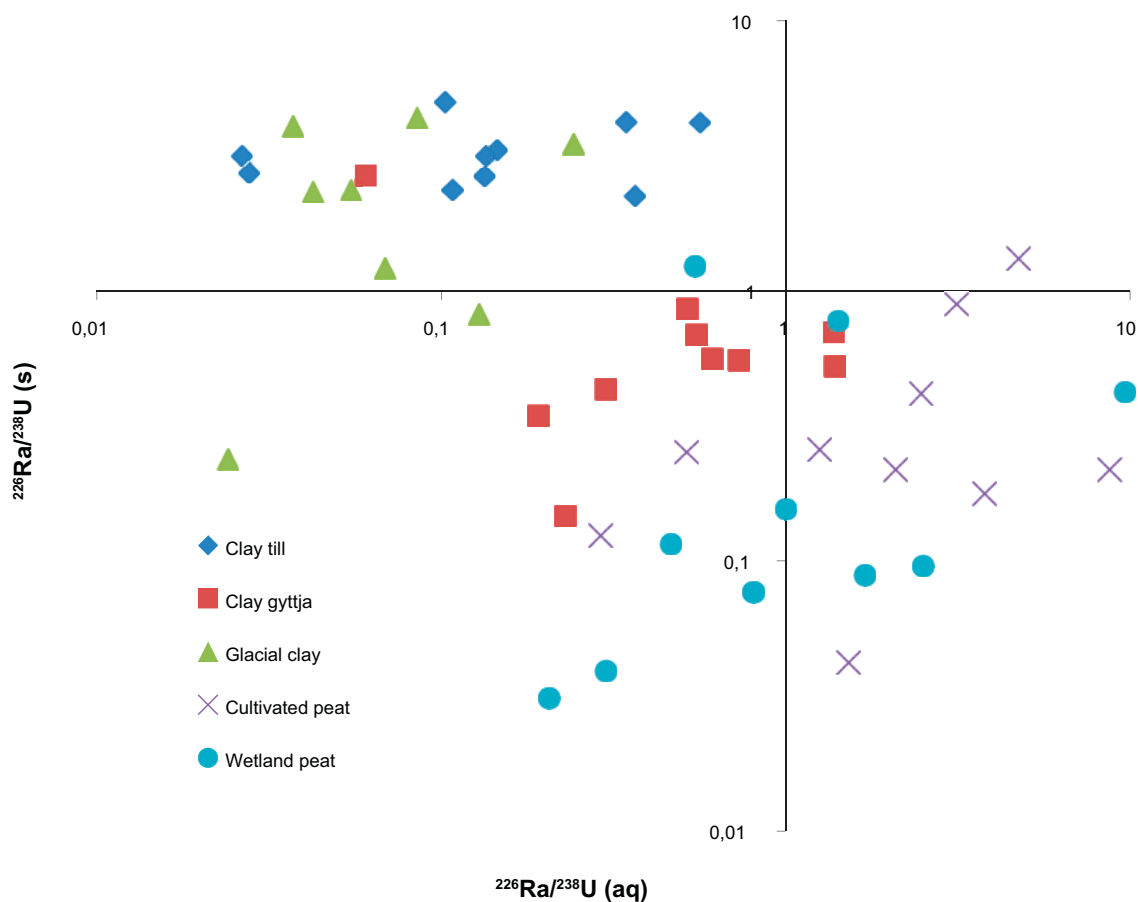


**Figure 6-12.**  $^{226}\text{Ra}/^{238}\text{U}$  activity ratios in soils vs.  $^{226}\text{Ra}/^{238}\text{U}$  ratios in pore water.



The clay gyttja is in most cases characterized by an excess of U both in the aqueous phase and in the solid phase, while the clay till samples consistently have an excess of Ra in the solid phase and an excess of U only in the aqueous phase. Almost all glacial clay samples follow this pattern too. However, since this type of samples naturally contains both Ra and U, the interpretation of the disequilibria becomes more ambiguous. However, one should expect the mobility of U to increase significantly where the carbonate concentrations are high enough to allow the formation of Ca-uranyl-carbonate complexes. This is a likely explanation to the excess of U in the pore waters of the clay gyttja and the glacial clay. These are the two types of soils that are most likely to contain significant amounts of calcite. Hence, a plausible interpretation of the clay gyttja and glacial clay samples is that there is a preferential mobilization of U from these soils. This also implies that there is some process (or processes) that limits the mobility of Ra in these environments. The saturation indices with respect to barite for these samples suggest that coprecipitation of Ra with barite possibly could be one such process in some – but probably not all – of the clay till and glacial clay samples. Active accumulation of Ra (not only lack of mobilization) may of course contribute to the high  $^{226}\text{Ra}/^{238}\text{U}$  ratios in these samples, but the occurrence of such accumulation is not possible to infer unambiguously from these observations.

In the case of the gyttja clay one might generally expect more organic matter and perhaps also less influence from calcite. Both these factors would lower the mobility of U so although there still is an excess of U in the pore water, the excess is still generally smaller than in the clay till and the glacial clay. However, the excess of U in the pore water also coincides with an excess of U in the solid phase. All these samples are oversaturated with respect to barite ( $\text{SI} > 0.6$ ). Together with the fact that the gyttja probably was formed in marine or brackish waters this suggests that barite should be present in these samples. As noted above, however, any Ra present in the barite should largely not be detected in these measurements. One possible explanation to the observed pattern is that a fair part of the Ra that is produced from the decay of U is mobilized and subsequently incorporated into barite. This hypothesis could be tested by measuring the  $^{226}\text{Ra}/^{238}\text{U}$  ratio in the residual remaining after the aqua regia extraction.

When looking at the  $K_d$  values one could also hypothesise that the Ra  $K_d$  values could be influenced by U, particularly if the total extraction would have been used. Since partial extraction was used instead, the potential impact of U on the Ra  $K_d$  values should be limited. In the measured samples there are no trends in any of the soil types that the Ra  $K_d$  values would be particularly high in samples containing high concentrations of U or exhibiting high  $K_d$  values for U. The lack of clear relationships between U and Ra is positive and indicates that the measured  $K_d$  values mainly reflect the geochemical behaviour of Ra than its occurrence in the environment as a member of the uranium decay chain.

## 6.6 Compilation of reported $K_d$ values

A compilation of  $K_d$  values for Ca, Sr, Ba, Ra and U used in various SKB reports – either from site specific measurements or from generic datasets – is given in Table 6-3. There is clear tendency that Ba often exhibits higher  $K_d$  values than Ca and Sr – both in the site specific and the generic data. Since not all samples can be expected to contain barite and those, which do, sometimes are measured without including the barite, there are good reasons to believe that Ba indeed is less mobile than Sr in many environments. Table 6-3 also shows that the most extreme differences between Sr and Ba are, however, observed in samples, which are likely to contain barite, e.g. marine sediments (Engdahl et al. 2008). The potential importance of barite on the  $K_d$  values of Ba are well illustrated by the few measurements, where both partial extraction and total digestion were used (Sheppard et al. 2011). The latter method leads roughly to a tenfold increase in the  $K_d$  values for Ba.

The different techniques that were used to determine the site specific  $K_d$  values also leads to a bias in the dataset because total digestion was used for marine sediments, whereas partial extraction was used in the other environments. Should barite be present also in some of the terrestrial environments, as the thermodynamic modelling indicates, one should expect higher  $K_d$  values for Ba in these environments too. With the present dataset there is a risk that the mobility of Ra is overestimated in many types of soils as compared to marine sediments, where all barite also was dissolved and accounted for.

**Table 6-3. Compilation of reported  $K_d$  values [ $\text{l kg}^{-1}$ ] for Ra, Ba, Ca, Sr and U for soils, sieved bedrock, marine sediments and freshwater sediments from different SKB reports. Ranges of the  $K_d$  values are given in parenthesis. The  $K_d$  values for Ba in soils presented by Sheppard et al. (2009) are given in brackets, since they probably are incorrect (Section 6.4.1).**

Reference	Matrix	Ra	Ba	Ca	Sr	U	Number of samples
(Sheppard et al. 2009)	<b>Soils:</b>						
	Agricultural soils Clay till, peat etc.		210 [27 (15–92)]	120 130 (13–450)	250 160 (33–1,300)	410 4,000 (610–44,000)	GM of 200 GM of 7
	Sand	12,000 <sup>a</sup>					GM of 9
	Loam Clay	3,100 1,100 38,000					IAEA 2010. 51 values from 8 reports
(Nordén et al. 2010)	Inorganic deposits	7,300		34	320	1,500	GM
	Organic deposits	2,300		15	120	6,300	GM of 6
(Sheppard et al. 2011)	All (clay-wetland)	3,600 (550–28,000)	1,300 (260–7,100)	190 (40–490)	210 (43–800)	2,300 (110–40,000)	GM of 50
	Clay till	8,700 (2,400–28,000)	1,600 (910–4,200)	260 (41–790)	200 (53–570)	410 <sup>b</sup> (160–890)	GM of 5
	Clay gyttja	2,600 (870–6,400)	1,300 (260–490)	44 (23–110)	78 (144–150)	3,100 (610–4,400)	GM of 4
	Glacial clay	5,500 (1,900–22,000)	1,900 (610–7,100)	180 (26–350)	250 (43–800)	420 (110–18,000)	GM of 6
	Cultivated peat	2,000 (550–5,400)	910 (280–1,500)	240 (67–500)	270 (74–510)	15,000 (6,100–33,000)	GM of 5
	Wetland peat	2,100 (780–8,000)	950 (330–1,800)	340 (130–560)	350 (130–610)	14,000 (3,500–40,000)	GM of 5
	Sandy till	1,300	190	280	110	17	GM of 8
(Byegård et al. 2008)	<b>Sieved bedrock 1–2 mm:</b>						
	Fresh water <sup>g</sup> Marine <sup>g</sup>	93 (78–110) 17 (10–27)			4.6 (0.7–11) 0.38 (–1.3–3.4)	1 (0.9–12) 2.9 (26.–3.3)	
(Sheppard et al. 2009)	<b>Marine sediments:</b>						
	Marine sediments	30 <sup>c</sup>			5	860	
	IAEA Pelagic $K_d$	4,000			200	500	
	IAEA Coastal $K_d$	2,000			8	1,000	
	SKB benthic $K_d$ SKB susp. $K_d$				77 130	2,500 1,900	
(Nordén et al. 2010)	Susp. particulate matter	4,000		270	19	1,200	
(Sheppard et al. 2011)	Aqua regia digestion <sup>d</sup>	4,530, 1,000 <sup>e</sup>	3,400, 410	39, 26	27, 16	7,400, 3,600	5 and 25 cm depth
	Total digestion <sup>d</sup>		24,000, 3,600	82, 69	110, 82	15,000, 6,900	5 and 25 cm depth
(Engdahl et al. 2008)	Total digestion		5,300 (2,600–12,000)	70 (46–95)	77 (65–100)		GM of 6
(Sheppard et al. 2009)	<b>Freshwater sediments:</b>						
	Susp. $K_d$ (in situ) <sup>f</sup>	7,400			1,200		
	Lit $K_d$				480	15,000	
	SKB benthic $K_d$ SKB susp. $K_d$				410 1,300	5,900 8,400	
(Nordén et al. 2010)	Susp. particulate matter	7,400		700	1,100	6,300	
(Engdahl et al. 2008)	Freshwater sediments		2,200 (770–5,800)	340 (140–860)	410 (210–840)		

a) Ra  $K_d$  values: Vandenhove and Van Hees 2007.

b) In report R-11-24 (Sheppard et al. 2011) the value 77,000 is given, but this is considered a miscalculation.

c) Ra  $K_d$  values: Rama and Moore 1996.

d) In report R-11-24 the columns for aqua regia and total digestion are interchanged.

e) In report R-11-24 the value 35  $\text{m}^3 \text{kg}^{-1}$  is given, but this is a miscalculation.

f) IAEA 2010.

g) Spiked samples,  $t=180$  days.

In Table 6-3 the  $K_d$  values for sieved bedrock stand out, since the  $K_d$  values for Ra, Sr and U are substantially lower than in other matrices (Crawford 2010). In the case of Ra the numbers are partly based on site specific measurements by Byegård et al. (2008) and Selnert et al. (2009). Crawford (2010) recommends Ra  $K_d$  values in the range 0.0039–1.5 L kg<sup>-1</sup>, which at first sight do not seem to agree well  $K_d$  data of Sheppard et al. (2011). However, the  $K_d$  values presented by Crawford (2010) are not directly comparable to those presented by Sheppard et al. (2011) for a number of reasons. Firstly, Crawford (2010) uses a narrower definition of sorption, which means that some of the processes considered by Sheppard et al. (2011) are not included. Whereas Sheppard et al. (2011) considers all possible mechanisms by which an element can be retained in the soil matrix Crawford (2010) strictly focuses on adsorptive interaction with mineral surfaces by electrostatic or covalent chemical bonding. Hence, for elements like Ba and Ra, for which processes such as precipitation and coprecipitation are likely to be important, the two definitions will inevitably lead to different  $K_d$  values. All samples, in which precipitation of barite was suspected to occur, were deliberately excluded by Crawford (2010). Secondly, the values presented by Crawford (2010) are valid for the bedrock only due to the differences in surface area between soils and bedrock. Although the measurements were made using crushed and sieved bedrock, the values were then adjusted for differences in surface area, mechanical damage, cation exchange capacity and groundwater chemistry between the natural conditions and the laboratory conditions. The values presented by Sheppard et al. (2011), on the other hand, were based on soil samples and were not normalized in any way. Since the surface area of bedrock is much lower than the surface area of a normal soil, it is not surprising that the estimated  $K_d$  values for the bedrock are much lower. After all, the sorption is more dependent on the surface area than on the mass, which is the parameter used to calculate the  $K_d$  value. The recommendations of Crawford (2010) are partly based on measurements in fresh bedrock from the Forsmark area with a grain size of 1–2 mm. After a contact time of 180 days  $K_d$  values for Ra in the range 0.16–110 L kg<sup>-1</sup> were observed (Byegård et al. 2008). As shown in Table 6-3, this is in reasonable agreement with the 2011  $K_d$  data given the differences in methodology and material. Hence, there are no reasons to distrust either of the two studies.

## 6.7 The mechanisms behind the $K_d$ values

### 6.7.1 Radium in soils

Besides coprecipitation of radium with barite, there are of course also other retention mechanisms that influence the mobility of radium, e.g. ion exchange and the formation of surface complexes. Since many of the investigated samples show no signs of the presence of barite, coprecipitation of radium with barite is certainly not the only relevant process in the site investigation areas. It is not particularly well known in what soil fractions Ra generally occurs, but a few attempts to answer this question have been made using sequential extraction. Schmid and Wiegand (2003) studied sediments from the Lippe river, a tributary to the Rhine, in Germany. In most samples, the “residual” was the dominating soil fraction. This fraction was believed to mainly represent barite. The “mobile fraction” (leachable by NH<sub>4</sub>NO<sub>3</sub>), the exchangeable fraction and the organic fraction were also of some importance, while Mn and Fe oxyhydroxides were of less importance. Beneš et al. (1983) also used sequential extraction (albeit another analysis protocol) in order to investigate particulate Ra and Ba in waste water from a Czechoslovakian U mine, in nearby river water and in river sediments. Barite was the dominating fraction for both Ba and Ra in all water samples that were affected by the mine (> 80% in most cases). In the uncontaminated water, barite was less important (17–69%), while the “acid soluble” fraction (HCl + H<sub>2</sub>SO<sub>4</sub>) and “crystalline detritus” became more important. Sequential extraction has also been attempted for Swedish soils collected in the Stockholm esker and in Kloten in northern Västmanland (Edsfeldt 2001). In the latter soils most of the extractable Ra was found in the “exchangeable” fraction, while Fe oxides or possibly Fe-organic complexes were more important in the Stockholm soils. The most comprehensive study of the geochemistry of Ra in soils is probably the work of Greeman et al. (1999). Besides investigating <sup>226</sup>Ra/<sup>238</sup>U ratios in soils they also used sequential extraction to study the fractionation of Ra in soils throughout the Eastern USA. The “exchangeable” fraction occasionally contributed with up to 21% of the total Ra, but generally this fraction did not exceed a few percent. The “organic” fraction was often more important, containing up to 26% of the total Ra. In some soils Fe oxides were also important (up to 12%). In total, between 16 and 50% of the Ra was found in pedogenic soil fractions. In relation to U

and Th, Ra was often enriched in the “exchangeable” and “organic” soil fractions. (All soil fractions mentioned in this paragraph are given with citation marks because different extraction methods were used in different studies. Hence, they are not directly comparable. This also illustrates an even more important point, namely that the different soil fractions acquired by sequential extraction ultimately are interpretations.)

### 6.7.2 Radium and manganese

Radium itself is not a redox sensitive element, but it is well-known that Ra has a high affinity for Fe and, in particular, Mn oxyhydroxides (Sun and Torgersen 2001, Charette and Sholkovitz 2006). Mn, in turn, is an element, which is strongly redox dependent. Mn mainly occurs as  $Mn^{2+}$  in reducing environments or as  $Mn^{4+}$  in oxidizing environments. While  $Mn^{2+}$  is fairly mobile in most environments,  $Mn^{4+}$  easily precipitates as  $MnO_2$ . This means that Mn – just like Fe – usually is more mobile under reducing conditions. Due to the association with Mn, Ra can sometimes be indirectly dependent on redox. For instance, Todd et al. (1988) observed a sharp maximum in the activities of  $^{226}Ra$  just below the  $O_2/H_2S$  interface in a Norwegian fjord. The maximum Ra activities coincided with the maxima of  $Fe^{2+}$  and  $Mn^{2+}$ , suggesting that Ra was released from Fe and Mn oxyhydroxides as they were dissolved.

In the evaluation of the 2011  $K_d$  data Sheppard et al. (2011) observed that Mn  $K_d$  values had a distinct bipolar distribution with generally high  $K_d$  values in clay till and low  $K_d$  values in clay gyttja, glacial clay, cultivated peat and wetland peat. At least partly, this should be related to the oxidation state of Mn in different types of soils, i.e. relatively high mobility of  $Mn^{2+}$  in reducing environments and low solubility of  $Mn^{4+}$  in oxidizing environments. As for all elements, the mobility can be governed by a wide range of processes, but high  $K_d$  values for Mn could be in indication that significant amounts of  $MnO_2$  are present. Often this implies that Fe oxyhydroxides also might be present.

When comparing the Ra  $K_d$  values and the Ba  $K_d$  values in the 2011  $K_d$  data, Ba can explain 54% of the variability in Ra on a log scale ( $p < 0.001$ ). Ra is also significantly dependent on Mn ( $r^2 = 0.49$ ) and Fe ( $r^2 = 0.44$ ), indicating that Ra is less mobile in environments where Mn and Fe have low mobility ( $p < 0.001$  for both). Due to the redox behaviour of Fe and Mn this suggests that Ra generally is less mobile in oxidizing environments. One explanation to this relationship could be sorption of Ra onto Fe and Mn oxyhydroxides. It is particularly interesting to note that the dependence on Mn remains even when accounting for the dependence on Ba. A multiple linear regression based on Ba and Mn without interaction terms can explain 63% of the variability in the Ra  $K_d$  ( $L\ kg^{-1}$ ) values ( $p < 0.01$ ):

$$\log_{10}(Ra) = 0.94 + 0.62 \times \log_{10}(Ba) + 0.13 \times \log_{10}(Mn) \quad (6-1)$$

This relationship is illustrated in Figure 6-13.

### 6.7.3 Dealing with barite in transport models

In safety assessments precipitation and coprecipitation are often not considered to contribute to the retention of radionuclides. This is not because these processes are thought to be unimportant, but rather because they are considered difficult to implement adequately in transport models (Crawford 2010). In the geosphere it is easy to justify the exclusion of precipitation and coprecipitation as a conservative assumption – neglecting precipitation and coprecipitation will invariably result in higher mobility for the radionuclides in question and, accordingly, higher transport to the biosphere. However, the consequences of a similar assumption in the biosphere are harder to foresee without careful considerations and testing. The outcome will partly depend on which compartments that are assumed to contain barite and which are not. Hence, whether or not the effects of barite should be included in the biosphere  $K_d$  values is not a straightforward question to answer. As discussed in Section 2.1.1, a linear  $K_d$  model is not ideal for describing the mobility of substances that are controlled by precipitation-dissolution processes. On the other hand, where barite is present, coprecipitation of Ra with barite clearly has the potential to be the dominating retention mechanism. Hence, not considering barite may lead to a considerable overestimation of the mobility of Ra.

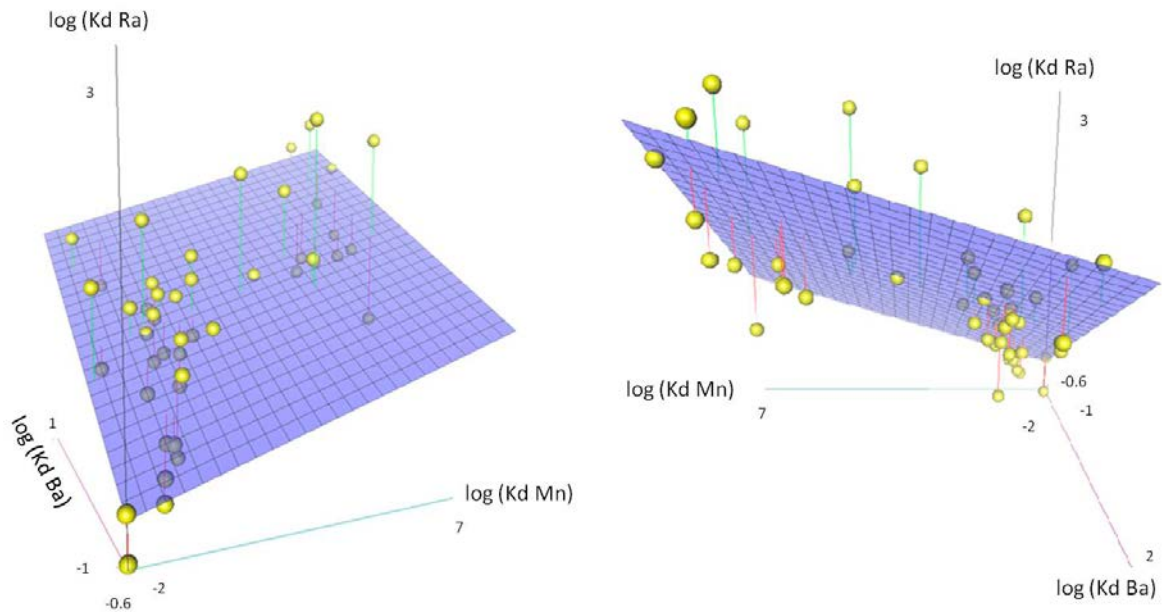


**Figure 6-13.** *Ra  $K_d$  values as a function of Ba and Mn  $K_d$  values in the 2011  $K_d$  dataset (Sheppard et al. 2011). The same graph is shown from two different angles. All axes are on a log scale. The regression surface represents Equation 6-1.*

Currently, the sediment  $K_d$  values are based on total digestion. These samples are characterised by clear differences between Ba on one hand and Ca and Sr on the other, which probably are caused by the presence of barite. However, the 2011  $K_d$  values are based on partial extraction by aqua regia so the impact of barite in these samples should be limited. Not all samples show signs of being saturated with respect to barite, but some do, and in these cases the observed  $K_d$  values for Ba and Ra should probably be regarded as minimum  $K_d$  values – unless one wishes to entirely neglect the effects of barite for some reason. Regardless of whether one chooses to include or exclude the effects of barite in the  $K_d$  values, there is an imbalance between the soil  $K_d$  values and the sediment  $K_d$  values due to the different analysis methods. This results in seemingly lower mobility of Ra and Ba in sediments as compared to soils, which is not a fair representation of the actual conditions.

What effect barite will have on the apparent  $K_d$  values for Ra and Ba will ultimately depend on what amounts of barite that are present in different environments. This issue is not easy to assess, since the barite has not yet been observed in the soils, let alone quantified. Still, one can get some sense of what to expect by considering the two samples, where both total digestion and partial extraction by aqua regia were used to quantify Ba in the solid phase. Both these samples were marine sediments so they should represent an environment where the amount of barite should be relatively high in comparison to other environments. When comparing the differences between total digestion and aqua regia extraction, the  $K_d$  values for most elements, including Ca and Sr, in these samples were approximately doubled (Table 6-3). In the case of Ba, however, there was almost a tenfold increase in the  $K_d$  values. In this sense Ba is similar to elements like Si, Zr and Hf, which usually occur in resistant minerals such as zircon and various silicates. By analogy with Ca and Sr one can estimate the Ba  $K_d$  to be doubled when including resistant minerals other than barite, in which Ba may occur. If we assume that the rest of the increase is caused by barite, this would imply an increase by a factor 3–5. However, one must also consider that fact the extractions using aqua regia potentially could be affected by the presence of barite, although its solubility in aqua regia is low. One reason to suspect this is that the  $K_d$  values for Ba in the youngest sediments are roughly 100 times higher than those for Ca and Sr, when using aqua regia. It is not unlikely that the barite-free  $K_d$  values of Ba should be higher than those of Ca and Sr, but if we for the sake of argument rely on the chemical similarities between these three elements and assume that the barite-free  $K_d$  values for Ba are comparable to those of Ca and Sr, the barite could potentially have caused an increase in the observed  $K_d$  value for Ba in marine sediments by a factor 200. This latter estimate is also more consistent with the observations in Borholmsfjärden, where Ba was 50–100 times more abundant than Ca and Sr in suspended particles in relation to their concentration in the aqueous phase (Engdahl et al. 2008).

As regards Ra, its  $K_d$  values are further affected by the efficiency of the coprecipitation. However, whether one assumes solid solution to be ideal, as Crawford (2010), or slightly non-ideal, as in this study, the relative uptake of Ra and Ba into barite will be reasonably similar. Hence, one could expect the Ra  $K_d$  values to increase by more or less the same factor as the Ba  $K_d$  values if barite was to be accounted for.

#### **6.7.4 Barite in the future landscape**

In the long-term perspective – on timescales of thousands of years and beyond – it is obvious that the  $K_d$  values are likely to change as the landscape ages. In order to assess such changes in the chemical behavior of various radionuclides it is important to have some idea about what processes that the  $K_d$  values represent. It is beyond the scope of this report to go through all changes in the soil and water chemistry that are likely to occur, but it may be worth to make some remarks concerning the potential role of barite in the future. As far as we know, the precipitation of barite in marine environments is likely to continue. As the land rise advances, the emerging soils will all have the potential to contain barite due to their marine origin. It is possible that this also is the reason why many soils in the site investigation areas today seem to be saturated with respect to barite. How long this saturation may continue to control the mobility of Ba and Ra depends on how active the barite is and how large amounts of barite there are. Based on the available data it is hard to give a conclusive answer to this question, but there are good reasons to believe that barite will remain the controlling phase for Ba in parts of the soils of the site investigation areas in the future. This suggests that the role of coprecipitation of radium with barite will be important also in the future landscape.

## 7 Conclusions

The results of this study have demonstrated that there are good reasons to believe that barite is present in parts of both the Forsmark and Simpevarp areas and that it is likely to have far-reaching effects on the mobility of Ba and Ra. Thermodynamic modelling of the local hydrochemistry has shown that the near-surface groundwater and surface water in many cases are saturated with respect to barite. This implies that the aqueous concentrations – and hence the mobility – of Ba at many sites seems to be controlled by barite. In addition, a thorough literature review has shown that the presence of barite in marine environments is a well-known and widely established fact. Therefore, it appears likely that barite should be present in areas with a recent marine history such as Forsmark and Simpevarp. The available data also suggest that large amounts of Ba in sediments are present in a more resistant mineral fraction than Ca and Sr, which may very well be barite. Furthermore, it has been observed that Ba, in relative terms, is more common in the particulate phase of sea water than Ca and Sr, which again is consistent with the assumption that barite is present. The thermodynamic modelling has also demonstrated that many types of waters, in particular in the Forsmark area, are saturated with respect to aragonite/calcite. This is in full accordance with the high concentrations of  $\text{CaCO}_3$  that previously have been observed.

As regards Ra, all available literature suggests that the occurrence of barite in soils and sediments will lead to coprecipitation of Ra, thereby decreasing the mobility of Ra. Thermodynamic modelling of the coprecipitation of Ra with barite also indicates that the presence of barite should have a considerable influence on  $K_d$  values of Ra at certain sites, e.g. marine sediments. Ca and Sr, on the other hand, are not expected to be affected to the same extent by coprecipitation with barite. Therefore, barite presents a plausible explanation to some of the differences that have been observed in the site investigation areas between Ca and Sr on one hand and Ba and Ra on the other.

If barite indeed is present in some of the samples used for  $K_d$  measurements, the choice of extraction method is likely to have a profound impact on the site specific  $K_d$  values – as suggested by the investigated marine sediment samples (Sheppard et al. 2011). In the sediment  $K_d$  dataset, total digestion was used, so any barite that was present in the sediments was included in the  $K_d$  values. In the soil  $K_d$  measurements (both 2009 and 2011) partial extraction by aqua regia was used. Since barite has very low solubility in aqua regia, most barite – if present – would not dissolve. Hence, the soil  $K_d$  values would not fully reflect the effect of barite on the retention of Ba. Due to anomalously high concentrations of Ba in the pore water of the 2009  $K_d$  samples (Sheppard et al. 2009) it is recommended that these  $K_d$  values are not used.

Since the role of barite for the mobility of Ra is dependent on the amount of barite, it is hard to make a quantitative estimation of its effects on the  $K_d$  values for Ra, especially in samples where the total Ba concentration is unknown. Based on the thermodynamic modelling of Ra coprecipitation with barite and the available experimental data it was not possible to achieve as high  $K_d$  values for Ra as were observed in by Sheppard et al. (2011). This may depend on uncertainties in the parametrisation of the model or the influence of other mechanisms than coprecipitation.

Without more detailed measurements of barite and its content of Ra from the Forsmark and Simpevarp areas it is hard to draw any certain conclusions concerning the quantitative effects of barite on the mobility of Ra. However, there are good reasons to believe that barite is present in parts of the site investigation areas and that coprecipitation of Ra with barite potentially might constitute the most important retention mechanism for radium. Accordingly, neglecting coprecipitation of Ra with barite might lead to an appreciable overestimation of its mobility.

In short, the main findings of this report can be summarised in the following points:

- Thermodynamic modelling indicates that many waters throughout the site investigation areas are saturated with respect to barite and calcite. The presence of calcite is well-known and has been confirmed before, above all in Forsmark, whereas barite so far only has been observed in the bedrock.
- Precipitation of barite is well-known to occur in sea water so given the marine history of the Forsmark and Simpevarp areas it would not be surprising if barite was present, especially in old sediment soils. Furthermore, barite can also occur as a primary mineral in Swedish soils.

- Although direct observations are lacking, the occurrence of barite is consistent with previous observations from the site investigation areas, e.g. higher relative concentrations of particulate Ba relative to Sr and Ca and higher relative concentrations of Ba in insoluble mineral fractions.
- All relevant literature and the thermodynamic modelling suggest that Ra will coprecipitate with barite. The uptake of Ra in barite is potentially the most important retention mechanism for Ra wherever barite is present. Neglecting it would therefore lead to an overestimation of the mobility of Ra.
- Occurrence of barite is one possible explanation to the observed differences in the site specific  $K_d$  values for Ba and Ra on one hand and Ca and Sr on the other hand.
- Different measurement techniques have caused a potential bias in the site specific  $K_d$  dataset, leading to high  $K_d$  values for Ba in marine sediments (based on total digestion) and low  $K_d$  values for Ba in soils (based on partial extraction, which does not dissolve barite). Hence, the effects of barite are probably not fully accounted for in the soil  $K_d$  values.
- The  $K_d$  values for Ba presented by Sheppard et al. (2009) are probably incorrect due to anomalously high concentration of Ba in the pore water.



## References

SKB's (Svensk Kärnbränslehantering AB) publications can be found at [www.skb.se/publications](http://www.skb.se/publications).

- Ansari T M, Marr I L, Coats A M, 2001.** Characterisation of mineralogical forms of barium and trace heavy metal impurities in commercial barytes by EPMA, XRD and ICP-MS. *Journal of Environmental Monitoring: JEM* 3, 133–138.
- Appelo C A J, Postma D, 2005.** *Geochemistry, groundwater and pollution*. 2nd ed. Leiden: Balkema.
- Baker P, Bloomer S, 1988.** The origin of celestite in deep-sea carbonate sediments. *Geochimica et Cosmochimica Acta* 52, 335–339.
- Beneš P, Šebesta F, Sedláček J, Obdržálek M, Šandrik R, 1983.** Particulate forms of radium and barium in uranium-mine waste-waters and receiving river waters. *Water Research* 17, 619–624.
- Bernstein R E, Byrne R H, 2004.** Acantharions and marine barite. *Marine Chemistry* 86, 45–50.
- Bishop J K B, 1988.** The barite-opal-organic carbon association in oceanic particulate matter. *Nature* 332, 341–343.
- Bosbach D, Böttle M, Metz V, 2010.** Experimental study on  $Ra^{2+}$  uptake by barite ( $BaSO_4$ ). Kinetics of solid solution formation via  $BaSO_4$  dissolution and  $Ra_xBa_{1-x}SO_4$  (re) precipitation. SKB TR-10-43, Svensk Kärnbränslehantering AB.
- Byegård J, Selnert E, Tullborg E-L, 2008.** Bedrock transport properties. Data evaluation and retardation model. Site descriptive modelling, SDM-Site Forsmark. SKB R-08-98, Svensk Kärnbränslehantering AB.
- Böttcher M E, Lepland A, 2000.** Biogeochemistry of sulfur in a sediment core from the west-central Baltic Sea: evidence from stable isotopes and pyrite textures. *Journal of Marine Systems* 25, 299–312.
- Caron D A, Swanberg N R, 1990.** The ecology of planktonic sarcodines. *Reviews in Aquatic Sciences* 3, 147–180.
- Charette M A, Sholkovitz E R, 2006.** Trace element cycling in a subterranean estuary: Part 2. Geochemistry of the pore water. *Geochimica et Cosmochimica Acta* 70, 811–826.
- Church T M, Wolgemuth K, 1972.** Marine barite saturation. *Earth and Planetary Science Letters* 15, 35–44.
- Crawford J, 2010.** Bedrock  $K_d$  data and uncertainty assessment for application in SR-Site geosphere transport calculations. SKB R-10-48, Svensk Kärnbränslehantering AB.
- Curti E, 1999.** Coprecipitation of radionuclides with calcite: estimation of partition coefficients based on a review of laboratory investigations and geochemical data. *Applied Geochemistry* 14, 433–445.
- Curti E, Fujiwara K, Iijima K, Tits J, Cuesta C, Kitamura A, Glaus M A, Muller W, 2010.** Radium uptake during barite recrystallization at  $23 \pm 2^\circ C$  as a function of solution composition: an experimental  $^{133}Ba$  and  $^{226}Ra$  tracer study. *Geochimica et Cosmochimica Acta* 74, 3553–3570.
- Dehairs F, Chesselet R, Jedwab J, 1980.** Discrete suspended particles of barite and the barium cycle in the open ocean. *Earth and Planetary Science Letters* 49, 528–550.
- Dietzel M, Gussone N, Eisenhauer A, 2004.** Co-precipitation of  $Sr^{2+}$  and  $Ba^{2+}$  with aragonite by membrane diffusion of  $CO_2$  between 10 and  $50^\circ C$ . *Chemical Geology* 203, 139–151.
- Doerner H A, Hoskins W M, 1925.** Co-precipitation of Ra and Ba sulphates. *Journal of the American Chemical Society* 47, 662–675.
- Drake H, Tullborg E-L, 2007.** Oskarshamn site investigation. Fracture mineralogy. Results from drill cores KLX03, KLX04, KLX06, KLX07A, KLX08 and KLX10A. SKB P-07-74, Svensk Kärnbränslehantering AB.

- Dymond J, Suess E, Lyle M, 1992.** Barium in deep-sea sediment: a geochemical proxy for paleo-productivity. *Paleoceanography* 7, 163–181.
- Edsfeldt C, 2001.** The radium distribution in some Swedish soils and its effect on radon emanation. PhD thesis. Royal Institute of Technology, Stockholm. Available at: <http://kth.diva-portal.org/smash/get/diva2:8981/FULLTEXT01>
- Engdahl A, Rådén R, Borgiel M, Omberg L-G, 2008.** Oskarshamn and Forsmark site investigation. Chemical composition of suspended material, sediment and pore water in lakes and sea bays. SKB P-08-81, Svensk Kärnbränslehantering AB.
- Fairclough A, Plater A, Appleby P, 2006.** Determination of Holocene sedimentation rates from a carbonate lake using excess  $^{226}\text{Ra}$  profiles. *Earth and Planetary Science Letters* 243, 115–127.
- Gingele F, Dahmke A, 1994.** Discrete barite particles and barium as tracers of paleoproductivity in south Atlantic sediments. *Paleoceanography* 9, 151–168.
- Glynn P D, Reardon E J, 1990.** Solid-solution aqueous-solution equilibria: thermodynamic theory and representation. *American Journal of Science* 290, 164–201.
- Gnanapragasam E K, Lewis B-A G, 1995.** Elastic strain energy and the distribution coefficient of radium in solid solutions with calcium salts. *Geochimica et Cosmochimica Acta* 59, 5103–5111.
- Gonnea M E, Paytan A, 2006.** Phase associations of barium in marine sediments. *Marine Chemistry* 100, 124–135.
- Gonzalez-Muñoz M T, Martinez-Ruiz F, Morcillo F, Martin-Ramos J D, Paytan A, 2012.** Precipitation of barite by marine bacteria: a possible mechanism for marine barite formation. *Geology* 40, 675–678.
- Gooday A J, Nott J A, 1982.** Intracellular barite crystals in two xenophyophores, *Aschemonella ramuliformis* and *Galatheaamina* sp. (Protozoa, Rhizopoda) with comments on the taxonomy of *A. ramuliformis*. *Journal of the Marine Biological Association of the United Kingdom* 62, 595–605.
- Grandia F, Merino J, Bruno J, 2008.** Assessment of the radium-barium co-precipitation and its potential influence on the solubility of Ra in the near-field. SKB TR-08-07, Svensk Kärnbränslehantering AB.
- Greeman D J, Rose A W, Washington J W, Dobos R R, Ciolkosz E J, 1999.** Geochemistry of radium in soils of the Eastern United States. *Applied Geochemistry* 14, 365–385.
- Gustafsson J P, 2012.** Visual MINTEQ ver 3.0. Available at: <http://www2.lwr.kth.se/english/OurSoftware/Vminteq/index.html>
- Hannu S, Karlsson S, 2006.** Forsmark site investigation. Chemical characterisation of deposits and biota. SKB P-06-220, Svensk Kärnbränslehantering AB.
- Hedenström A, Sohlenius G, 2008.** Description of the regolith at Forsmark. Site descriptive modelling, SDM-Site Forsmark. SKB R-08-04, Svensk Kärnbränslehantering AB.
- Helgeson H C, Delany J M, Nesbitt H W, Bird D K, 1978.** Summary and critique of the thermodynamic properties of rock-forming minerals. *American Journal of Science* 278, 1–229.
- IAEA, 2010.** Handbook of parameter values for the prediction of radionuclide transfer in terrestrial and freshwater environments. Vienna: International Atomic Energy Agency. (Technical Reports Series 472) Available at: [http://www-pub.iaea.org/MTCD/publications/PDF/trs472\\_web.pdf](http://www-pub.iaea.org/MTCD/publications/PDF/trs472_web.pdf)
- Jones M J, Butchins L J, Charnock J M, Patrick R A D, Small J S, Vaughan D J, Wincott P L, Livens F R, 2011.** Reactions of radium and barium with the surfaces of carbonate minerals. *Applied Geochemistry* 26, 1231–1238.
- Langmuir D, Riese A C, 1985.** The thermodynamic properties of radium. *Geochimica et Cosmochimica Acta* 49, 1593–1601.
- Lauria D C, Almeida R M R, Sracek O, 2004.** Behavior of radium, thorium and uranium in groundwater near the Buena Lagoon in the Coastal Zone of the State of Rio de Janeiro, Brazil. *Environmental Geology* 47, 11–19.

- Lin C-C, Tsai T-L, Lung C-C, 2012.** Impact of water environmental change and migration of radionuclides on Hokutulite conservation in Peito (Taiwan). *Radiochimica Acta* 100, 329–338.
- McManus J, Berelson W M, Klinkhammer G P, Kilgore T E, Hammond D E, 1994.** Remobilization of barium in continental margin sediments. *Geochimica et Cosmochimica Acta* 58, 4899–4907.
- Monnin C, Cividini D, 2006.** The saturation state of the world's ocean with respect to (Ba,Sr)SO<sub>4</sub> solid solutions. *Geochimica et Cosmochimica Acta* 70, 3290–3298.
- Monnin C, Jeandel C, Cattaldo T, Dehairs F, 1999.** The marine barite saturation state of the world's oceans. *Marine Chemistry* 65, 253–261.
- Nordén S, Avila R M, de la Cruz I, Stenberg K, Grolander S, 2010.** Element-specific and constant parameters used for dose calculations in SR-Site. SKB TR-10-07, Svensk Kärnbränslehantering AB.
- Paige C R, Kornicker W A, Hileman O E, Snodgrass W J, 1998.** Solution equilibria for uranium ore processing: the BaSO<sub>4</sub>–H<sub>2</sub>SO<sub>4</sub>–H<sub>2</sub>O System and the RaSO<sub>4</sub>–H<sub>2</sub>SO<sub>4</sub>–H<sub>2</sub>O system. *Geochimica et Cosmochimica Acta* 62, 15–23.
- Paytan A, Mearon S, Cobb K, Kastner M, 2002.** Origin of marine barite deposits: Sr and S isotope characterization. *Geology* 30, 747–750.
- Paytan A, Moore W S, Kastner M, 1996.** Sedimentation rate as determined by <sup>226</sup>Ra activity in marine barite. *Geochimica et Cosmochimica Acta* 60, 4313–4319.
- Pierret M C, Chabaux F, Leroy S A G, Causse C, 2012.** A record of Late Quaternary continental weathering in the sediment of the Caspian Sea: evidence from U–Th, Sr isotopes, trace element and palynological data. *Quaternary Science Reviews* 51, 40–55.
- Plummer L N, Busenberg E, 1982.** The solubilities of calcite, aragonite and vaterite in CO<sub>2</sub>–H<sub>2</sub>O solutions between 0 and 90°C, and an evaluation of the aqueous model for the system CaCO<sub>3</sub>–CO<sub>2</sub>–H<sub>2</sub>O. *Geochimica et Cosmochimica Acta* 46, 1011–1040.
- Rama, Moore W S, 1996.** Using the radium quartet for evaluating groundwater input and water exchange in salt marshes. *Geochimica et Cosmochimica Acta* 60, 4645–4652.
- Rihs S, Condomines M, 2002.** An improved method for Ra isotope (<sup>226</sup>Ra, <sup>228</sup>Ra, <sup>224</sup>Ra) measurements by gamma spectrometry in natural waters: application to CO<sub>2</sub>–rich thermal waters from the French Massif Central. *Chemical Geology* 182, 409–421.
- Rihs S, Condomines M, Sigmarsson O, 2000.** U, Ra and Ba incorporation during precipitation of hydrothermal carbonates: implications for <sup>226</sup>Ra–Ba dating of impure travertines. *Geochimica et Cosmochimica Acta* 64, 661–671.
- Schmid S, Wiegand J, 2003.** Radionuclide contamination of surface waters, sediments, and soil caused by coal mining activities in the Ruhr District (Germany). *Mine Water and the Environment* 22, 130–140.
- Scholz F, Neumann T, 2007.** Trace element diagenesis in pyrite-rich sediments of the Achterwasser lagoon, SW Baltic Sea. *Marine Chemistry* 107, 516–532.
- Selnert E, Byegård J, Widestrand H, Carlsten S, Döse C, Tullborg E, 2009.** Bedrock transport properties. Data evaluation and retardation model. Site descriptive modelling SDM-Site Laxemar. SKB R-08-100, Svensk Kärnbränslehantering AB.
- Sheppard S, Long J, Sanipelli B, Sohlenius G, 2009.** Solid/liquid partition coefficients (K<sub>d</sub>) for selected soils and sediments at Forsmark and Laxemar-Simpevarp. SKB R-09-27, Svensk Kärnbränslehantering AB.
- Sheppard S, Sohlenius G, Omberg L-G, Borgiel M, Grolander S, Nordén S, 2011.** Solid/liquid partition coefficients (K<sub>d</sub>) and plant/soil concentration ratios (CR) for selected soils, tills and sediments at Forsmark. SKB R-11-24, Svensk Kärnbränslehantering AB.
- Siegel M D, Bryan C R, 2007.** Environmental geochemistry of radioactive contamination. In Sherwood Lollar B (ed). *Treatise on geochemistry*. Vol 9, Environmental geochemistry. Amsterdam: Elsevier, 205–262.

- Smieja-Król B, Fialkiewicz-Koziel B, Sikorski J, Palowski B, 2010.** Heavy metal behaviour in peat – a mineralogical perspective. *The Science of the Total Environment* 408, 5924–5931.
- Smith R M, Martell A E, Motekaitis R, 2003.** NIST critically selected stability constants of metal complexes database. Available at: [http://www.nist.gov/srd/upload/46\\_8.htm](http://www.nist.gov/srd/upload/46_8.htm)
- Sun Y, Torgersen T, 2001.** Adsorption-desorption reactions and bioturbation transport of  $^{224}\text{Ra}$  in marine sediments: a one-dimensional model with applications. *Marine Chemistry* 74, 227–243.
- Sverjensky D A, Molling P A, 1992.** A linear free energy relationship for crystalline solids and aqueous ions. *Nature* 356, 231–234.
- Tang J, Dietzel M, Kohler S J, 2007.** Co-precipitation of  $\text{Sr}^{2+}$  with calcite from 5 to 40°C. *Geochimica et Cosmochimica Acta* 71, A999–A999.
- Todd J F, Elsinger R J, Moore W S, 1988.** The distributions of uranium, radium and thorium isotopes in two anoxic fjords: Framvaren Fjord (norway) and Saanich Inlet (British Columbia). *Marine Chemistry* 23, 393–415.
- Tribovillard N, Algeo T J, Lyons T, Riboulleau A, 2006.** Trace metals as paleoredox and paleo-productivity proxies: an update. *Chemical Geology* 232, 12–32.
- Tröjbom M, Söderbäck B, 2006.** Chemical characteristics of surface systems in the Forsmark area. Visualisation and statistical evaluation of data from shallow groundwater, precipitation, and regolith. SKB R-06-19, Svensk Kärnbränslehantering AB.
- Tröjbom M, Söderbäck B, Johansson P-O, 2007.** Hydrochemistry in surface water and shallow groundwater. Site descriptive modelling, SDM-Site Forsmark. SKB R-07-55, Svensk Kärnbränslehantering AB.
- Tröjbom M, Söderbäck B, Kalinowski B, 2008.** Hydrochemistry of surface water and shallow groundwater. Site descriptive modelling, SDM-Site Laxemar. SKB R-08-46, Svensk Kärnbränslehantering AB.
- van Beek P, Reyss J-L, 2001.**  $^{226}\text{Ra}$  in marine barite: new constraints on supported  $^{226}\text{Ra}$ . *Earth and Planetary Science Letters* 187, 147–161.
- van Beek P, Sternberg E, Reyss J-L, Souhaut M, Robin E, Jeandel C, 2009.**  $^{228}\text{Ra}/^{226}\text{Ra}$  and  $^{226}\text{Ra}/\text{Ba}$  ratios in the Western Mediterranean Sea: barite formation and transport in the water column. *Geochimica et Cosmochimica Acta* 73, 4720–4737.
- Vandenhove H, Van Hees M, 2007.** Predicting radium availability and uptake from soil properties. *Chemosphere* 69, 664–674.
- Yoshida Y, Yoshikawa H, Nakanishi T, 2008.** Partition coefficients of Ra and Ba in calcite. *Geochemical Journal* 42, 295–304.
- Zhu C, 2004a.** Coprecipitation in the barite isostructural family: 1. Binary mixing properties. *Geochimica et Cosmochimica Acta* 68, 3327–3337.
- Zhu C, 2004b.** Coprecipitation in the barite isostructural family: 2. Numerical simulations of reactions and mass transport. *Geochimica et Cosmochimica Acta* 68, 3339–3349.
- Zielinski R A, Otton J K, Budahn J R, 2001.** Use of radium isotopes to determine the age and origin of radioactive barite at oil-field production sites. *Environmental Pollution* 113, 299–309.

### Measured $K_d$ values

Figure A-1 and Figure A-2 shows the measured  $K_d$  values for the sediment  $K_d$  data (Engdahl et al. 2008) and the 2009  $K_d$  data for soils (Sheppard et al. 2009).

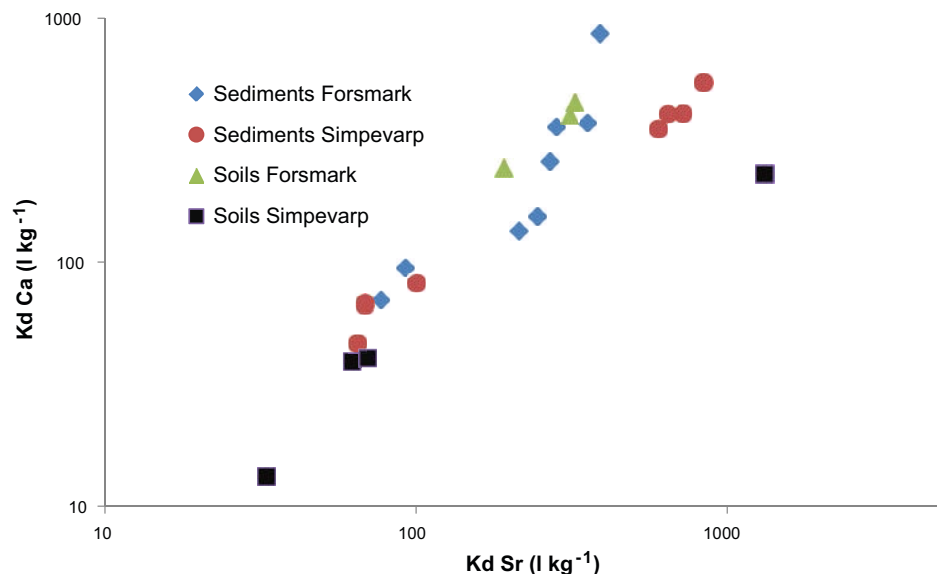


Figure A-1.  $K_d$  values for Sr vs.  $K_d$  values for Ca based on Engdahl et al. (2008) and Sheppard et al. (2009).

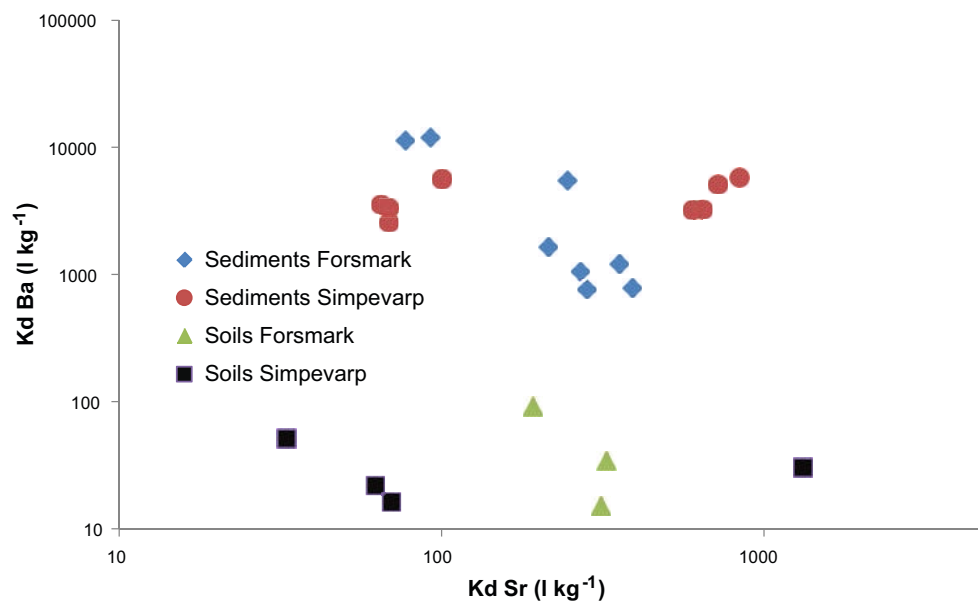
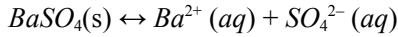


Figure A-2.  $K_d$  values for Sr vs.  $K_d$  values for Ba based on Engdahl et al. (2008) and Sheppard et al. (2009). Note that the  $K_d$  samples for Ba in the soil samples most likely are underestimated – see Section 6.4.1.

### Basic theory of solubility products and saturation indices

The solubility of an ionic compound is governed by the ion activity product (IAP). For instance, in the case of barite, the precipitation/dissolution is described by the following reaction formula:



The solubility product for this reaction,  $K_{sp}$ , is the ion activity product for which the solution is saturated with respect to barite.

$$K_{sp} = \frac{\{Ba^{2+}\}\{SO_4^{2-}\}}{\{BaSO_4(s)\}} = \{Ba^{2+}\}\{SO_4^{2-}\} \quad (B-1)$$

By comparing  $K_{sp}$  to the actual ion activity product (IAP) in the solution, in this case the product of the Ba and sulphate activities, it is possible to predict whether barite will dissolve or precipitate. The saturation index, SI, is defined as

$$SI = \log IAP - \log K_{sp} \quad (B-2)$$

At saturation, SI equals zero. Hence, a value close to zero could indicate that the Ba and sulphate concentrations are controlled by the presence of barite. A negative SI means that the solution is undersaturated with respect to barite ( $IAP < K_{sp}$ ). Any barite present in the solid phase is thermodynamically unstable and could be expected to dissolve. If SI is greater than zero, the solution is oversaturated and barite could be expected to precipitate.

### Basic theory of solid solutions

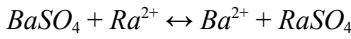
In the case of Ra coprecipitation with barite the two pure end-members would be barite ( $BaSO_4$ ) and  $RaSO_4$ . If the solid solution of barite and  $RaSO_4$  is in equilibrium with the aqueous solution two mass action equations need to be satisfied at the same time, namely saturation with respect to barite

$$K_{BaSO_4} = \frac{\{Ba^{2+}\}\{SO_4^{2-}\}}{\{BaSO_4\}} \quad (C-1)$$

and saturation with respect to  $RaSO_4$

$$K_{RaSO_4} = \frac{\{Ra^{2+}\}\{SO_4^{2-}\}}{\{RaSO_4\}} \quad (C-2)$$

where K denotes the solubility products for barite and  $RaSO_4$  respectively. We can also formulate a solubility product for the solid solution by considering the following equilibrium between barite and  $RaSO_4$  in the solid solution and Ra and Ba ions in the aqueous phase



Hence, the solubility for the solid solution must be described by the mass action expression

$$K_{SS} = \frac{\{Ba^{2+}\}\{RaSO_4\}}{\{Ra^{2+}\}\{BaSO_4\}} = \frac{K_{BaSO_4}}{K_{RaSO_4}} \quad (C-3)$$

where the last equality follows from the definition of the solubility products for barite and  $RaSO_4$  respectively (Equation C-1 and Equation C-2).

For an ideal solid solution the activity of the solid phase will be equal to its mole fraction in the solid solution, X. For instance, the activity for  $RaSO_4$  in solid solution with barite is given by

$$\{RaSO_4\} = X_{RaSO_4} = \frac{mol_{Ra}}{mol_{Ra} + mol_{Ba}} \quad (C-4)$$

In the general, non-ideal case, however, the activity for  $RaSO_4$  is given by

$$\{RaSO_4\} = X_{RaSO_4} \lambda_{RaSO_4} \quad (C-5)$$

where  $\lambda$  is an activity coefficients that corrects for the non-ideal behaviour of the solid solution.  $\lambda$ , in turn, is a function of the free energy of mixing of the two end-member phases. One of the problems when trying to make calculations involving solid solutions is to find an adequate determination of  $\lambda$ , since solid solutions as a rule behave nonideally (Appelo and Postma 2005). One common method is to use a Guggenheim series expansion, which for a binary solid solution describes the excess free-energy of mixing,  $\Delta G^E$ , as

$$\Delta G^E = (X_{Ba}X_{Ra})RT(a_0 + a_1(X_{Ba}-X_{Ra}) + a_2(X_{Ba}-X_{Ra})^2 + \dots) \quad (C-6)$$

Where R denotes the gas constant, T the temperature and  $a_i$  are dimensionless empirical coefficients often referred to as Guggenheim parameters. Once the Guggenheim parameters have been determined they can be used to calculate the activity coefficient. If  $a_0$  is non-zero and all other Guggenheim parameters are zero the solid solution is said to be regular. If both  $a_0$  and  $a_1$  are non-zero and all other Guggenheim parameters are zero the solid solution is said to be subregular. In both cases the activity coefficients can be calculated as

$$\ln \lambda_{Ra} = X_{Ba}^2 (a_0 - a_1(4X_{Ra} - 1)) \quad (C-7)$$

and

$$\ln \lambda_{Ba} = X_{Ra}^2 (a_0 - a_1(4X_{Ba} - 1)) \quad (C-8)$$

For an ideal solid solution all Guggenheim parameters are zero. In an ideal solid solution the energy of the solid solution will always be lower than the energy of a corresponding mechanical mixture. It follows that for an ideal solid solution the components may be mixed in any proportions. Depending on the values of the Guggenheim parameters this is not always the case for nonideal solid solutions. In some cases the activity coefficients may become so high that the solid solution becomes unstable. In that case there will be a so-called miscibility gap, a range of mole ratios where the solid solution is not stable. However, it is thought that barite and  $RaSO_4$  are completely miscible, i.e. they form a solid solution series where barite and  $RaSO_4$  can be mixed in any proportions without loss of stability (Zhu 2004a).

In literature dealing with solid solutions one often encounters a partitioning coefficient or distribution factor. Often it is denoted as  $K_d$  or  $D$ , but in order to avoid confusion with the soil-water partitioning coefficient the denomination  $D$  will be used throughout this report.  $D$  is defined as

$$D = \frac{[Ba^{2+}][RaSO_4]}{[Ra^{2+}][BaSO_4]} = \frac{([RaSO_4] / [BaSO_4])}{([Ra^{2+}] / [Ba^{2+}])} \quad (C-9)$$

As suggested by the last equality,  $D$  is the Ra/Ba ratio in the solid solution divided by the Ra/Ba ratio in the aqueous solution. If  $D > 1$ , it implies that there is a preferential incorporation of Ra into the barite as compared to the composition of the aqueous phase. If  $D < 1$ , Ra will instead be repelled from the barite and the incorporation of Ba will be favoured instead. Note, however, that Equation C-9 involves concentrations whereas Equation C-3 involves activities. In order to relate the partitioning coefficient ( $D$ ) to the mass action expression of the solid solution, it is therefore necessary to take the activity coefficients into account. For the aqueous solution the activity coefficients are determined by the ionic strength of the solution, but since both Ba and Ra are divalent they will have the same activity coefficients for the aqueous phase. Hence, they will cancel in the division. The activity coefficients for the components of the solid solution ( $\lambda_{Ra}$  and  $\lambda_{Ba}$ ), on the other hand, will as a rule not be equal. Hence, we get

$$K_{SS} = \frac{K_{BaSO_4}}{K_{RaSO_4}} = \frac{\{Ba^{2+}\} \{RaSO_4\}}{\{Ra^{2+}\} \{BaSO_4\}} = \frac{[Ba^{2+}][RaSO_4]\lambda_{Ra}}{[Ra^{2+}][BaSO_4]\lambda_{Ba}} = D \frac{\lambda_{Ra}}{\lambda_{Ba}} \quad (C-10)$$

For all applications in this report Ra will only occur in trace amounts in the barite. In other words, the mole fraction of Ba in the solid solution ( $X_{Ba}$ ) will be close to 1, while the mole fraction of Ra ( $X_{Ra}$ ) will be very low. If the Guggenheim approach is used, it follows from Equation C-8 that  $\lambda_{Ba} \approx 1$ . Hence, Equation C-10 simplifies to

$$K_{SS} = \frac{K_{BaSO_4}}{K_{RaSO_4}} = D\lambda_{Ra} \quad (C-11)$$

Since the solubility product of  $RaSO_4$  is greater than that of barite,  $K_{SS}$  will be less than unity under standard conditions, which at least in the ideal case implies that there will be a preferential incorporation of Ra into the solid solution. However, since the value of  $\lambda_{Ra}$  varies with the composition of the solid solution and the degree of nonideality that is assumed, the positive value of  $K_{SS}$  does not automatically imply that there is a preferential incorporation of Ra into barite under all circumstances. If  $\lambda_{Ra}$  increases too much, it will force  $D$  to become less than one, which means that there will be a repulsion of Ra from the solid solution. It is also important to bear in mind the solubility of minerals is dependent on temperature so the value of  $K_{SS}$  will be temperature dependent. Hence, the thermodynamic properties of a solid solution will change with temperature and composition.

A more comprehensive description of the thermodynamic background to solid solutions can be found in Glynn and Reardon (1990).



## Saturation indices

Table D-1. Calculated saturation indices for near surface ground water sites. Saturation indices above -0.5 are considered possible saturation and highlighted in red.

ID code	Sample date	Sampling depth (m)	Barite SI	Gypsum SI	Celestite SI	Witherite SI	Calcite SI	Strontianite SI
SFM0002	2003-10-28	4.71	0.11	-1.89	-3.03	-3.53	-0.14	-2.44
SFM0002	2002-09-20	4.71	-0.19	-2.12	-3.23	-3.37	0.09	-2.19
SFM0002	2004-10-12	4.71	-0.08	-2.03	-3.17	-3.57	-0.13	-2.43
SFM0002	2005-04-11	4.71	-0.14	-2.09	-3.24	-3.61	-0.16	-2.48
SFM0002	2004-07-06	4.71	-0.17	-2.11	-3.25	-3.58	-0.12	-2.43
SFM0002	2004-04-19	4.71	-0.19	-2.13	-3.25	-3.61	-0.15	-2.44
SFM0002	2003-01-13	4.71	0.12	-1.71	-2.82	-3.30	0.27	-2.01
SFM0005	2004-07-13	2.71	-0.65	-2.46	-3.79	-3.89	-0.30	-2.80
SFM0005	2004-04-20	2.71	-0.40	-2.15	-3.46	-3.98	-0.34	-2.81
SFM0005	2004-01-12	2.71	-0.41	-2.09	-3.40	-3.98	-0.25	-2.74
SFM0005	2005-04-08	2.71	-0.69	-2.41	-3.76	-4.24	-0.56	-3.09
SFM0008	2003-10-29	5.64	0.36	-1.44	-2.54	-3.67	-0.08	-2.35
SFM0008	2004-01-13	5.64	0.38	-1.31	-2.51	-3.68	0.02	-2.35
SFM0008	2004-04-20	5.64	0.33	-1.36	-2.52	-3.68	0.02	-2.30
SFM0008	2005-04-07	5.64	0.27	-1.42	-2.59	-3.79	-0.09	-2.43
SFM0008	2004-07-05	5.64	0.24	-1.44	-2.59	-3.64	0.07	-2.24
SFM0008	2004-10-15	5.64	0.05	-1.65	-2.80	-3.76	-0.06	-2.38
SFM0049	2007-08-08	3.4	-1.40	-3.13	-4.31	-4.65	-0.99	-3.34
SFM0049	2007-01-23	4.5	-0.83	-2.62	-3.80	-4.50	-0.89	-3.24
SFM0049	2006-01-24	4.5	-1.90	-3.57	-4.77	-4.64	-0.92	-3.29
SFM0049	2008-01-16	3.4	-1.18	-2.95	-4.13	-4.42	-0.80	-3.14
SFM0049	2007-03-27	4.5	-1.26	-3.02	-4.20	-4.52	-0.88	-3.24
SFM0049	2006-04-19	4.5	-2.09	-3.74	-4.95	-4.77	-1.02	-3.40
SFM0049	2006-01-24	4.5	-1.92	-3.56	-4.76	-4.54	-0.79	-3.15
SFM0049	2006-10-10	4.5	-0.58	-2.22	-3.42	-4.65	-0.90	-3.27
SFM0049	2005-10-04	4.5	-1.66	-3.25	-4.48	-4.75	-0.95	-3.34
SFM0049	2005-04-12	4.5	-2.12	-3.80	-4.99	-4.74	-1.02	-3.38
SFM0049	2004-07-12	4.5	-1.90	-3.52	-4.70	-4.54	-0.76	-3.11
SFM0049	2004-10-12	4.5	-1.22	-2.79	-3.97	-4.86	-1.03	-3.38
SFM0057	2004-07-06	3.95	0.00	-1.90	-3.05	-3.78	-0.28	-2.60
SFM0057	2004-10-13	3.95	0.01	-1.90	-3.02	-3.77	-0.28	-2.57
SFM0057	2004-01-20	3.95	-0.07	-1.92	-3.02	-3.62	-0.07	-2.34
SFM0057	2003-11-04	3.95	-0.30	-2.18	-3.30	-3.81	-0.29	-2.58

**Table D-2. Calculated saturation indices for lakes in Forsmark, part one.**

ID code	Sample date	Sampling depth (m)	Barite SI	Gypsum SI	Celestite SI	Witherite SI	Calcite SI	Strontianite SI
PFM102270	2006-04-18	0.5	-0.94	-2.52	-3.64	-4.66	-0.84	-3.14
PFM000135	2003-01-15	0.5	-0.43	-2.18	-3.19	-3.58	0.06	-2.12
PFM000135	2004-01-14	0.5	-0.47	-2.06	-3.13	-4.33	-0.52	-2.77
PFM000135	2004-04-21	0.5	-0.84	-2.43	-3.46	-3.65	0.16	-2.04
PFM000135	2004-07-06	0.5	-0.86	-2.65	-3.45	-2.93	0.67	-1.29
PFM000135	2004-10-11	0.5	-0.91	-2.69	-3.49	-3.19	0.43	-1.54
PFM000127	2003-10-27	1	-0.75	-2.58	-3.38	-3.39	0.17	-1.79
PFM000127	2002-08-12	1	-0.83	-2.65	-3.51	-2.93	0.64	-1.38
PFM000127	2002-07-15	1	-0.85	-2.63	-3.53	-3.22	0.39	-1.68
PFM000127	2002-07-15	0.5	-0.87	-2.64	-3.54	-4.42	-0.79	-2.86
PFM000117	2005-01-17	1.5	-1.03	-2.65	-3.92	-4.06	-0.28	-2.72
PFM000117	2003-01-15	1.5	-1.11	-2.74	-3.95	-3.80	-0.04	-2.42
PFM000117	2006-01-24	1.5	-1.14	-2.73	-4.02	-4.08	-0.27	-2.73
PFM000117	2008-01-15	1.5	-0.87	-2.48	-3.73	-4.03	-0.23	-2.65
PFM000117	2003-01-15	0.5	-1.23	-2.83	-4.02	-3.52	0.28	-2.08
PFM000117	2005-05-12	0.5	-1.23	-2.79	-4.08	-3.79	0.05	-2.41
PFM000117	2004-04-20	0.5	-1.10	-2.68	-3.95	-3.64	0.17	-2.26
PFM000117	2005-01-17	0.5	-1.19	-2.78	-3.96	-4.01	-0.20	-2.56
PFM000117	2008-04-06	0.5	-1.08	-2.59	-3.89	-3.55	0.34	-2.13
PFM000117	2006-01-24	0.5	-1.30	-2.83	-4.04	-4.00	-0.14	-2.51
PFM000117	2003-05-06	0.5	-1.28	-2.86	-4.11	-3.42	0.40	-2.02
PFM000117	2004-01-14	0.5	-1.08	-2.66	-3.89	-3.97	-0.15	-2.55
PFM000117	2008-01-15	0.5	-1.15	-2.73	-3.94	-3.90	-0.09	-2.47
PFM000117	2007-05-07	0.5	-1.17	-2.67	-3.94	-3.27	0.62	-1.81
PFM000117	2003-07-08	0.5	-1.33	-2.94	-4.08	-3.15	0.64	-1.67
PFM000117	2004-07-05	0.5	-1.28	-2.88	-4.02	-3.42	0.38	-1.94
PFM000117	2006-10-09	0.5	-1.59	-3.13	-4.26	-3.66	0.20	-2.10
PFM000117	2002-07-16	1.5	-1.55	-3.01	-4.20	-3.55	0.38	-1.97
PFM000117	2005-07-11	0.5	-1.52	-3.06	-4.19	-3.23	0.63	-1.68
PFM000117	2007-10-08	0.5	-1.37	-2.89	-4.02	-3.67	0.21	-2.09
PFM000117	2002-07-16	0.5	-1.56	-3.02	-4.22	-3.56	0.37	-1.99
PFM000117	2006-07-18	0.5	-1.53	-3.04	-4.17	-3.18	0.71	-1.59
PFM000117	2005-10-04	0.5	-1.54	-3.07	-4.21	-4.89	-1.03	-3.33
PFM000117	2007-08-06	0.5	-1.41	-2.85	-3.96	-3.44	0.52	-1.76
PFM000107	2008-01-14	1	-0.01	-1.67	-2.31	-3.90	-0.16	-1.98
PFM000107	2007-10-08	0.5	-0.03	-1.70	-2.25	-3.86	-0.12	-1.85
PFM000107	2005-01-17	1	-0.11	-1.79	-2.42	-4.54	-0.82	-2.62
PFM000107	2006-01-23	1	-0.64	-2.33	-3.28	-4.10	-0.40	-2.52
PFM000107	2008-01-14	0.5	-0.42	-2.04	-2.93	-4.42	-0.65	-2.70
PFM000107	2007-05-07	0.5	-0.28	-1.95	-2.70	-2.96	0.76	-1.16
PFM000107	2006-01-23	0.5	-0.65	-2.25	-3.30	-4.34	-0.55	-2.77
PFM000107	2007-08-06	0.5	-0.25	-1.90	-2.50	-2.68	1.06	-0.71
PFM000107	2006-10-09	0.5	-0.52	-2.24	-2.99	-3.75	-0.07	-1.98
PFM000107	2003-01-21	1	-0.64	-2.34	-3.34	-4.07	-0.37	-2.54
PFM000107	2005-01-17	0.5	-0.75	-2.37	-3.47	-4.38	-0.61	-2.87
PFM000107	2007-01-15	0.5	-0.33	-1.97	-2.75	-4.00	-0.24	-2.19
PFM000107	2005-05-11	0.5	-0.43	-2.10	-2.95	-3.81	-0.08	-2.10
PFM000107	2005-07-11	0.5	-0.59	-2.34	-3.20	-3.10	0.54	-1.49
PFM000107	2004-01-13	1	-0.68	-2.33	-3.44	-4.06	-0.31	-2.59
PFM000107	2002-07-15	0.5	-0.72	-2.45	-3.37	-3.08	0.59	-1.50
PFM000107	2003-01-16	0.5	-0.73	-2.46	-3.45	-4.15	-0.48	-2.64
PFM000107	2004-01-13	0.5	-0.75	-2.35	-3.50	-4.54	-0.75	-3.07
PFM000107	2008-04-06	0.5	-0.62	-2.18	-3.08	-3.63	0.21	-1.87

**Table D-3. Calculated saturation indices for lakes in Forsmark, part two. Saturation indices above -0.5 are considered possible saturation and highlighted in red.**

ID code	Sample date	Sampling depth (m)	Barite SI	Gypsum SI	Celestite SI	Witherite SI	Calcite SI	Strontianite SI
PFM000107	2005-10-03	0.5	-0.69	-2.40	-3.26	-3.49	0.20	-1.83
PFM000107	2006-07-17	0.5	-0.73	-2.42	-3.24	-2.76	0.94	-1.04
PFM000107	2003-07-07	0.5	-0.89	-2.63	-3.57	-2.87	0.79	-1.33
PFM000107	2002-07-15	1	-0.82	-2.45	-3.38	-3.18	0.59	-1.51
PFM000107	2004-10-11	0.5	-0.91	-2.61	-3.49	-3.57	0.12	-1.92
PFM000107	2004-04-20	0.5	-0.96	-2.53	-3.57	-3.66	0.17	-2.04
PFM000107	2002-04-17	0.5	-0.76	-2.32	-3.23	-3.82	0.01	-2.07
PFM000107	2004-07-05	0.5	-0.93	-2.63	-3.50	-3.09	0.61	-1.42
PFM000107	2003-05-04	0.5	-0.95	-2.53	-3.61	-3.47	0.35	-1.89
PFM000097	2004-01-13	0.5	-0.28	-2.01	-3.00	-3.97	-0.30	-2.47
PFM000097	2003-01-15	0.5	-0.57	-2.27	-3.26	-3.95	-0.26	-2.42
PFM000097	2002-07-15	0.5	-0.64	-2.40	-3.30	-3.65	-0.01	-2.08
PFM000097	2004-04-20	0.5	-0.87	-2.46	-3.46	-3.68	0.13	-2.03
PFM000097	2002-04-17	0.5	-0.80	-2.34	-3.24	-3.99	-0.14	-2.21
PFM000097	2003-05-06	0.5	-0.98	-2.57	-3.61	-3.37	0.43	-1.77
PFM000097	2003-07-08	0.5	-1.06	-2.82	-3.58	-2.59	1.04	-0.89
PFM000087	2003-01-15	1.5	-0.05	-1.90	-3.12	-3.63	-0.08	-2.47
PFM000087	2003-01-15	0.5	-0.07	-1.91	-3.12	-3.76	-0.20	-2.57
PFM000087	2004-01-12	1.5	0.10	-1.72	-2.96	-3.72	-0.14	-2.55
PFM000087	2002-07-14	1.5	-0.94	-2.72	-3.89	-3.39	0.23	-2.10
PFM000087	2002-07-14	0.5	-0.95	-2.71	-3.87	-3.22	0.41	-1.92
PFM000087	2004-01-12	0.5	-0.59	-2.24	-3.49	-4.20	-0.46	-2.87
PFM000087	2004-04-20	0.5	-0.67	-2.38	-3.58	-3.62	0.06	-2.31
PFM000087	2003-05-06	0.5	-0.70	-2.41	-3.62	-3.51	0.18	-2.20
PFM000087	2003-10-27	0.5	-0.64	-2.43	-3.43	-3.10	0.52	-1.65
PFM000087	2002-08-11	1.5	-1.15	-2.78	-3.92	-3.57	0.19	-2.12
PFM000087	2003-07-07	0.5	-1.00	-2.81	-3.79	-2.95	0.64	-1.51
PFM000074	2003-01-16	0.5	-0.36	-2.02	-3.27	-4.11	-0.37	-2.79
PFM000074	2003-10-27	0.5	-1.11	-2.78	-3.97	-3.97	-0.24	-2.61
PFM000074	2005-07-11	0.5	-1.23	-2.94	-4.14	-3.64	0.05	-2.32
PFM000074	2007-05-08	0.5	-0.68	-2.33	-3.56	-3.53	0.22	-2.18
PFM000074	2007-08-07	0.5	-0.92	-2.60	-3.76	-3.34	0.38	-1.96
PFM000074	2006-01-24	0.5	-0.73	-2.29	-3.59	-4.28	-0.45	-2.92
PFM000074	2002-07-14	0.5	-1.27	-2.93	-4.18	-3.67	0.07	-2.36
PFM000074	2004-07-06	0.5	-1.19	-2.89	-4.05	-3.79	-0.10	-2.43
PFM000074	2005-10-03	0.5	-1.16	-2.82	-4.03	-3.15	0.59	-1.79
PFM000074	2003-07-07	0.5	-1.08	-2.80	-3.95	-3.40	0.27	-2.04
PFM000074	2007-10-09	0.5	-1.14	-2.79	-3.97	-3.65	0.10	-2.25
PFM000074	2006-10-10	0.5	-1.20	-2.87	-4.01	-3.72	0.01	-2.30
PFM000074	2008-01-15	0.5	-0.49	-2.09	-3.35	-4.33	-0.54	-2.96
PFM000074	2006-07-17	0.5	-1.12	-2.83	-3.94	-3.18	0.51	-1.77
PFM000074	2004-10-12	0.5	-1.26	-2.90	-4.05	-3.54	0.21	-2.11
PFM000074	2004-01-14	0.5	-0.81	-2.40	-3.67	-4.34	-0.54	-2.98
PFM000074	2004-04-20	0.5	-1.02	-2.67	-3.91	-4.02	-0.28	-2.69
PFM000074	2008-04-07	0.5	-0.82	-2.41	-3.68	-4.01	-0.20	-2.64
PFM000074	2005-01-18	0.5	-0.79	-2.38	-3.65	-4.41	-0.60	-3.04
PFM000074	2003-05-06	0.5	-0.82	-2.45	-3.70	-4.10	-0.34	-2.76
PFM000074	2005-05-11	0.5	-1.18	-2.82	-4.10	-4.24	-0.49	-2.94
PFM000074	2006-04-18	0.5	-1.12	-2.73	-4.04	-4.53	-0.75	-3.22

**Table D-4. Calculated saturation indices for lake water in Simpevarp. Saturation indices above -0.5 are considered possible saturation and highlighted in red.**

ID code	Sample date	Sampling depth (m)	Barite SI	Gypsum SI	Celestite SI	Witherite SI	Calcite SI	Strontianite SI
PSM002065	2003-06-23	2.50	-1.06	-3.24	-3.77	-6.17	-2.95	-4.65
PSM002065	2003-06-23	0.50	-1.06	-3.27	-3.80	-5.96	-2.78	-4.48
PSM002065	2005-08-23	0.00	-1.04	-3.31	-3.85	-5.58	-2.46	-4.17
PSM002065	2005-08-23	1.50	-1.05	-3.32	-3.86	-5.51	-2.39	-4.09
PSM002065	2005-12-13	0.00	-0.98	-3.25	-3.79	-5.99	-2.87	-4.58
PSM002065	2005-12-13	1.50	-0.97	-3.25	-3.80	-5.81	-2.70	-4.41
PSM002065	2006-03-21	0.50	-0.70	-2.98	-3.55	-6.76	-3.64	-5.38
PSM002065	2006-03-21	2.00	-0.72	-2.98	-3.57	-6.74	-3.60	-5.36
PSM002065	2006-05-30	0.00	-0.85	-3.13	-3.71	-5.90	-2.78	-4.53
PSM002065	2006-05-30	2.50	-0.85	-3.17	-3.76	-6.05	-2.97	-4.73
PSM002065	2006-08-22	0.00	-0.94	-3.21	-3.75	-5.26	-2.13	-3.85
PSM002065	2006-08-22	1.00	-0.96	-3.21	-3.75	-5.21	-2.06	-3.76
PSM002065	2006-12-12	1.00	-0.69	-3.07	-3.61	-5.80	-2.79	-4.50
PSM002065	2006-12-12	3.50	-0.81	-3.08	-3.63	-5.95	-2.82	-4.55
PSM002065	2007-03-20	0.00	-0.81	-3.07	-3.63	-6.66	-3.52	-5.25
PSM002065	2007-03-20	2.50	-0.81	-3.07	-3.63	-6.66	-3.53	-5.25
PSM002065	2007-05-23	0.00	-0.75	-3.03	-3.58	-5.97	-2.85	-4.58
PSM002065	2007-05-23	2.00	-0.74	-3.02	-3.57	-6.49	-3.37	-5.09
PSM002065	2007-08-22	0.00	-0.86	-3.10	-3.64	-5.58	-2.42	-4.13
PSM002065	2007-08-22	1.50	-0.84	-3.09	-3.64	-5.64	-2.50	-4.21
PSM002065	2007-12-11	0.00	-0.85	-3.09	-3.65	-6.39	-3.24	-4.97
PSM002065	2007-12-11	2.50	-0.81	-3.08	-3.65	-6.34	-3.21	-4.95
PSM002065	2008-03-12	0.00	-0.79	-3.07	-3.62	-6.27	-3.16	-4.88
PSM002065	2008-03-12	2.50	-0.80	-3.06	-3.60	-6.21	-3.07	-4.78
PSM002065	2008-05-20	1.00	-0.82	-3.04	-3.61	-6.18	-3.01	-4.75
PSM002065	2008-05-20	2.00	-0.80	-3.02	-3.60	-6.14	-2.96	-4.71
PSM002065	2008-08-19	1.00	-0.79	-2.98	-3.52	-5.69	-2.48	-4.19
PSM002065	2008-08-19	1.50	-0.83	-3.02	-3.56	-5.68	-2.47	-4.19

**Table D-5. Calculated saturation indices for sea water in Forsmark, part one. Saturation indices above -0.5 are considered possible saturation and highlighted in red.**

ID code	Sample date	Sampling depth (m)	Barite SI	Gypsum SI	Celestite SI	Witherite SI	Calcite SI	Strontianite SI
PFM005865	2006-07-20	55	-0.08	-1.49	-1.62	-4.78	-0.80	-2.10
PFM005865	2006-07-20	0.5	-0.09	-1.50	-1.62	-4.35	-0.36	-1.65
PFM005865	2006-07-20	30	-0.09	-1.50	-1.62	-4.75	-0.76	-2.05
PFM000082	2003-01-13	6.5	-0.04	-1.54	-1.67	-4.19	-0.29	-1.60
PFM000082	2003-01-13	0.5	-0.04	-1.54	-1.68	-4.03	-0.14	-1.44
PFM000082	2006-01-23	6	-0.09	-1.45	-1.61	-4.59	-0.56	-1.88
PFM000082	2006-01-23	0.5	-0.09	-1.46	-1.62	-4.59	-0.56	-1.89
PFM000065	2003-05-05	0.5	-0.10	-1.70	-2.03	-4.10	-0.30	-1.79
PFM000065	2002-08-12	0.5	-0.06	-1.64	-1.85	-3.77	0.05	-1.33
PFM000065	2003-01-13	0.5	0.01	-1.62	-1.96	-4.45	-0.69	-2.20
PFM000065	2002-07-15	0.5	-0.04	-1.56	-1.72	-3.92	-0.03	-1.37
PFM000065	2004-01-12	0.5	-0.25	-1.86	-2.70	-4.71	-0.93	-2.94
PFM000065	2003-07-07	0.5	-0.04	-1.56	-1.71	-4.05	-0.17	-1.49
PFM000065	2004-04-19	0.5	-0.11	-1.60	-1.89	-4.29	-0.39	-1.85
PFM000065	2003-10-28	0.5	-0.10	-1.52	-1.66	-4.43	-0.45	-1.76
PFM000065	2002-10-21	0.5	-0.14	-1.58	-1.72	-4.34	-0.37	-1.69
PFM000064	2002-07-15	1	0.00	-1.55	-1.72	-4.07	-0.22	-1.56
PFM000064	2002-07-15	0.5	-0.01	-1.55	-1.72	-4.16	-0.31	-1.65
PFM000064	2002-08-12	0.5	-0.03	-1.60	-1.79	-3.78	0.04	-1.32
PFM000064	2003-07-07	0.5	0.00	-1.54	-1.67	-4.06	-0.20	-1.50
PFM000064	2004-01-12	0.5	-0.23	-1.83	-2.54	-4.71	-0.92	-2.79
PFM000064	2003-10-28	0.5	-0.04	-1.53	-1.67	-4.50	-0.59	-1.90
PFM000064	2004-04-19	0.5	-0.07	-1.59	-1.86	-4.28	-0.41	-1.85
PFM000064	2002-10-21	1	-0.09	-1.57	-1.72	-4.40	-0.48	-1.81
PFM000064	2004-01-12	1	-0.07	-1.51	-1.70	-4.85	-0.89	-2.25
PFM000064	2002-10-21	0.5	-0.11	-1.57	-1.73	-4.34	-0.40	-1.73
PFM000063	2002-08-12	4.5	0.05	-1.56	-1.69	-4.65	-0.86	-2.16
PFM000063	2003-01-14	1	0.00	-1.53	-1.67	-4.53	-0.66	-1.97
PFM000063	2002-10-21	4.5	-0.03	-1.57	-1.70	-4.37	-0.52	-1.82
PFM000063	2003-01-14	0.5	-0.02	-1.53	-1.68	-4.46	-0.57	-1.89
PFM000063	2002-08-12	0.5	-0.04	-1.56	-1.70	-4.24	-0.37	-1.67
PFM000063	2003-07-07	0.5	-0.05	-1.55	-1.67	-4.18	-0.28	-1.57
PFM000063	2002-07-15	4.5	-0.07	-1.54	-1.69	-4.49	-0.56	-1.88
PFM000063	2002-07-15	0.5	-0.08	-1.55	-1.70	-4.29	-0.36	-1.68
PFM000063	2003-05-05	0.5	-0.10	-1.56	-1.69	-4.26	-0.32	-1.62
PFM000063	2004-04-19	0.5	-0.05	-1.48	-1.63	-4.34	-0.38	-1.70
PFM000063	2003-10-28	0.5	-0.10	-1.51	-1.64	-4.50	-0.52	-1.82
PFM000063	2002-10-21	0.5	-0.17	-1.57	-1.71	-4.41	-0.42	-1.73

**Table D-6. Calculated saturation indices for sea water in Forsmark, part two.**

ID code	Sample date	Sampling depth (m)	Barite SI	Gypsum SI	Celestite SI	Witherite SI	Calcite SI	Strontianite SI
PFM000062	2002-08-12	0.5	-0.06	-1.59	-1.72	-4.36	-0.50	-1.80
PFM000062	2005-07-11	0.5	-0.03	-1.51	-1.61	-4.22	-0.30	-1.56
PFM000062	2002-08-12	3	-0.06	-1.58	-1.72	-4.27	-0.40	-1.70
PFM000062	2003-07-07	0.5	-0.05	-1.56	-1.68	-4.47	-0.58	-1.87
PFM000062	2004-04-19	0.5	-0.02	-1.47	-1.61	-4.23	-0.28	-1.59
PFM000062	2005-05-11	0.5	-0.05	-1.48	-1.58	-4.27	-0.29	-1.56
PFM000062	2005-10-03	0.5	-0.04	-1.45	-1.58	-4.58	-0.59	-1.89
PFM000062	2005-01-18	0.5	-0.08	-1.50	-1.64	-4.48	-0.51	-1.82
PFM000062	2002-07-15	0.5	-0.10	-1.53	-1.70	-4.21	-0.25	-1.59
PFM000062	2003-10-28	0.5	-0.08	-1.51	-1.64	-4.56	-0.59	-1.88
PFM000062	2007-01-15	0.5	-0.09	-1.49	-1.67	-4.73	-0.74	-2.09
PFM000062	2008-04-06	0.5	-0.08	-1.49	-1.64	-4.09	-0.10	-1.42
PFM000062	2007-10-08	0.5	-0.09	-1.50	-1.61	-4.39	-0.41	-1.68
PFM000062	2008-01-14	0.5	-0.09	-1.50	-1.59	-4.49	-0.52	-1.77
PFM000062	2003-05-05	0.5	-0.10	-1.54	-1.67	-4.31	-0.35	-1.65
PFM000062	2006-04-18	0.5	-0.10	-1.49	-1.63	-4.48	-0.48	-1.78
PFM000062	2006-07-17	0.5	-0.11	-1.51	-1.63	-4.36	-0.36	-1.66
PFM000062	2004-10-11	0.5	-0.08	-1.48	-1.62	-4.39	-0.39	-1.69
PFM000062	2004-07-05	0.5	-0.09	-1.50	-1.63	-4.43	-0.45	-1.75
PFM000062	2006-10-09	0.5	-0.12	-1.50	-1.63	-4.57	-0.56	-1.86
PFM000062	2007-05-07	0.5	-0.11	-1.51	-1.62	-4.36	-0.36	-1.64
PFM000062	2007-08-06	0.5	-0.16	-1.50	-1.63	-4.38	-0.33	-1.63
PFM000062	2002-10-21	3	-0.18	-1.57	-1.70	-4.31	-0.30	-1.60

**Table D-7. Calculated saturation indices for sea water in Simpevarp, part one. Saturation indices above -0.5 are considered possible saturation and highlighted in red.**

ID code	Sample date	Sampling depth (m)	Barite SI	Gypsum SI	Celestite SI	Witherite SI	Calcite SI	Strontianite SI
PSM002060	2003-06-23	0.50	-0.03	-1.41	-1.49	-4.20	-0.19	-1.44
PSM002060	2003-06-23	28.50	-0.03	-1.38	-1.48	-4.43	-0.39	-1.66
PSM002061	2003-06-23	0.50	-0.01	-1.37	-1.48	-4.19	-0.15	-1.42
PSM002061	2003-06-23	7.50	-0.05	-1.41	-1.51	-4.36	-0.32	-1.59
PSM002062	2003-06-24	0.50	-0.09	-1.57	-1.70	-4.25	-0.33	-1.63
PSM002062	2003-06-24	2.50	-0.05	-1.52	-1.64	-4.38	-0.45	-1.74
PSM002064	2003-06-24	0.50	-0.08	-1.50	-1.62	-4.33	-0.35	-1.64
PSM002064	2003-06-24	15.50	-0.04	-1.43	-1.54	-4.88	-0.87	-2.15
PSM002064	2005-05-23	0.00	-0.01	-1.39	-1.46	-4.16	-0.14	-1.39
PSM002064	2005-08-23	15.50	-0.02	-1.37	-1.45	-5.19	-1.14	-2.39
PSM002064	2005-12-13	0.00	0.02	-1.35	-1.45	-4.44	-0.41	-1.68
PSM002064	2005-12-13	16.50	0.01	-1.35	-1.46	-4.46	-0.42	-1.71
PSM002064	2006-03-21	0.50	0.04	-1.38	-1.50	-4.89	-0.91	-2.19
PSM002064	2006-03-21	16.00	-0.04	-1.31	-1.41	-4.97	-0.84	-2.11
PSM002064	2006-05-30	0.00	-0.06	-1.44	-1.59	-4.47	-0.46	-1.77
PSM002064	2006-05-30	17.50	-0.05	-1.37	-1.50	-5.13	-1.05	-2.35
PSM002064	2006-08-22	0.00	0.01	-1.36	-1.50	-4.07	-0.05	-1.35
PSM002064	2006-08-22	16.00	-0.01	-1.37	-1.47	-5.24	-1.20	-2.47
PSM002064	2006-12-12	0.00	0.00	-1.44	-1.55	-4.64	-0.68	-1.97
PSM002064	2006-12-12	16.50	0.00	-1.37	-1.48	-5.00	-0.98	-2.25
PSM002064	2007-03-20	0.00	-0.04	-1.45	-1.59	-4.74	-0.76	-2.06
PSM002064	2007-03-20	16.50	0.00	-1.37	-1.50	-4.96	-0.94	-2.23
PSM002064	2007-05-23	0.00	-0.01	-1.41	-1.51	-4.27	-0.27	-1.55
PSM002064	2007-05-23	16.50	0.03	-1.38	-1.48	-5.26	-1.28	-2.55
PSM002064	2007-08-21	0.00	-0.17	-1.41	-1.53	-4.51	-0.35	-1.64
PSM002064	2007-08-21	15.50	0.00	-1.38	-1.51	-5.08	-1.07	-2.37
PSM002064	2007-12-11	0.00	0.04	-1.55	-1.71	-4.67	-0.87	-2.19
PSM002064	2007-12-11	16.50	0.02	-1.40	-1.53	-4.68	-0.71	-2.00
PSM002064	2008-03-12	0.00	-0.02	-1.41	-1.51	-4.37	-0.37	-1.63
PSM002064	2008-03-12	16.50	-0.03	-1.39	-1.48	-4.52	-0.48	-1.74
PSM002064	2008-05-20	1.00	-0.01	-1.40	-1.51	-4.17	-0.16	-1.44
PSM002064	2008-05-20	15.50	-0.03	-1.38	-1.49	-5.03	-0.98	-2.26
PSM002064	2008-08-19	1.00	0.06	-1.35	-1.44	-4.18	-0.19	-1.45
PSM002064	2008-08-19	16.00	0.04	-1.36	-1.45	-5.17	-1.18	-2.44

**Table D-8. Calculated saturation indices for sea water in Simpevarp, part two.**

ID code	Sample date	Sampling depth (m)	Barite SI	Gypsum SI	Celestite SI	Witherite SI	Calcite SI	Strontianite SI
PSM007097	2005-08-23	0.00	0.06	-1.34	-1.44	-3.92	0.07	-1.19
PSM007097	2005-08-23	5.50	0.03	-1.39	-1.52	-5.00	-1.03	-2.32
PSM007097	2005-12-13	0.00	0.04	-1.38	-1.49	-4.46	-0.48	-1.76
PSM007097	2005-12-13	5.50	0.04	-1.36	-1.46	-4.47	-0.47	-1.74
PSM007097	2006-03-21	0.50	0.08	-1.45	-1.57	-5.01	-1.14	-2.43
PSM007097	2006-03-21	6.00	0.04	-1.35	-1.45	-5.33	-1.32	-2.59
PSM007097	2006-05-30	0.00	-0.03	-1.56	-1.75	-4.61	-0.75	-2.11
PSM007097	2006-05-30	6.50	0.10	-1.38	-1.51	-5.21	-1.28	-2.58
PSM007097	2006-08-22	0.00	0.06	-1.39	-1.54	-3.63	0.31	-1.01
PSM007097	2006-08-22	6.00	0.04	-1.41	-1.51	-4.85	-0.90	-2.18
PSM007097	2006-12-12	0.00	0.07	-1.46	-1.59	-4.61	-0.75	-2.05
PSM007097	2006-12-12	6.50	0.02	-1.38	-1.50	-4.64	-0.65	-1.94
PSM007097	2007-03-20	0.00	-0.04	-1.63	-1.78	-4.93	-1.12	-2.44
PSM007097	2007-03-20	6.50	-0.04	-1.37	-1.50	-5.35	-1.29	-2.59
PSM007097	2007-05-23	0.00	0.01	-1.44	-1.56	-4.22	-0.28	-1.56
PSM007097	2007-05-23	6.00	0.06	-1.39	-1.50	-5.00	-1.06	-2.33
PSM007097	2007-08-21	0.00	0.01	-1.48	-1.62	-4.03	-0.13	-1.43
PSM007097	2007-08-21	5.00	-0.14	-1.42	-1.55	-4.84	-0.72	-2.01
PSM007097	2007-12-11	0.00	0.08	-1.68	-1.86	-4.88	-1.25	-2.59
PSM007097	2007-12-11	6.00	0.03	-1.43	-1.56	-4.84	-0.90	-2.20
PSM007097	2008-03-12	0.00	-0.04	-1.46	-1.59	-4.44	-0.47	-1.76
PSM007097	2008-03-12	6.00	-0.01	-1.39	-1.50	-4.76	-0.75	-2.02
PSM007097	2008-05-20	1.00	-0.01	-1.45	-1.58	-4.26	-0.30	-1.60
PSM007097	2008-05-20	5.50	0.00	-1.38	-1.49	-4.83	-0.80	-2.09
PSM007097	2008-08-19	1.00	0.08	-1.37	-1.45	-4.09	-0.14	-1.39
PSM007097	2008-08-19	6.00	0.06	-1.37	-1.46	-4.12	-0.15	-1.41



**Table D-9. Calculated saturation indices for stream water in Forsmark. Saturation indices above -0.5 are considered possible saturation and highlighted in red.**

ID code	Sample date	Sampling depth (m)	Barite SI	Gypsum SI	Celestite SI	Witherite SI	Calcite SI	Strontianite SI
PFM000073	2003-05-05	0.05	0.00	-1.62	-2.70	-2.96	0.82	-1.43
PFM000073	2004-01-14	0.05	0.06	-1.55	-2.61	-3.31	0.48	-1.76
PFM000073	2004-04-21	0.05	-0.05	-1.63	-2.67	-2.83	0.98	-1.22
PFM000072	2003-01-16	0.1	0.06	-1.88	-2.77	-4.68	-1.22	-3.29
PFM000072	2003-10-29	0.1	-0.01	-1.92	-2.82	-4.55	-1.06	-3.13
PFM000072	2003-07-08	0.1	-0.97	-2.87	-3.76	-3.86	-0.36	-2.42
PFM000072	2004-01-14	0.1	-0.51	-2.30	-3.29	-4.55	-0.94	-3.10
PFM000072	2004-04-19	0.1	-0.60	-2.36	-3.36	-4.24	-0.60	-2.77
PFM000072	2003-05-05	0.1	-0.80	-2.44	-3.42	-4.51	-0.76	-2.91
PFM000071	2003-01-15	0.1	-0.87	-2.47	-3.79	-3.72	0.07	-2.41
PFM000071	2002-07-16	0.1	-1.44	-3.01	-4.33	-3.31	0.52	-1.97
PFM000070	2003-07-08	0.1	-1.66	-3.34	-4.57	-4.16	-0.44	-2.85
PFM000070	2003-01-16	0.1	-1.18	-2.77	-3.99	-3.82	-0.01	-2.40
PFM000070	2004-07-05	0.1	-1.46	-3.16	-4.38	-4.29	-0.59	-2.98
PFM000070	2003-10-28	0.1	-0.56	-2.18	-3.44	-5.02	-1.24	-3.67
PFM000070	2003-05-06	0.1	-1.28	-2.83	-4.09	-3.85	-0.02	-2.44
PFM000070	2004-01-14	0.1	-1.07	-2.66	-3.87	-4.32	-0.51	-2.89
PFM000070	2002-07-16	0.2	-1.48	-3.07	-4.28	-4.19	-0.38	-2.76
PFM000069	2003-01-16	0.1	-0.57	-2.22	-3.35	-4.40	-0.65	-2.95
PFM000069	2002-10-22	0.05	-0.94	-2.56	-3.62	-4.06	-0.28	-2.52
PFM000069	2002-07-16	0.15	-0.97	-2.64	-3.76	-3.68	0.05	-2.24
PFM000069	2004-07-06	0.01	-0.88	-2.54	-3.61	-4.02	-0.28	-2.52
PFM000068	2002-10-22	0.5	-0.94	-2.56	-3.63	-3.86	-0.09	-2.33
PFM000068	2003-01-16	0.1	-0.71	-2.35	-3.49	-4.42	-0.66	-2.97
PFM000068	2003-07-08	0.5	-0.76	-2.42	-3.48	-3.63	0.10	-2.13
PFM000068	2003-10-29	0.5	-0.39	-2.05	-3.12	-4.36	-0.63	-2.87
PFM000068	2002-07-16	0.2	-1.15	-2.81	-3.93	-3.67	0.07	-2.22
PFM000068	2004-07-06	0.5	-0.88	-2.54	-3.59	-4.05	-0.32	-2.53
PFM000068	2004-01-13	0.5	-0.81	-2.42	-3.57	-4.65	-0.86	-3.18
PFM000068	2004-04-21	0.5	-0.91	-2.55	-3.69	-4.38	-0.63	-2.94
PFM000068	2003-05-05	0.5	-0.95	-2.61	-3.75	-4.42	-0.68	-2.99
PFM000067	2003-01-15	0.1	-0.47	-2.28	-3.29	-3.86	-0.27	-2.44
PFM000067	2002-07-15	0.1	-0.66	-2.41	-3.33	-3.75	-0.10	-2.19
PFM000067	2002-10-22	0.05	-0.60	-2.31	-3.23	-3.79	-0.11	-2.19
PFM000067	2004-01-13	0.05	-0.70	-2.35	-3.47	-4.54	-0.79	-3.08
PFM000067	2003-07-08	0.05	-0.82	-2.57	-3.53	-3.17	0.48	-1.65
PFM000067	2004-04-20	0.05	-0.93	-2.50	-3.51	-3.76	0.07	-2.11
PFM000067	2003-10-28	0.05	-0.83	-2.56	-3.44	-4.04	-0.38	-2.43
PFM000067	2003-05-06	0.1	-1.05	-2.64	-3.71	-3.51	0.30	-1.94
PFM000066	2003-01-13	0.1	-0.39	-2.01	-3.29	-3.95	-0.17	-2.63
PFM000066	2002-07-16	0.2	-1.25	-2.88	-4.16	-3.41	0.35	-2.10
PFM000066	2003-10-27	0.1	-0.64	-2.25	-3.50	-4.12	-0.34	-2.75
PFM000066	2004-04-19	0.1	-1.03	-2.67	-3.94	-4.14	-0.38	-2.82
PFM000066	2003-07-08	0.1	-1.14	-2.79	-4.00	-3.88	-0.12	-2.50
PFM000066	2004-01-12	0.1	-0.85	-2.42	-3.75	-4.26	-0.43	-2.92
PFM000066	2003-05-06	0.1	-0.89	-2.51	-3.79	-4.06	-0.28	-2.73
PFM000066	2004-07-06	0.1	-1.32	-2.95	-4.15	-3.97	-0.21	-2.58

**Table D-10. Calculated saturation indices for stream water in Simpevarp, part one. Saturation indices above -0.5 are considered possible saturation and highlighted in red.**

ID code	Sample date	Sampling depth (m)	Barite SI	Gypsum SI	Celestite SI	Witherite SI	Calcite SI	Strontianite SI
PSM000347	2006-03-21	0.50	-0.42	-2.72	-3.35	-6.81	-3.72	-5.51
PSM000347	2006-05-30	0.50	-0.70	-2.94	-3.56	-6.26	-3.10	-4.90
PSM000347	2006-12-12	0.50	-0.17	-2.76	-3.32	-6.94	-4.14	-5.86
PSM000347	2007-03-20	0.50	-0.59	-2.87	-3.46	-7.00	-3.89	-5.65
PSM000347	2007-12-11	0.50	-0.63	-3.01	-3.54	-7.42	-4.40	-6.10
PSM000347	2008-03-12	0.50	-0.75	-2.98	-3.57	-6.51	-3.34	-5.10
PSM002071	2003-06-24	0.10	-1.00	-3.21	-3.74	-6.15	-2.97	-4.67
PSM002072	2003-06-24	0.10	-1.80	-4.13	-4.60	-6.92	-3.86	-5.50
PSM002076	2003-06-24	0.10	-1.28	-3.30	-3.85	-5.90	-2.52	-4.24
PSM002079	2003-06-24	0.10	-0.96	-3.15	-3.69	-5.77	-2.56	-4.27
PSM002079	2005-08-24	0.50	-0.82	-3.03	-3.57	-5.29	-2.11	-3.82
PSM002079	2005-12-14	0.50	0.04	-2.28	-2.83	-7.03	-3.95	-5.67
PSM002079	2006-03-22	0.50	-0.28	-2.64	-3.22	-7.06	-4.03	-5.78
PSM002079	2006-05-31	0.50	-0.73	-3.05	-3.62	-6.72	-3.65	-5.38
PSM002079	2006-08-23	0.50	-0.40	-2.57	-3.12	-5.27	-2.04	-3.76
PSM002079	2006-12-13	0.50	0.23	-2.39	-2.94	-7.79	-5.01	-6.73
PSM002079	2007-03-20	0.50	-0.46	-2.83	-3.39	-7.59	-4.57	-6.30
PSM002079	2007-05-24	0.50	-0.50	-2.68	-3.23	-5.58	-2.38	-4.09
PSM002079	2007-08-22	0.50	-0.71	-2.88	-3.43	-5.43	-2.20	-3.92
PSM002079	2007-12-12	0.50	-0.44	-2.87	-3.42	-8.20	-5.23	-6.95
PSM002079	2008-03-13	0.50	-0.63	-2.90	-3.45	-6.37	-3.24	-4.96
PSM002079	2008-05-20	0.50	-0.65	-2.74	-3.32	-5.33	-2.02	-3.77
PSM002079	2008-08-20	0.50	-0.04	-2.32	-2.83	-6.46	-3.34	-5.02
PSM002082	2003-06-24	0.10	-1.18	-3.29	-3.91	-6.23	-2.94	-4.73
PSM002083	2003-06-23	0.10	-1.17	-3.24	-3.77	-6.12	-2.79	-4.49
PSM002083	2005-08-24	0.50	-0.70	-2.80	-3.35	-5.73	-2.43	-4.16
PSM002083	2005-12-14	0.50	-0.18	-2.36	-2.96	-6.92	-3.69	-5.47
PSM002083	2006-03-22	0.50	-0.43	-2.66	-3.27	-7.12	-3.95	-5.72
PSM002083	2006-05-31	0.50	-0.78	-2.97	-3.59	-6.56	-3.35	-5.14
PSM002083	2006-08-26	0.50	-0.50	-2.60	-3.27	-5.77	-2.48	-4.31
PSM002083	2006-12-13	0.50	0.08	-2.45	-3.03	-7.41	-4.54	-6.29
PSM002083	2007-03-20	0.50	-0.62	-2.89	-3.49	-7.62	-4.50	-6.26
PSM002083	2007-05-24	0.50	-0.41	-2.55	-3.14	-5.92	-2.67	-4.43
PSM002083	2007-08-21	0.50	-0.39	-2.53	-3.10	-5.80	-2.53	-4.28
PSM002083	2007-12-12	0.50	-0.76	-3.10	-3.69	-7.82	-4.76	-6.52
PSM002083	2008-03-13	0.50	-0.82	-2.99	-3.59	-6.58	-3.36	-5.13
PSM002083	2008-05-20	0.50	-0.57	-2.69	-3.30	-5.97	-2.69	-4.46

**Table D-11. Calculated saturation indices for stream water in Simpevarp, part two.**

ID code	Sample date	Sampling depth (m)	Barite SI	Gypsum SI	Celestite SI	Witherite SI	Calcite SI	Strontianite SI
PSM002084	2003-06-23	0.10	-0.69	-2.64	-3.34	-5.46	-2.02	-3.89
PSM002085	2003-06-23	0.10	-0.67	-2.35	-3.21	-4.05	-0.34	-2.36
PSM002085	2005-12-13	0.50	0.04	-1.94	-2.65	-4.65	-1.23	-3.11
PSM002085	2006-03-22	0.50	-0.18	-2.05	-2.93	-4.65	-1.13	-3.18
PSM002085	2006-05-30	0.50	-0.39	-2.25	-3.07	-4.12	-0.58	-2.57
PSM002085	2006-12-12	0.50	0.36	-1.59	-2.36	-4.74	-1.29	-3.23
PSM002085	2007-03-20	0.50	-0.22	-2.08	-2.93	-4.88	-1.34	-3.35
PSM002085	2007-05-23	0.50	-0.58	-2.38	-3.12	-3.99	-0.40	-2.31
PSM002085	2007-12-12	0.50	-0.17	-2.06	-2.95	-4.78	-1.27	-3.33
PSM002085	2008-03-12	0.50	-0.32	-2.08	-2.95	-4.25	-0.61	-2.66
PSM002085	2008-05-20	0.50	-0.62	-2.32	-3.15	-4.10	-0.41	-2.41
PSM002085	2008-08-19	0.50	0.00	-1.89	-2.63	-4.81	-1.31	-3.22
PSM002086	2003-06-24	0.10	-0.52	-2.58	-3.28	-5.47	-2.13	-3.99
PSM002086	2008-03-13	0.50	-0.06	-2.16	-2.86	-5.73	-2.44	-4.30
PSM002086	2008-05-21	0.50	-0.14	-2.06	-2.82	-4.96	-1.48	-3.41
PSM002086	2008-08-20	0.50	-0.01	-2.15	-2.84	-5.76	-2.51	-4.36
PSM002087	2003-06-23	0.10	-0.88	-2.98	-3.54	-5.56	-2.27	-3.99
PSM002087	2005-08-24	0.50	-0.76	-2.96	-3.51	-5.35	-2.16	-3.88
PSM002087	2005-12-14	0.50	0.13	-2.19	-2.74	-6.42	-3.34	-5.06
PSM002087	2006-03-22	0.50	-0.24	-2.57	-3.17	-6.72	-3.65	-5.42
PSM002087	2006-05-31	0.50	-0.32	-2.92	-3.51	-6.01	-3.21	-4.97
PSM002087	2006-08-23	0.50	-0.10	-2.18	-2.69	-5.02	-1.71	-3.38
PSM002087	2006-12-13	0.50	0.41	-2.28	-2.85	-7.26	-4.56	-6.30
PSM002087	2007-03-20	0.50	-0.43	-2.77	-3.34	-7.45	-4.39	-6.13
PSM002087	2007-05-24	0.50	-0.42	-2.55	-3.12	-5.37	-2.11	-3.84
PSM002087	2007-08-22	0.50	-0.82	-2.74	-3.29	-5.45	-1.97	-3.68
PSM002087	2007-12-12	0.50	-0.39	-2.78	-3.34	-7.86	-4.85	-6.58
PSM002087	2008-03-13	0.50	-0.56	-2.80	-3.37	-6.10	-2.95	-4.69
PSM002087	2008-05-21	0.50	-0.43	-2.53	-3.06	-5.06	-1.76	-3.45
PSM002087	2008-08-20	0.50	-0.06	-2.28	-2.80	-5.95	-2.78	-4.47
PSM107795	2008-03-13	0.50	-0.44	-2.52	-3.16	-6.29	-2.97	-4.79
PSM107795	2008-05-21	0.50	-0.69	-2.48	-3.16	-5.34	-1.74	-3.59

**Table D-12.  $K_d$  values and calculated saturation indices for the 2011 soil samples.**

<b>Id code</b>	<b>Depth</b>		<b><math>K_d</math> Ba</b>	<b><math>K_d</math> Ca</b>	<b><math>K_d</math> <sup>226</sup>Ra</b>	<b><math>K_d</math> Sr</b>	<b><math>K_d</math> U</b>	<b>Barite SI</b>
AFM001356	20–25	Clay Till	1,200	93	13,000	100	560	-0.035
AFM001356	55–55	Clay Till	4,200	500	28,000	460	590	-0.547
AFM001357	20–25	Clay Till	1,500	268	11,000	210	890	-0.603
AFM001357	55–55	Clay Till	2,300	790	4,100	570	550	-0.764
AFM001359	20–25	Clay Till	910	210	23,000	110	230	-0.08
AFM001359	55–55	Clay Till	1,300	600	20,000	320	160	-0.33
AFM001361	20–25	Clay Till	1,000	41	5,200	53	240	-0.331
AFM001361	55–55	Clay Till	2,000	250	5,400	170	230	-0.912
AFM001376	20–25	Clay Till	1,600	210	5,100	160	260	-0.703
AFM001376	55–55	Clay Till	1,300	460	2,400	340	380	-0.814
AFM001362	20–25	Clay Gyttja	260	35	870	44	610	1.24
AFM001362	55–55	Clay Gyttja	1,200	23	1,800	33	3,600	1.007
AFM001363	20–25	Clay Gyttja	610	26	1,900	43	1,100	1.26
AFM001363	55–55	Clay Gyttja	4,600	350	9,800	230	220	0.655
AFM001365	20–25	Clay Gyttja	760	110	1,600	150	2,500	0.735
AFM001365	55–55	Clay Gyttja	1,800	38	3,000	88	3,200	0.62
AFM001367	20–25	Clay Gyttja	1,200	78	3,300	120	4,400	0.903
AFM001367	55–55	Clay Gyttja	4,900	46	3,500	120	2,800	0.613
AFM001368	20–25	Clay Gyttja	870	30	4,300	57	11,000	1.202
AFM001368	55–55	Clay Gyttja	3,600	38	6,400	86	3,900	0.663
AFM001369	20–25	Glacial Clay	820	82	2,500	89	260	0.833
AFM001369	55–55	Glacial Clay	2,700	140	4,800	800	110	0.407
AFM001371	20–25	Glacial Clay	710	0.19		0.24	1.1	0.075
AFM001371	55–55	Glacial Clay	2,300	0.34		0.55	18	-0.027
AFM001372	20–25	Glacial Clay	830	0.041	2.7	0.062	0.43	0.34
AFM001372	55–55	Glacial Clay	3,200	0.12	6.4	0.63	0.12	0.389
AFM001373	20–25	Glacial Clay	2,200	0.29	4.6	0.22	0.32	-0.345
AFM001373	55–55	Glacial Clay	4,800	1.1	16	0.76	0.31	-0.821
AFM001374	20–25	Glacial Clay	1,200	0.1	4.3	0.1	0.24	0.283
AFM001374	55–55	Glacial Clay	7,100	1.1	22	0.78	0.2	-0.487
AFM001379	20–25	Cultivated Peat	810	0.21	1.5	0.26	15	0.975
AFM001379	55–55	Cultivated Peat	690	0.23	0.81	0.22	33	1.04
AFM001381	20–25	Cultivated Peat	400	0.086	0.88	0.092	19	1.373
AFM001381	55–55	Cultivated Peat	280	0.067	0.55	0.074	20	1.22
AFM001382	20–25	Cultivated Peat	1,200	0.29	2	0.34	9.8	0.455
AFM001382	55–55	Cultivated Peat	1,300	0.3	3	0.35	6.1	0.312
AFM001383	20–25	Cultivated Peat	1,500	0.39	5.4	0.43	19	-0.081
AFM001383	55–55	Cultivated Peat	1,400	0.5	4.3	0.51	26	-0.151
AFM001384	20–25	Cultivated Peat	1,500	0.44	3.5	0.49	13	-0.222
AFM001384	55–55	Cultivated Peat	1,300	0.36	3.7	0.39	8.5	0.82
AFM001385	20–25	Wetland Peat	1,300	0.48	8	0.55	3.5	-1.002
AFM001385	55–55	Wetland Peat	1,800	0.52	4	0.61	7.3	-0.991
AFM001387	20–25	Wetland Peat	1,700	0.56	2.7	0.6	11	0.176
AFM001387	55–55	Wetland Peat	1,300	0.46	1.8	0.48	19	0.093
AFM001388	20–25	Wetland Peat	490	0.18	1.1	0.17	8.4	-1.002
AFM001388	55–55	Wetland Peat	1,100	0.41	2.4	0.42	16	-0.507
AFM001389	20–25	Wetland Peat	330	0.13	0.78	0.13	18	-0.196
AFM001389	55–55	Wetland Peat	470	0.19	1.1	0.17	29	-0.175
AFM001391	20–25	Wetland Peat	1,200	0.44	2.5	0.46	16	-0.521
AFM001391	55–55	Wetland Peat	1,100	0.44	2	0.42	40	0.219

## Ra speciation

Table E-1. Calculated Ra speciation in the sediment  $K_d$  samples.

IDCODE	Min depth (cm)	Sediment type	Ra <sup>2+</sup> (%)	RaOH <sup>+</sup> (%)	RaCl <sup>+</sup> (%)	RaCO <sub>3</sub> (%)	RaSO <sub>4</sub> (%)	Org-Ra (%)
PFM000074	0	Lake	98.9	1.7E-05	0.06	0.12	0.18	0.75
PFM000074	25	Lake	98.6	1.8E-05	0.07	0.07	0.37	0.90
PFM000107	0	Lake	97.9	5.7E-05	0.53	0.17	0.47	0.93
PFM000107	25	Lake	97.8	6E-05	0.33	0.16	0.80	0.96
PFM000117	0	Lake	98.2	6.8E-05	0.02	0.32	0.43	1.00
PFM000117	25	Lake	97.7	7E-05	0.01	0.22	0.71	1.38
PSM002065	0	Lake	95.4	1.9E-06	0.05	0.00	1.22	3.34
PSM002065	20	Lake	97.1	3.3E-06	0.09	0.00	0.18	2.62
PSM002067	0	Lake	93.5	2.1E-08	0.03	0.00	1.31	5.21
PSM002067	15	Lake	95.3	5.5E-07	0.03	0.00	0.38	4.33
PFM000063	0	Marine	91.4	2.2E-05	1.99	0.04	6.53	0.07
PFM000063	20	Marine	93.0	2.5E-05	2.05	0.07	4.79	0.09
PSM002064	0	Marine	94.6	8.6E-06	2.58	0.03	2.45	0.32
PSM002064	25	Marine	96.7	1.1E-05	2.66	0.09	0.30	0.28
PSM007090	0	Marine	92.6	3.3E-06	2.67	0.01	4.65	0.07
PSM007090	25	Marine	96.6	1.5E-06	2.80	0.01	0.38	0.25

Effects of barite on the  $K_d$  for Ra

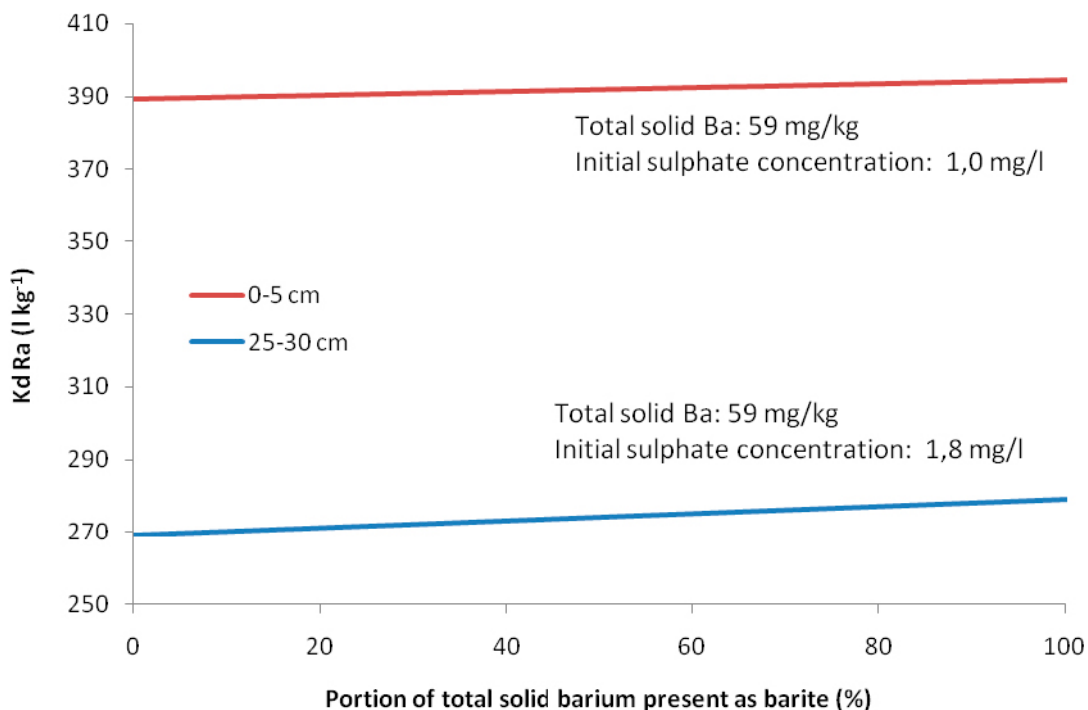


Figure F-1. Modelled effect of barite on Ra  $K_d$ -values at site PFM000074, depth 0–5 and 25–30 cm.

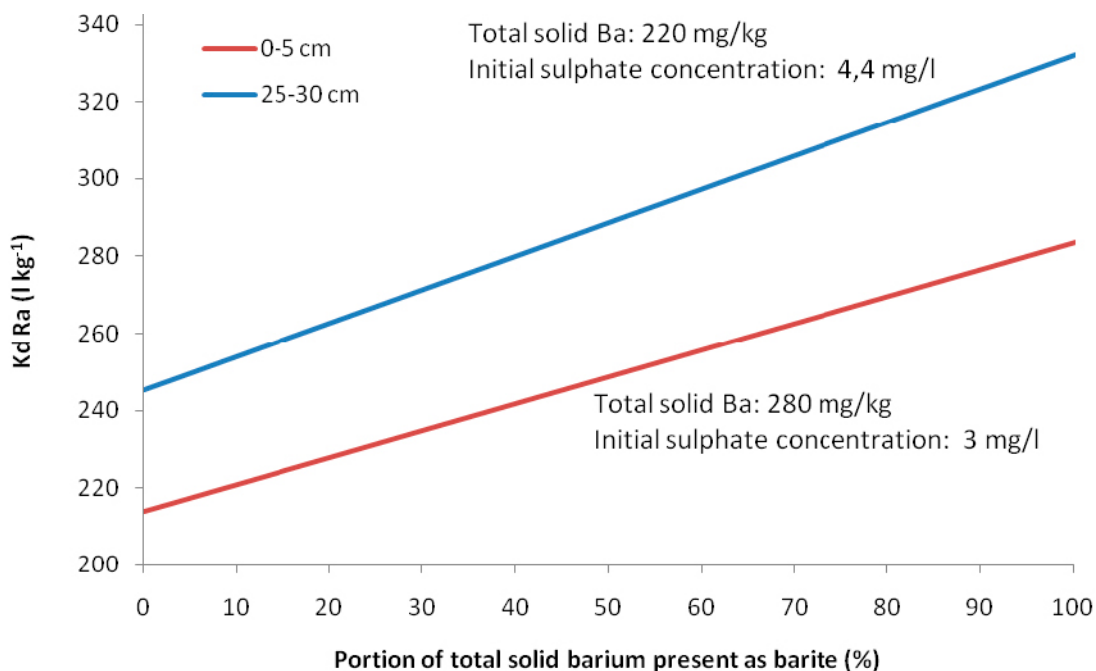


Figure F-2. Modelled effect of barite on Ra  $K_d$ -values at site PFM000107, depth 0–5 and 25–30 cm.

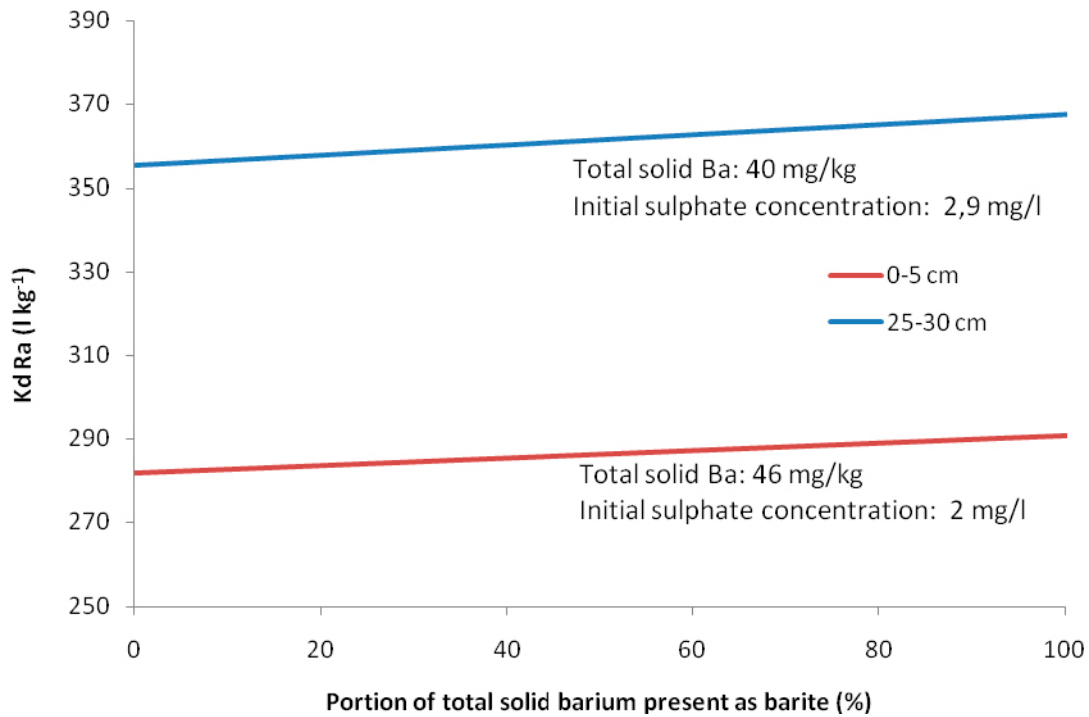


Figure F-3. Modelled effect of barite on  $Ra\ K_d$ -values at site PFM000117, depth 0–5 and 25–30 cm.

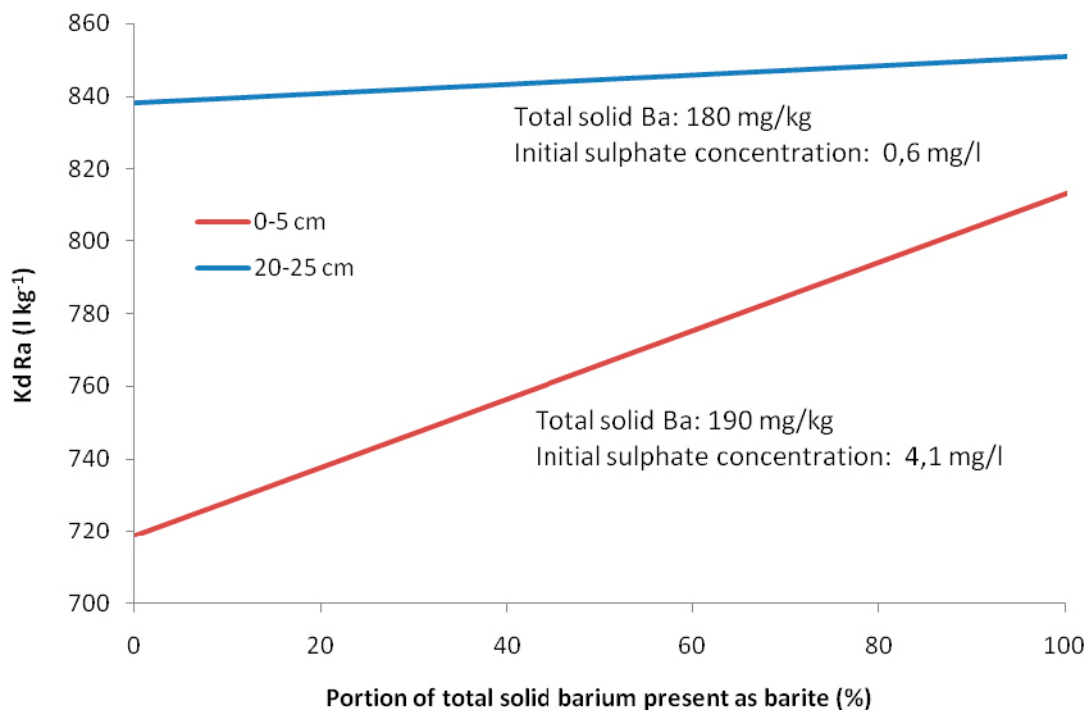


Figure F-4. Modelled effect of barite on  $Ra\ K_d$ -values at site PFM002065, depth 0–5 and 20–25 cm.

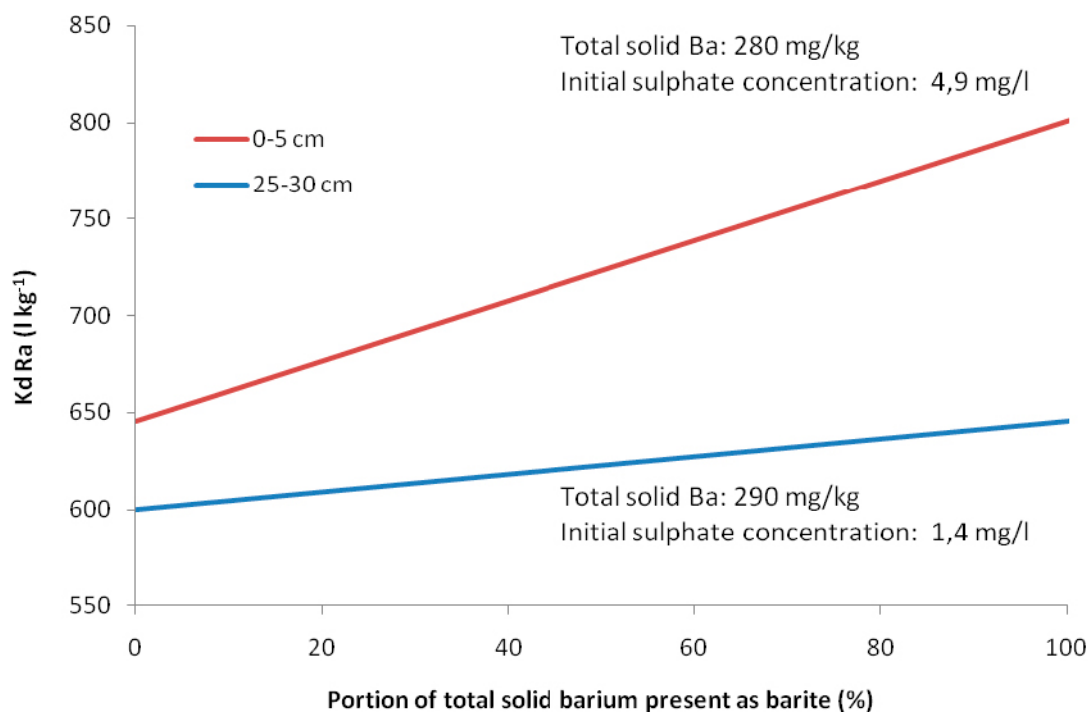


Figure F-5. Modelled effect of barite on Ra  $K_d$ -values at site PFM002067, depth 0–5 and 25–30 cm.

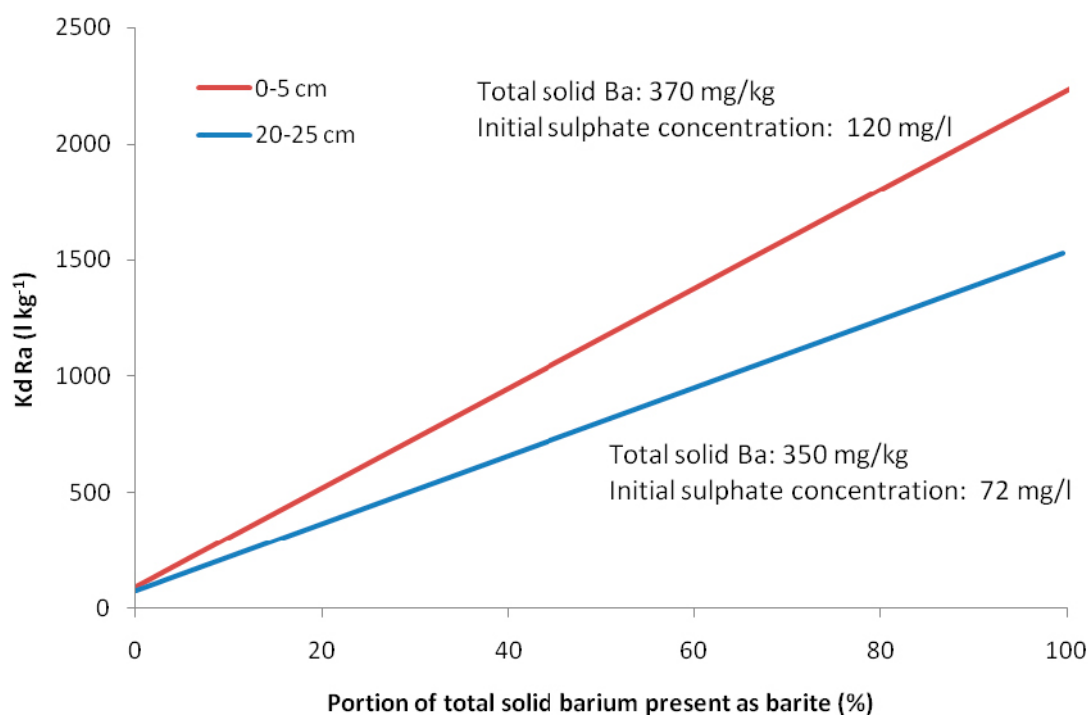


Figure F-6. Modelled effect of barite on Ra  $K_d$ -values at site PFM000063, depth 0–5 and 20–25 cm.



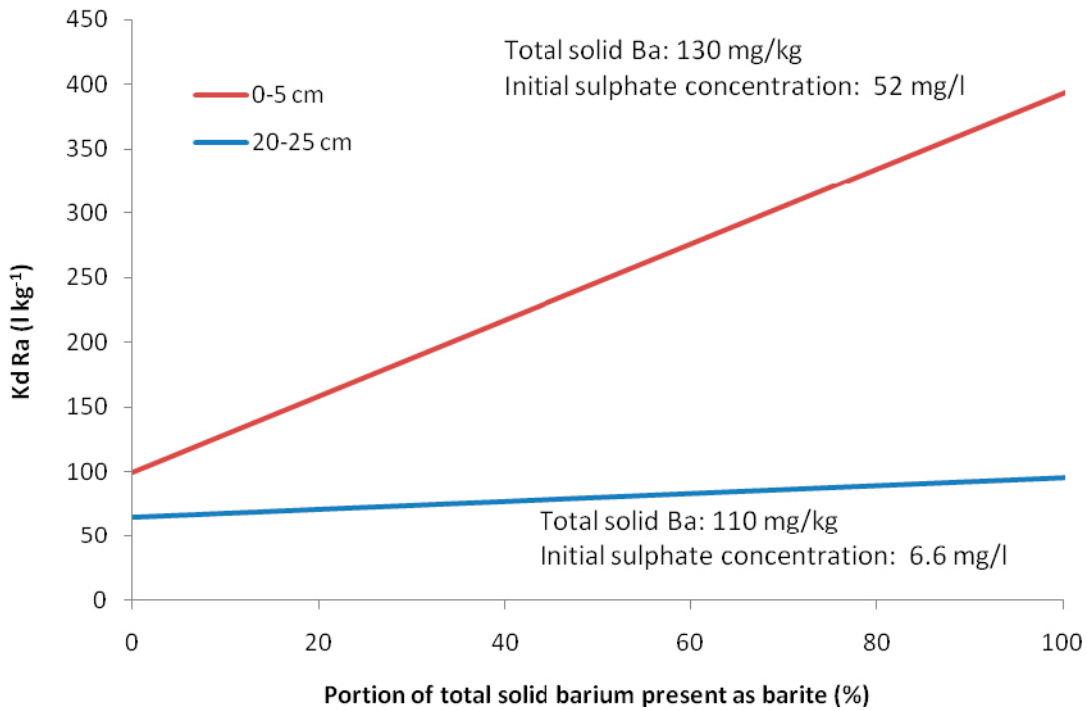


Figure F-7. Modelled effect of barite on Ra  $K_d$ -values at site PFM002064, depth 0–5 and 20–25 cm.

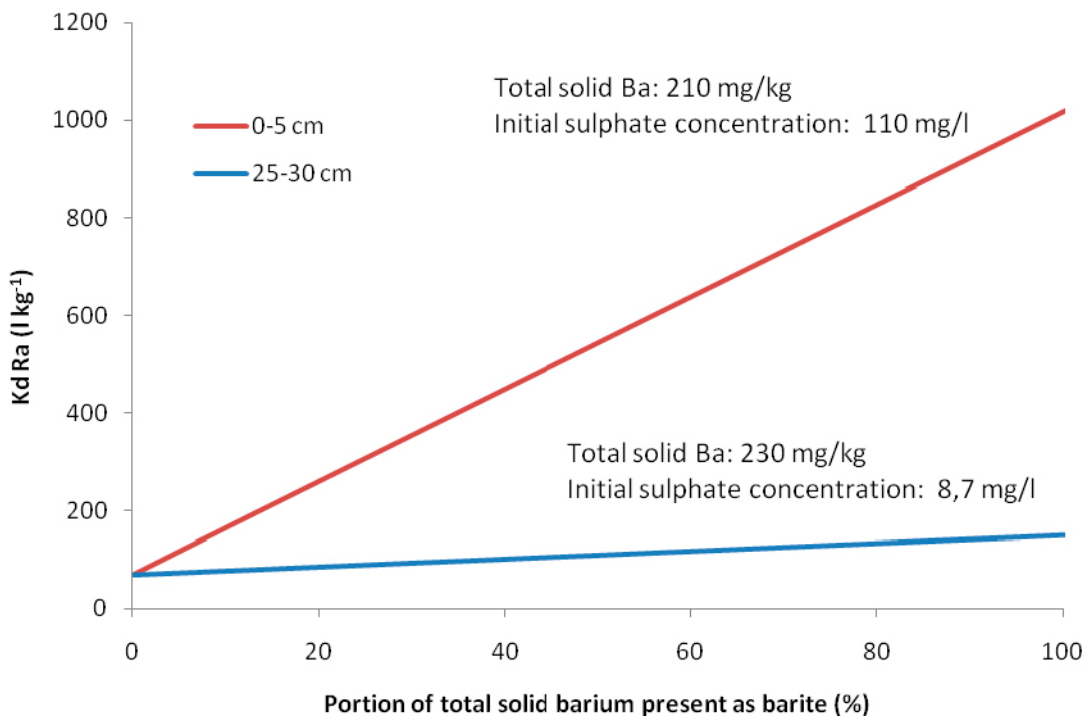
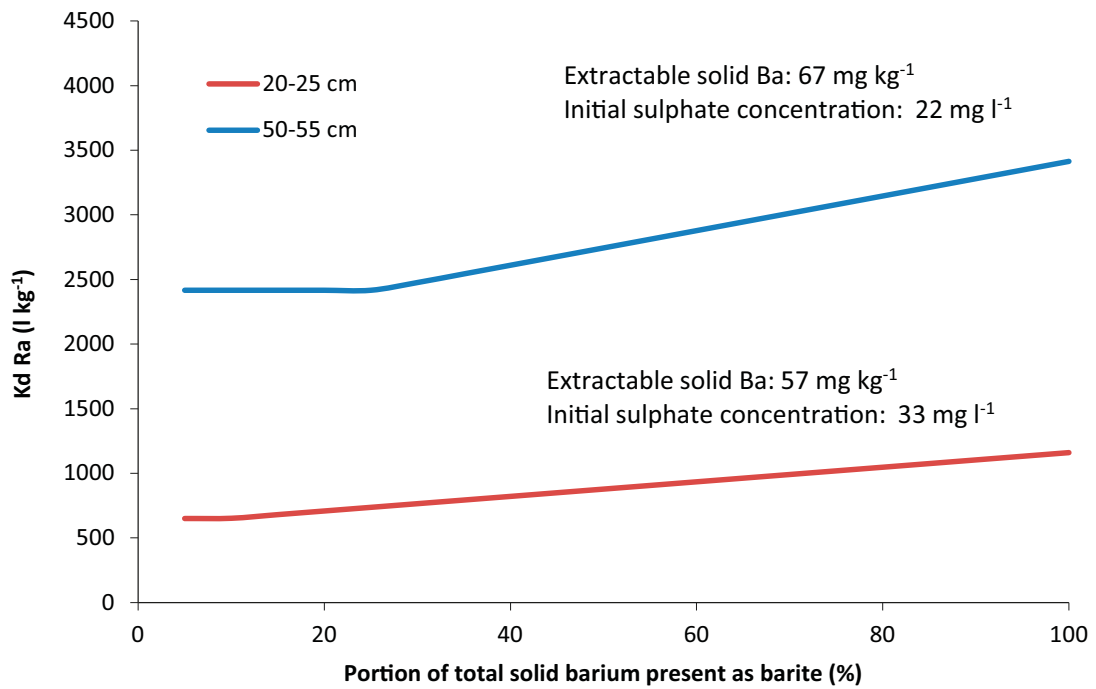
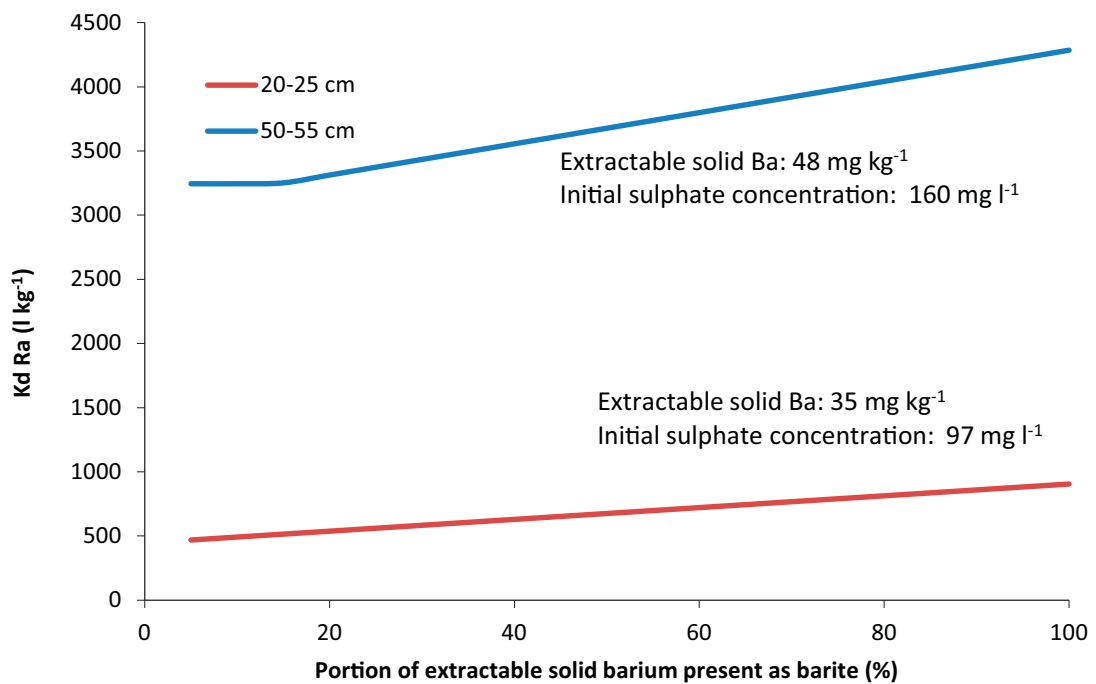


Figure F-8. Modelled effect of barite on Ra  $K_d$ -values at site PFM007090, depth 0–5 and 25–30 cm.



**Figure F-9.** Modelled effect of barite on Ra  $K_d$ -values at the clay till site AFM001356, depth 20–25 and 50–55 cm.



**Figure F-10.** Modelled effect of barite on Ra  $K_d$ -values at the glacial clay site AFM001372, depth 20–25 and 50–55 cm.